Hydration and Hydrolysis with Water Tolerant Lewis Acid Catalysis in High Temperature Water

by

Natalie A. Rebacz

A dissertation submitted in partial fulfillment
of the requirements for the degree of
Doctor of Philosophy
(Chemical Engineering)
in The University of Michigan
2011

Doctoral Committee:

Professor Phillip E. Savage, Chair
Professor Johannes W. Schwank
Professor Edwin Vedejs
Emeritus Professor Walter J. Weber Jr.
Associate Professor Suljo Linic

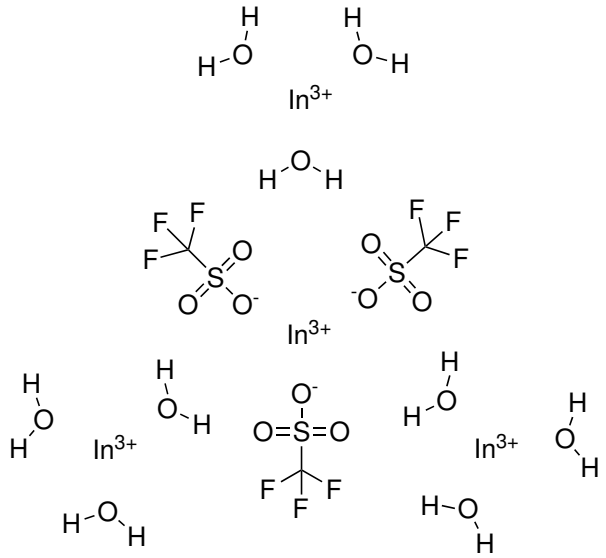

to Debe Williams

and to WAB

ACKNOWLEDGEMENTS

I would first like to thank all of my mentors during college who inspired me to continue studies in graduate school. These include Dennis Compton, Dotti Miller, Marina Miletic, Debbie Williams, Jeffrey Weber, and especially Bill Boulanger.

I was happy to have had the opportunity to mentor several undergraduate students: Alex Cohen, Christopher Rausche, Lauren E. Ludlow, Kazi M. Munabbir, and Valerie A. Lee. I learned just as much from them about mentoring as they learned from me about experimental techniques. Alex Cohen contributed greatly to the work in chapters 7 and 5; Chris Rausche, to material in chapters 4 and 5; and Lauren, Kazi, and Valerie, to much of the experimental work in chapter 4. I wish them all success and happiness in their careers. During my research, I also worked closely with Master's student Dongil Kang, who contributed greatly to the experimental work in chapter 6. Dongil performed excellently in the lab, and I greatly enjoyed his calm, genial, and endearing personality. I wish him the best in his endeavors.

I greatly enjoyed the friendship of many of my colleagues. It would be impossible to thank them all, but I would like to extend thanks in particular to Tanawan Pinnarat, Ayse Bilge Ozel, and Eranda Nikola for their friendship and support.

I thank former Savage group member Craig Comisar for helping me find my way around lab as a first-year student. Tanawan Pinnarat and I joined the Savage group together and shared many experiences. We took courses together, attended conferences, and pursued fun and enjoyment outside of lab. I greatly appreciate her friendship. I wish the best of luck to all of our junior members, and I especially thank

Chad Huelsman for his good humor and deep appreciation of irony, Peter Valdez for the order he brings to our lab, Jake Dickinson for his ability to fix things, and Changi for his good nature. I would like to thank post-doctoral student Tylisha Brown for her encouragement and good discussions.

I thank Kent Pruss from the machine shop for his help in fixing lab equipment. I thank Harald Eberhart for making a large fraction of the equipment that went into this study.

I thank my committee members for their support and criticism over the years. I especially thank Phil Savage for serving as my research advisor.

I acknowledge the National Science Foundation (CTS-0625641) for funding this work.

I thank all the individuals who developed and documented LaTeX and gnuplot – formally or informally – which this work uses extensively. Together, they made a more aesthetic dissertation.

Finally, I thank my husband, Andrew Dalton, for his love and support throughout the last several years.

TABLE OF CONTENTS

LIST OF FIGURES

Figure

LIST OF TABLES

Table

LIST OF APPENDICES

Appendix

LIST OF ABBREVIATIONS

ANOVA analysis of variance

CI confidence interval as in "95% confidence interval"

DMF dimethylformamide

DOF degree(s) of freedom

GC gas chromatography

GC-FID gas chromatography-flame ionization detector

GC/MS gas chromatography/mass spectrometry

HTW high-temperature water

HCW hot-compressed water

ID inner diameter

MS_B between-group mean-square variance

MS_W within-group mean-square variance

MW molecular weight

OD outer diameter

Qz quartz

SS stainless steel

SSE sum of squared errors

THF tetrahydrofuran

WTLA water-tolerant Lewis acid

X conversion

$\mathbf{Y}$ yield, as a percent

Greek characters

μ average, arithmetic mean

σ standard deviation

ABSTRACT

Hydration and Hydrolysis with Water Tolerant Lewis Acid Catalysis in High Temperature Water

by

Natalie A. Rebacz

Chair: Phillip E. Savage

The purpose of this work was to develop the technique of performing organic reactions in high temperature water with water-tolerant Lewis acids (WTLAs). We define high temperature water (HTW), or hot compressed water (HCW), as liquid water above its normal boiling point. A water-tolerant Lewis acid is a Lewis acid that is not deactivated in the presence of water. The potential advantages that reaction in HTW with WTLAs may offer are many. Water is a benign solvent that is relatively safe to use. Post-reaction separation may be as simple as lowering temperature and pressure and decanting the organic phase from the liquid phase. The use of WTLAs may provide good reaction kinetics at low cost. WTLAs can often be reused in reactions without loss of activity. Our work is the first application of WTLAs to HTW reaction media.

We studied two basic reactions in HTW with WTLA catalysis: alkyne hydration to form ketones, and ether hydrolysis to form alcohols. We began our study of alkyne hydration with 1-phenyl-1-propyne hydration to propiophenone. We tested six different acid catalysts ($In(OTf)_3$, $InCl_3$, $Sc(OTf)_3$, $Yb(OTf)_3$, HCl, and H_2SO_4), and

found that $In(OTf)_3$ was the best catalyst for the hydration of 1-phenyl-1-propyne. We then performed experiments to discover that 1-phenyl-1-propyne hydration was first order in alkyne and first order in catalyst. Next, we determined the kinetics of hydration by collecting concentration vs time data at four different temperatures: 150, 175, 200, and 225°C. The rate of hydration of 1-phenyl-1-propyne in HTW with WTLAs was found to be similar to the rate of hydration carried out by conventional methods. Experimentally, activation energy and frequency factor were determined to be 21.4 ± 0.6 kcal/mol and $10^{8.8\pm0.3}$ L mol^{-1} s^{-1}, respectively. We concluded our studies in alkyne hydration with kinetics for related alkyne hydration systems. These additional experiments provided clues as to a reasonable mechanism and helped define the scope and limitations of the general method.

Our work on ether hydrolysis took a parallel path. Using anisole as a model ether, we tested the same six catalysts for their ability to hydrolyze anisole to form phenol. Again, $In(OTf)_3$ was found to be the best catalyst. The pseudo-first order method was used to show that the reaction was first order in ether and approximately first order in catalyst. Experiments at different temperatures (200, 225, 250, 275, and 300°C) with temporal variation allowed us to determine the kinetics of anisole hydrolysis. Again, rates and yields were found to be comparable to conventional techniques. We determined the activation energy to be 31 ± 1 kcal/mol and the frequency factor to be $10^{10.6\pm0.5}$ L mol^{-1} s^{-1}. Finally, we tested additional ethers toward hydrolysis to gain some insight into the mechanism, as well as the scope and limitations of the procedure.

As part of these studies in hydration and hydrolysis, we tested the effects that our reactor vessel may be exerting upon the reaction. For alkyne hydration, we found that the use of a capillary quartz reactor slowed the reaction dramatically. We hypothesized that the cause of this inhibition is a lack of favorable transport. For ether hydrolysis, we found that the presence of any surface tested – quartz or statinless

steel – decreased reaction progress. We hypothesize that this phenomenon is due to interaction between the surface and the $In(OTf)_3$ catalyst. These experimental results identify an important phenomenon that had previously gone unrecognized in the field. Examination of the surface-inhibition phenomenon was also invaluable in correctly interpreting the results from our kinetic studies.

The overall significance of our work is our demonstration that the use of WTLAs in HTW presents potential as a novel medium for organic synthesis. For hydration and hydrolysis, this previously unexplored reaction medium can be competitive with traditional techniques in terms of rate and yield.

CHAPTER I

Introduction

corpora non agunt nisi soluta

1.1 Motivation

Water is generally avoided in chemical synthesis. Many chemists have a stock of tales of the reactive destruction wrought by a few percent water in solution. Catalyst deactivation is one pathway by which water may wreak synthetic havoc. The Co/Mn/Br catalyst used in the industrial process of p-xylene oxidation to terephthalic acid, for example, is tranformed from the active octahedral configuration in glacial acetic acid to an inactive tetrahedral structure with just a few percent water. [1, 2] Dry conditions are insisted upon with the use of strong Lewis acids, as in Friedel-Crafts alkylations with $AlCl_3$ and others. [3] The fear of hydrolysis occurring when water is contacted with labile moieties such as esters is also well documented.

But alongside these horror stories are tales of success. After decades of scrupulously drying reaction vessels for Friedel-Crafts, it was discovered that the reaction will not occur under completely dry conditions. [3] The Diels-Alder reaction has had a similar sinusoidal history with regard to water. While water was the first reaction medium to carry out the Diels-Alder reaction in the history of man, water was shunned as a reaction medium for the next several decades, until Woodward and Baer

noted reaction acceleration of Diels-Alder in the presence of water [4]. Rideout and Breslow proceeded to quantify the rate acceleration [5]; their work was followed by many other investigations.

The term "on-water" was used for the observation that particular reactions are accelerated in a biphasic aqueous/organic system, as compared to reaction in organic solvent alone or in aqueous solvent alone.

Researchers have observed the "on-water" phenomenon for many polar reactions, such as the ene and cycloaddition reactions of azodicarboxylates [6], wherein the "on-water" reaction proceeds 3 to 10^5 times faster than reaction in non-polar organic solvent. Sharpless and co-workers also demonstrated the rate enhancements of "on-water" reaction for the aromatic Claisen rearrangement, and for the nucleophilic opening of an epoxide. Not all reactions were found to benefit from the presence of water. Jung and Marcus [7] made sense of the "on-water" data with an elegant synthesis of experimental rate data — rate data collected for differently modeled reactions (neat, aqueous homogeneous, and surface reactions) — and transition state theory. They concluded that "on-water" rate enhancement was an instance of transition-state stabilization by the reaction environment, by the solvent system. [7]

Reactions that do not necessarily benefit from transition-state stabilization by water are more limited in their applicability for reaction in water. Where such limitations do not stem from the necessity to avoid hydrolysis, they are oft due to rate retardation by a lack of solubility. Hence, hot-compressed water (HCW) is investigated here. The advantage gained is an increase in the solubility of organics relative to room-temperature water. Figure 1.1 portrays this effect with some simple, common organic substrates. An important process advantage is also gained with hot compressed water. Since the solubility of organics decreases as water temperature decreases, separation can be as simple as lowering vessel temperature and pressure, and decanting.

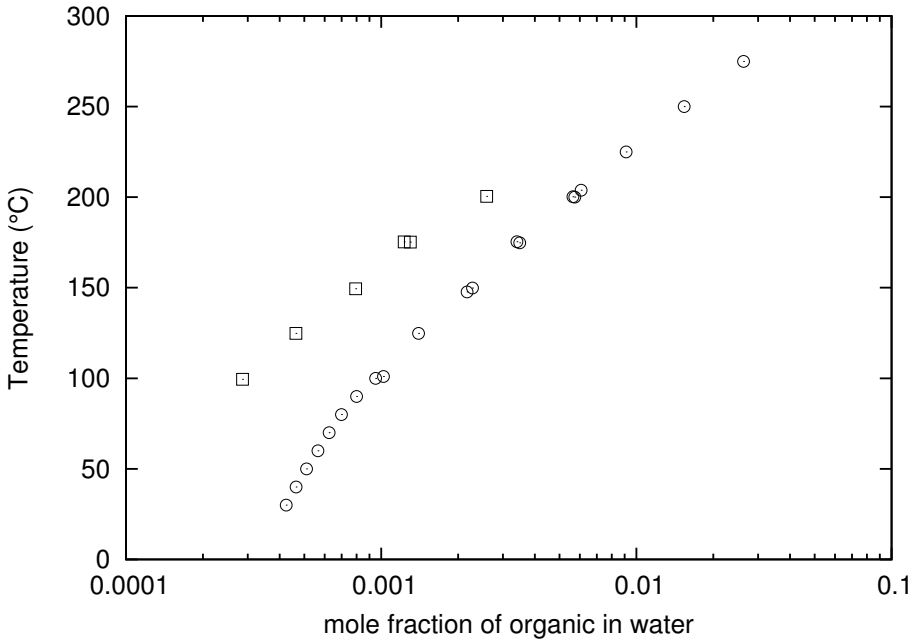

Figure 1.1: Temperature vs mole fraction of organic in water phase. Circles denote phase equilibria for benzene; squares, for toluene. Data were collected from [8–11]

One of the earliest papers on synthesis in high-temperature water (HTW) is a careful study on acid-catalyzed dehydration of alcohols in supercritical water. [12] The work demonstrated that low concentrations of mineral acids, such as 5 to 50 mM HCl or H_2SO_4, could be used to dehydrate simple small alcohols, diols, and polyols. Hence, ethanol affords ethene, propanol yields propene, diol ethylene glycol affords acetaldehyde which may then form crotonaldehyde, and polyol glycerol forms acrolein. The authors thought that the hydrothermal route could be of industrial interest. [12] However, a comparison with robust industrial processes such as the Wacker process for producing acetaldehyde from ethylene and oxygen, was not carried out.

This work was followed by research on Heck arylations with alkenes, Pd catalyst, and base in hot water. [13] Proof of concept was shown, though a number of drawbacks were also noted in comparison with reaction in organic solvents. Limited yields of coupling products (always less than 30%) were traced to deactivation of the Pd catalyst. Steric hindrance and electronic effects limited the procedure's general appli-

cability; sterically hindered α-methyl styrene and unactivated 1-hexene did not couple with iodobenzene, but styrene and allyl alcohol did. The prevalance of side reactions, such as alkene isomerization, oligomerization, and hydrogenation, also tempered the procedure's appeal. [13]

Another classic work in HTW organic synthesis is the study by Chandler et al. of Friedel-Crafts alkylation performed at 250 to 350°C without the use of any catalyst. [14, 15] The researchers showed that phenol could be alkylated to produce cresols in as much as 11% yield after two days. This work showed proof of concept, though it was riddled with some impracticable elements; namely, long reaction times and poor conversion. Further, the substrate used (phenol) was activated and thus relatively easy to alkylate. Non-activated compounds, such as benzene, could not be alkylated as readily.

Other exploratory work featuring the lack of any added catalysts included the Diels-Alder reaction with cyclopentadiene and electron-poor dienophiles [16], the Claisen-Schmidt condensation of benzaldehyde with 2-butanone [17], and Friedel-Crafts acylation of phenol and resorcinol [18]. Contributions from the Savage research group included cyclohexanol dehydration [19], condensation of benzaldehyde with acetone [20], tetrahydrofuran synthesis by way of 1,4-butanediol dehydration [21], and production of iso-propenyl-phenol from bisphenol A [22]. Hydrogenations could be carried out with the addition of formic acid to water, the decomposition of which yields hydrogen in situ. [23] Sodium formate, which behaves similarly, could be used to reduce nitrobenzene, acetophenone, cyclohexanone, and others. [24] In our lab, Shawn Hunter explored the use of added CO_2 to increase the acidity of water for the purpose of performing acid-catalyzed reaction in hot water. The underlying premise was that CO_2 would form carbonic acid at reaction conditions, lowering the solution pH and improving the rate of acid-catalyzed reactions. Mild rate enhancement was observed for cyclohexanol dehydration though advantages were less clear for

the example of p-cresol alkylation with isopropanol. [25] Perhaps the most successful high-temperature-water process was that of p-xylene oxidation to terephthalic acid by $MnBr_2$ catalysis. [26, 27] A rough economic comparison of the HTW process for terephthalic acid with the industrial process shows that the two processes could be economically comparable. [28]

In general, the synthetic procedures pursued in HTW media were uncompetitive with existing techniques. We supposed that water-tolerant Lewis acids (WTLAs) could be used to improve the applicability of hot compressed aqueous reaction media. Herein lies the impetus for the current work: organic reactions may be catalyzed in hot compressed water with WTLAs. This work will demonstrate that in terms of rate and yield, the WTLA-in-HTW approach can be competitive with traditional techniques.

1.2 Properties of Hot Compressed Water

Anyone who has carelessly poured a cup of piping hot water to find puddles of hot liquid splattered, seemingly everywhere, has experienced viscerally the changing properties of water with increasing temperature. HTW is a creature very different than its ambient counterpart. Relative to room-temperature water, HCW is less dense and less viscous; it has a lower dielectric constant and a higher ion product, K_W (until the critical point is neared). Changes in these bulk properties can be explained by changes in the structure of water as temperature rises. In turn, the structure of HTW can be essentially explained by hydrogen-bonding as the dominant intermolecular force. Note, in this work, "HTW" is used interchangeably with "HCW"; both refer to liquid water above its ambient pressure boiling point, kept in the liquid phase by pressurization.

Although some hydrogen bonds, as with the highly electronegative fluorine atom, can be as strong as 40 kcal/mol, those that persist in water are generally around 4

kcal/mol, about 0.17 eV. For the sake of comparison, the energy barrier for butane rotation from the "anti" configuration to the gauche costs 3.4 kcal/mol. As you increase temperature, the propensity for hydrogen bonds to break increases. Water at high temperatures has fewer and less persistent hydrogen bonds. Elevated temperatures encourage increased translation and rotation in the water molecules. At room temperature, water prefers a tetrahedral structure with a distinct outer solvation shell. As hydrogen-bonding becomes less predominant with higher temperatures, the average cluster size shrinks and the outer solvation shell loses order. These effects are indicated by the molecular pair-correlation function of water; with increasing temperature, the first and second nearest-neighbor peaks diminish in magnitude and shift to longer distances. At 500°C and 987 atm, the second-nearest neighbor peak is almost gone, indicating approach to a more gas-like state. [29]

In water at ambient conditions, it is hydrogen-bonding interactions that give water its elevated density compared to other liquids (excluding chlorinated methanes, whose high density is derived from strong intramolecular forces). With diminished hydrogen-bonding, the bulk density must decrease. Figure 1.2 shows how the density of water falls with temperature to match that of some organic solvents. For example, the room-temperature densities of THF, benzene, acetone, and diethyl ether are 0.889, 0.874, 0.79, and 0.714 g/mL respectively. Viscosity is a measure of internal resistance to flow. Figure 1.3 shows how the viscosity of water drops with temperature. For comparison, the room temperature viscosities of benzene, THF, acetone, and diethyl ether are 652, 480, 308, and 224 μPa$*$s respectively. Formally, the dielectric constant is a measure of the effect of a solvent upon an electric field. The material is placed between two oppositely charged plates and the ability of the solvent to screen the potential between the plates is measured. A solvent with a high degree of polarizability, a large molecular dipole, and hydrogen-bonding potential, will greatly screen the potential between two oppositely charged plates, and will have a large dielectric con-

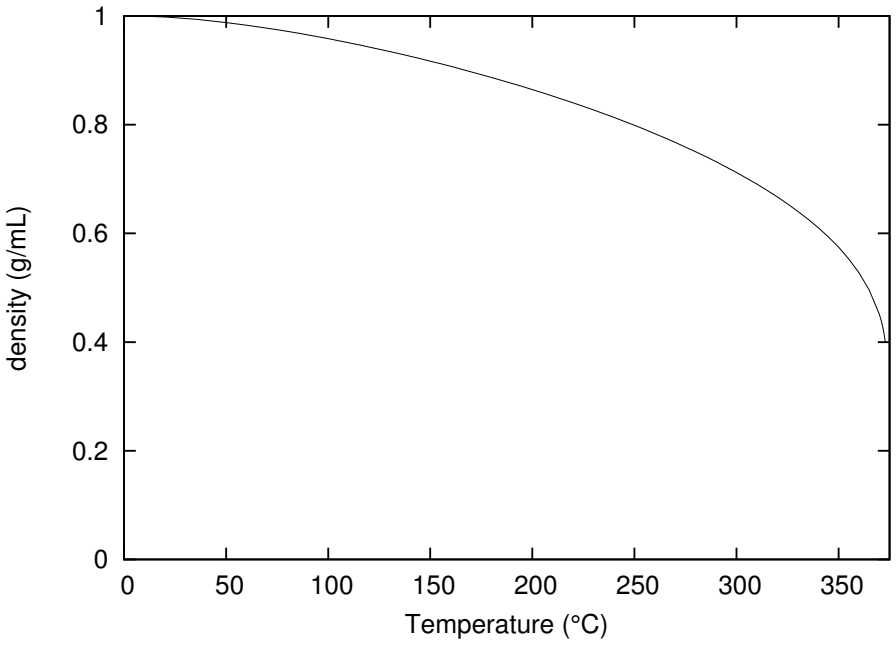

Figure 1.2: Change in density with temperature for HTW at its saturated condition. [31]

stant. As hydrogen bonding diminishes, of course, water's capacity to screen electric fields is compromised. For any temperature and density, Uematsu and Franck proposed the following relationship to describe the changing dielectric constant of water, where ρ^* is density in g/mL and T^* is temperature in Kelvin divided by 298.15 K. [30] Parameters A through J are estimated to be 7.62571, 244.003, -140.569, 27.7841, -96.2805, 41.7909, -10.2099, -45.2059, 84.6395, and -35.8644, respectively. Figure 1.4 uses this correlation to depict the behavior of the dielectric constant for the temperatures and pressures explored within the experiments of this work.

$$\begin{aligned} \epsilon &= 1 + \frac{A}{T^*}\rho^* + \left(\frac{B}{T^*} + C + DT^*\right)\rho^{*2} \\ &\quad + \left(\frac{E}{T^*} + FT^* + GT^{*2}\right)\rho^{*3} \\ &\quad + \left(\frac{H}{T^{*2}} + \frac{I}{T^*} + J\right)\rho^{*4} \end{aligned} \tag{1.1}$$

The dissociation constant, K_W, for HTW increases almost three orders of mag-

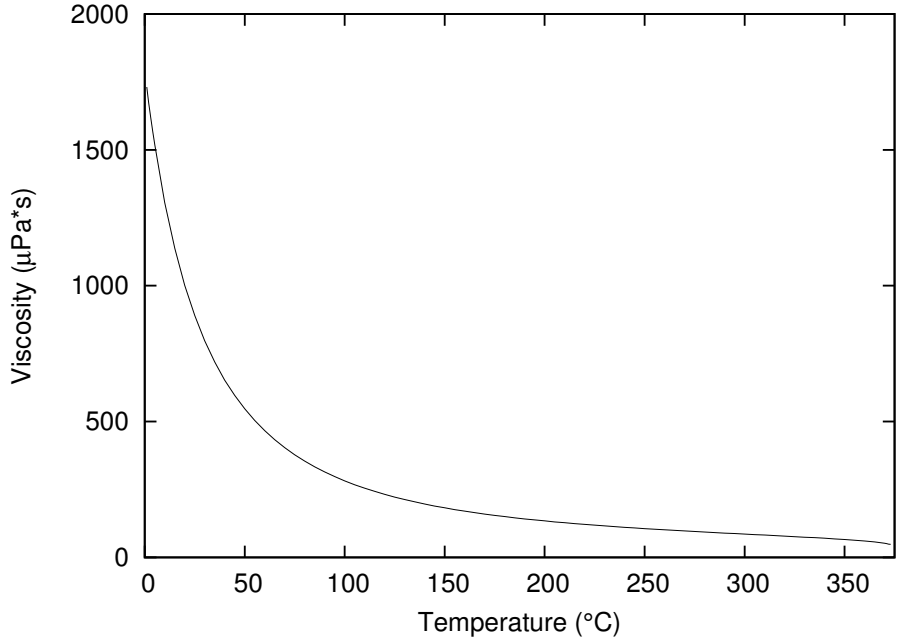

Figure 1.3: Change in viscosity with temperature for HTW at its saturated condition. [31]

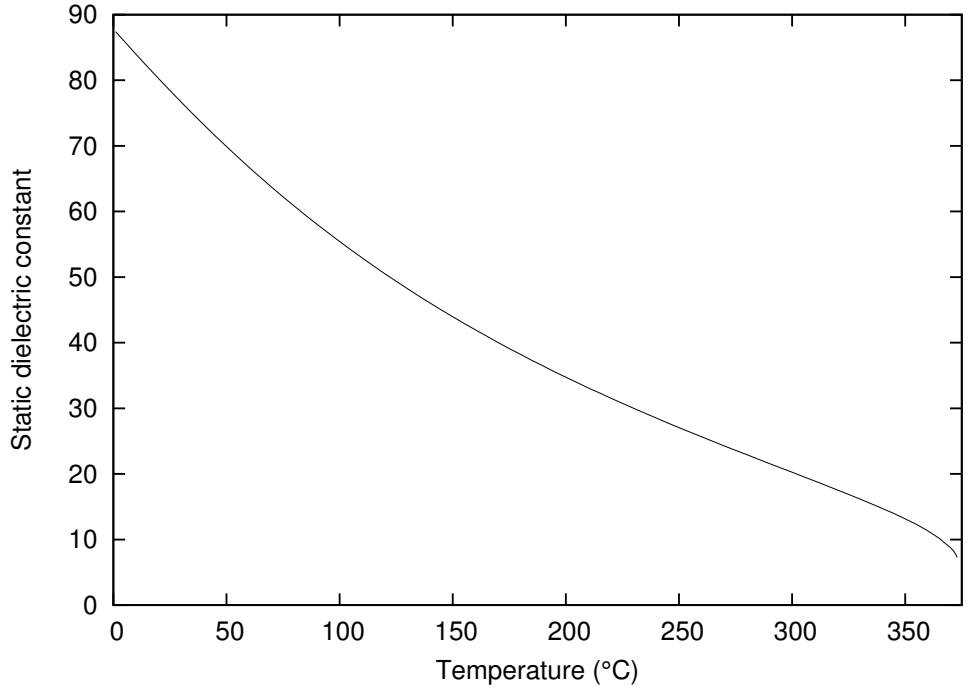

Figure 1.4: Static dielectric constant of saturated liquid water.

nitude from 10^{-14} (mol/kg)^2 at ambient conditions to nearly 10^{-11} (mol/kg)^2 near 275°C. Since the ion product is an equilibrium constant for the breaking of H−OH bonds to form H^+ and OH^-, which are stabilized by complexing to other water molecules, an increase in temperature will generally decrease the ΔH for the transformation. However, when the ability of water to stabilize the ions is compromised by a suppressed dielectric constant, the ion product will begin to decrease again. This behavior is seen as water nears the critical point, above 300°C. Beyond the critical point, water tends to behave more gas-like (unless the pressure is very high). It maintains only 10% of its room-temperature hydrogen bonds, it is much less dense, and the ion product is severely depressed, owing to its reduced ability to stabilize ions. Marshall and Franck provide a correlation for the ion product of water, K_W, in terms of temperature and density, given in Equation 1.2. [32] Here, K_W has units of (mol/kg)^2, temperature is in Kelvin, and density (ρ) has units of g/mL. The parameters A through G are estimated to be -4.098, -3245.2, 2.24x10^5, -3.98x10^7, 13.957, -1262.3, and 8.56x10^5, respectively.

$$K_W = A + \frac{B}{T} + \frac{C}{T^2} + \frac{D}{T^3} + \left(E + \frac{F}{T} + \frac{G}{T^2}\right) \log \rho \tag{1.2}$$

For the conditions explored as part of this work, Figure 1.5 depicts the behavior of K_W with increasing temperature at the saturated condition.

1.3 Water-tolerant Lewis acids

Conventional synthesis with Lewis acids in organic media demanded dry or nearly-dry conditions because most conventional Lewis acids are summarily deactivated by reaction with water. Once water was recognized as a desirable reaction medium for environmental reasons, the desire for water-tolerant Lewis acids naturally developed. WTLAs are defined phenomenologically as Lewis acid catalysts that are not

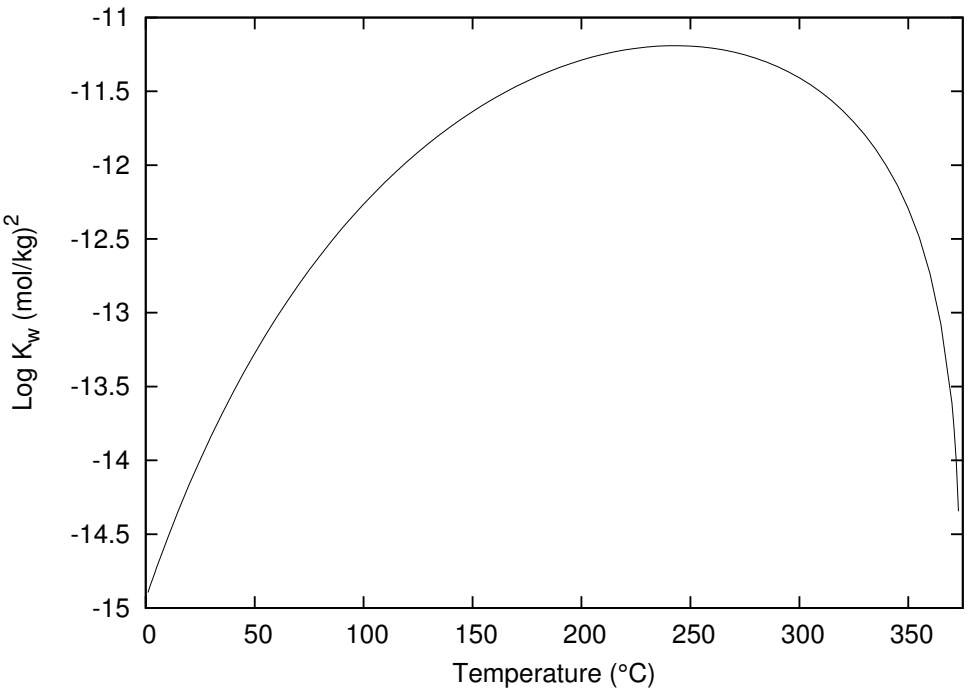

Figure 1.5: Ion product of saturated liquid water.

deactivated by the presence of water. Hence, a particular Lewis acid may show water tolerance for the purposes of one reaction, but not toward another reaction. One such example is $AlCl_3$, which is ineffective toward Friedel-Crafts alkylation in the presence of copious water [3], but is active toward the azidolysis of α,β-epoxycarboxylic acids in water [33] . For the latter reaction, the researchers believe $Al(H_2O)_6^{3+}$ to be the active catalytic species.

The reactivity of traditional Lewis acids, such as $AlCl_3$ is attributed to their willingness to accept an electron pair. Thus, the very behavior that makes Lewis acids successful, also makes them react with water, which readily presents an electron pair. Reaction with water will often leave the catalyst unavailable for reaction with the substrate.

It is thought that WTLAs work in a two-step process. First, upon addition to water, the WTLA dissociates and hydrates. Second, water molecules bonded to the metal continue to exchange during reaction. If substrate molecules are present, by

chance the metal will also interact with the substrate. [34] The substrate-metal interaction involves drawing electron density away from the active moiety on the substrate, facilitating reaction. [34]

Many reactions have been successfully carried out with WTLA. Kobayashi and Hachiya demonstrated that lanthanide triflates could catalyze aldol reactions of silyl enol ethers with aldehydes in water. [35] Of the catalysts tested by Hachiya and Kobayashi, $Yb(OTf)_3$ performed most ambirably, consistently offering high yields, usually around 80 to 94%. [35] The allylation of carbonyl compounds proceeded with allylic bromide and $In(Cl)_3$ in the presence of Al or Zn in THF/water solution. Good yields were obtained with a number of benzaldehydes. [36] $Sc(OTf)_3$ was found to catalyze the allylation of carbonyl compounds with tetraallyltin. This reaction proceeded well in both aqueous and anhydrous organic solvents. [37] Viswanathan and Li found that $In(OTf)_3$ catalyzed the coupling of alkynes with aldehydes in water at room temperature, though yields were typically less than 40%. [38] Crotti et al. were interested in the addition of lithium enolates of ketones to 1,2-epoxides, and found that $Sc(OTf)_3$ was the most active catalyst of those tested for this transformation. [39] Zhang et al. reported Friedel-Crafts hydroxyalkylation with $In(OTf)_3$ of highly activated trimethoxybenzenes in a number of solvents, including water. [40] Many other studies were carried out over the past 20 years showing the effectiveness of rare-earth metal triflates in catalyzing various nucleophilic additions (aldol, ene, cyanation, Michael), cyclization reactions (Diels-Alder), Baylis-Hillman reaction, ring-opening reactions, oxidations and reductions, rearrangements, and others. Clearly, the literature has established much potential for WTLAs.

Aside from their water tolerance, two important advantages are cited for the use of rare-earth metal triflates as WTLAs. One, only catalytic quantities of catalyst are used, in comparison to the stoichiometric equivalents of traditional Lewis acid catalysts employed for similar reactions. Most of the studies cited above use 10 mol%

WTLA catalyst or less. Two, evidence supports the reusability of these catalysts. For example, lanthanide triflates could be reused in aldol reactions (at least up to three times) with no significant decrease in yield. [35] Chen et al. found that the lanthanide triflates that catalyzed the double addition of indole to benzaldehyde could be used a second time with comparable activity to the first run. [41] Diels-Alder reactions with aqueous $Sc(OTf)_3$ reaction media reused twice experienced comparable results from all three successive runs. [42]

In summary, WTLA catalysts show promise for organic synthesis due to their demonstrable reactivity, stability toward water, and reusability.

CHAPTER II

Literature Review

> Don't work for my happiness, my brothers – show me yours – show me that it is possible – show me your achievement – and the knowledge of it will give me courage for mine. *Ayn Rand, The Fountainhead*

This chapter updates previous reviews [19, 43] on organic synthesis in high-temperature water. Studies of kinetic observables, e.g. rate constant, activation energy, frequency factor, are included, as are physical organic investigations concerned more with mechanistic pathways. However, supercritical water gasification and thermal decomposition studies are mostly neglected unless they are meant to feature some model transformation, as for example, decomposition of anisole to phenol as a model hydrolysis reaction.

2.1 Hydrogenation

Crittendon and Parsons first demonstrated the applicability of supercritical water for hydrogenation over Pd catalysts. [13, 44] Subsequently, decomposition of formic acid or formate salts was developed as a means of producing hydrogen in situ for HTW reductions. [23, 24] Poliakoff et al. investigated the reduction of simple aromatic nitro, ketone, and aldehyde compounds by the H_2 generated in situ. [24] Using HCO_2H as

the hydrogen source, nitrobenzene was hydrogenated to aniline with up to 75% yield within a residence time of around 11 seconds. Aniline was the only product observed at temperatures above 200°C. Surprisingly, formic acid provided little to no yield for the reductions of benzaldehyde and cyclohexanone. Sodium formate, however, successfully reduced benzaldehyde to benzyl alcohol in 65% yield after 19 seconds (247°C, 15.7 MPa) and reduced cyclohexanone to cyclohexanol in 28% yield in 24 seconds (250°C, 15.5MPa). The researchers surmise that CO poisoning of the stainless steel reactor surface is to blame for reaction failure with formic acid decomposition. CO was produced in much larger quantities from formic acid (31.0 mol% at 15 MPa) than from sodium formate (2.5 mol% at 15 MPa). As an alternative explanation, the researchers propose direct H-transfer from HCO_2^-, rather than hydrogenation by H_2. Unfortunately, no further work was presented to test these hypotheses, and the actual mechanism explaining these results is still poorly understood. Finally, acetophenone was successfully hydrogenated to 1-phenylethanol in 78% yield at 15.6 MPa, 250°C, 20 s of residence. A large molar ratio of sodium formate to acetophenone (at least 10:1) was needed to achieve reasonable yields. However, at these high loadings of sodium formate, no further reduction of 1-phenylethanol was observed, perhaps illustrating the typical relationship between selectivity and reactivity. [24] No added catalyst was used in this study, but the researchers suspected that the 316 stainless steel reactor wall (surface area = 5.7 cm^2, flow reactor volume = 0.23 cm^3), or stainless steel components that leached into solution were catalyzing the reaction. Though the transformations of this study proceed quickly and easily, the authors lament that the large quantity of reducing agent (HCOOH or HCOONa : substrate is as much as 10:1) limits the practicality of this procedure to bench scale preparations.

These studies of reductions with hydrogen generated in situ by decomposition reactions, present a flavor of the uncertainty found in many HTW studies regarding the activity of the reactor wall. This uncertainty is partly due to the dominance

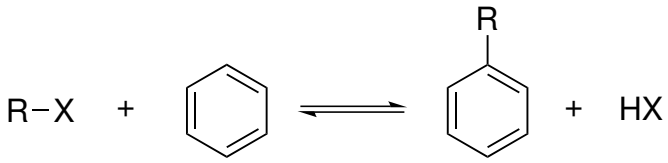

Figure 2.1: The most general representation of a Friedel-Crafts alkylation reaction.

of stainless steel as the choice material of construction for HTW reaction vessels. Experiments in other vessels, such as quartz, would help test some of the hypotheses attributing strange reaction behavior to stainless steel catalysis.

2.2 C−C Bond formation

The formation of new carbon-carbon bonds is the foundation of most synthetic routes in every chemical industry. The Friedel-Crafts reaction is likely the most important example within this class. Heck coupling is also useful, especially when Friedel-Crafts conditions cannot be tolerated. Both Friedel-Crafts alkylation and Heck coupling have been shown successful in HTW.

2.2.1 Friedel-Crafts alkylation

Friedel-Crafts alkylation is by far the most important method of attaching alkyl side chains to aromatic rings. [45] A general example of this transformation is shown in Figure 2.1.

Among the first Friedel-Crafts reactions carried out in HTW were the addition of tert-butanol to phenol and p-cresol to achieve about 20% yield in both cases after one to two days. [14] This result was promising because the reaction proceeded without a Lewis acid catalyst, but the working procedure was hardly practical for its low yields and long reaction times. Arai and co-workers built upon the promising results of Chandler et al. with a suite of investigations. [46–51] Sato et al.

showed that as much as 58% yield of o-isopropylphenol was possible at 400°C for the alkylation of phenol with 2-propanol. [46] Regioselectivity was demonstrated for the addition of propionaldehyde to phenol; low water densities at 400°C favored ortho addition. [47] High water densities seemed to increase the rate of both ortho and para substitution, but ortho-propylphenol was lost to dehydrogenation to form 2,3-dihydro-2-methylbenzofuran. Hence, the ortho/para ratio decreased with increasing water density. In a more thorough kinetic study of 2-propanol addition to phenol, the researchers again note that alkylation rates are increased with increasing water density, but this acceleration cannot entirely be attributed to $[H^+]$. [48] A study of the reverse reaction showed that the rate of dealkylation increased with increasing water density while the rate of rearrangement was independent of water density. [49] It then follows that phenol alkylation by 2-propanol to o-isopropylphenol is optimized at high water densities (0.5 g/mL). [50] Alkylation of phenol by t-BuOH at the para position increases with increasing water density; at the ortho position, it is independent of water density. [51]

Hunter and Savage demonstrated that the addition of CO_2 to a HTW reaction mixture can increase the rate of tert-butylation of p-cresol to achieve more than 10% yield of 2-tert-butyl-methylphenol in 120 minutes with CO_2 enrichment, compared to 7% yield without CO_2. [25, 52] The researchers attributed the rate enhancement to the lower pH achieved by formation of carbonic acid.

2.2.2 Heck Coupling

Palladium-catalyzed alkene-arene coupling reactions in HTW and SCW were studied by Parsons and co-workers. [13, 53] The general reaction studied was coupling of halobenzene with an alkene, as shown in Figure 2.2.

Gron and Tinsley further investigated Heck coupling of p-iodo-phenol with medium-sized cycloalkenes, producing, for instance, phenyl-cyclohexenes in 21% yield in 20

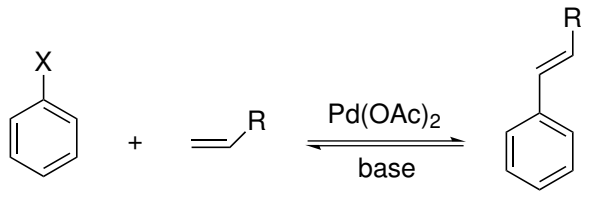

Figure 2.2: Heck coupling of a halobenzene with an alkene. [13]

minutes at 225°C at saturated liquid conditions in the presence of $Pd(OAc)_2$. [54] As is typical for Heck reactions, electron withdrawing groups on iodobenzene accelerated the reaction. Addition of LiCl decreased the yield of coupling products, but only slightly. Although salts are typically added to reaction mixtures to investigate the secondary salt effect, the researchers believe that the slight depression of yield (only 3 to 5 mol%) in this case is due to a salting-out effect, meaning that the salt simply made the starting materials, iodobenzene and cyclohexene, less soluble in water at 225°C, and therefore less able to react. Addition of $n-Bu_4NCl$ enhanced the yield of total coupling products and modified the distribution of isomers for the addition of cyclohexene to iodo-benzene. Interestingly, cyclopentene procured the least yield compared to cyclooctene, -heptene, and hexene. Coupling in DMF at room temperature typically achieved higher reactivity for cyclopentene than for the other cyclic alkenes. The authors suspected that hydrophobic effects explained the reactivity behavior in HTW.

Gron et al. went on to investigate the effects of batch reactor filling factor on the Heck coupling of iodo-benzene with cyclohexene, shown in Figure 2.3, at 225°C, [55] and observed that higher filling factors lead to increased yields. The best yield, 47%, was achieved at a water density of 0.84 g/mL (which achieved saturated liquid water at 225°C) in the presence of 1 m $n-Bu_4NBr$. This result can be explained by considering the meaning of "filling factor" for superheated water in a batch reactor. To achieve a saturated liquid phase at reaction conditions, the batch reactor must be

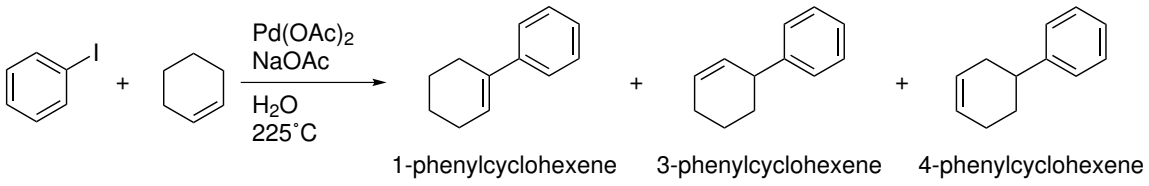

Figure 2.3: Researchers studied the Heck coupling of a iodobenzene with cyclohexene with respect to "filling factor" and ionic salts. [55]

filled at room temperature such that, given the expansion of water with increasing temperature and the thermophysical properties of water, the liquid phase almost completely fills the reactor at the reaction temperature. If the "filling factor" is less than what is needed to achieve the saturated liquid condition, then two situations are possible. If the filling factor is only slightly less than needed for saturated liquid water, then water will vaporize until the pressure within the reactor is high enough to keep the remaining volume of water within the liquid phase. This leads to complicated phase behavior, as reactants and products will partition between liquid and vapor phases, making the results more difficult to interpret correctly. If the filling factor is much less than what is needed for saturation, then the aqueous portion of the reaction mixture will be entirely in the vapor phase.

Finally, the researchers observed that the presence of tetrabutylammonium bromide altered the product isomer ratio from 8:31:62 for 1-:3-:4-phenylcyclohexene without the additive to 55:16:28. This effect is also seen in organic solvents. [55]

Zhang et al. investigated non-Pd-catalyzed Heck couplings in SCW with the more reactive olefin, styrene, which polymerizes somewhat during reaction. [56] In the presence of weak base potassium acetate at 650 K and 25 MPa, 55.6% yield of stilbene was achieved after 10 minutes with moderate selectivity: E:Z :: 45:10. The researchers found that when stronger bases such as K_2CO_3, Na_2CO_3, $NaHCO_3$, or NaOH were used, hydrogenation of iodo-benzene to phenol was the chief transforma-

tion. The coupling reaction yielded the same E:Z stereoselectivity regardless of base. Increasing water density accelerated the reaction, in accord with expectations for a simple bimolecular reaction with a negative volume of activation. [64] Water density, however, has no effect upon the E:Z selectivity. Hence, it was hypothesized that the transition state structure for E versus Z stilbene must have similar partial molar volumes. Two postulates regarding the role of water in the reaction were offered by the researchers. One is formation of carbanion by proton abstraction for the beta C of styrene. The other is a water-catalyzed proton transfer and Ar-sp2 C bond formation through an 8-membered ring involving two water molecules. [57]

2.2.3 Nazarov cyclization

Leikoski et al [58] discovered that the Nazarov reaction of trans,trans-dibenzylidene acetone, which normally produces 3,4-diphenyl-2-cyclopentanone in conventional media (acidic, chlorinated solvent at elevated temperatures), instead produces the abnormal [59, 60] Nazarov cyclization product 2,3-diphenyl-2-cyclopentenone in as much as 38% yield in CO_2-enriched HTW. The unusual product is thought to arise because of water or CO_2 addition to the intermediate oxyallyl cation formed after ring closure. Direct deprotonation of the intermediate leads to the ordinary 3,4-disubstituted-2-cyclopentanone. Without CO_2, yields of 2,3-diphenyl-2-cyclopentenone are only around 20%.

2.3 Condensation

Eckert et al. investigated the Claisen-Schmidt condensation of benzaldehyde with 2-butanone. [17] Most asymmetric ketones would attack benzaldehyde with the alpha carbon attached to the most hydrogens, but 2-butanone behaves differently as both but-2-en-ol and but-1-en-2-ol may add to benzaldehyde to form 4-phenyl-3-methyl-3-buten-2-one and 1-phenyl-1-penten-3-one respectively. See Figure 2.4. Experiments

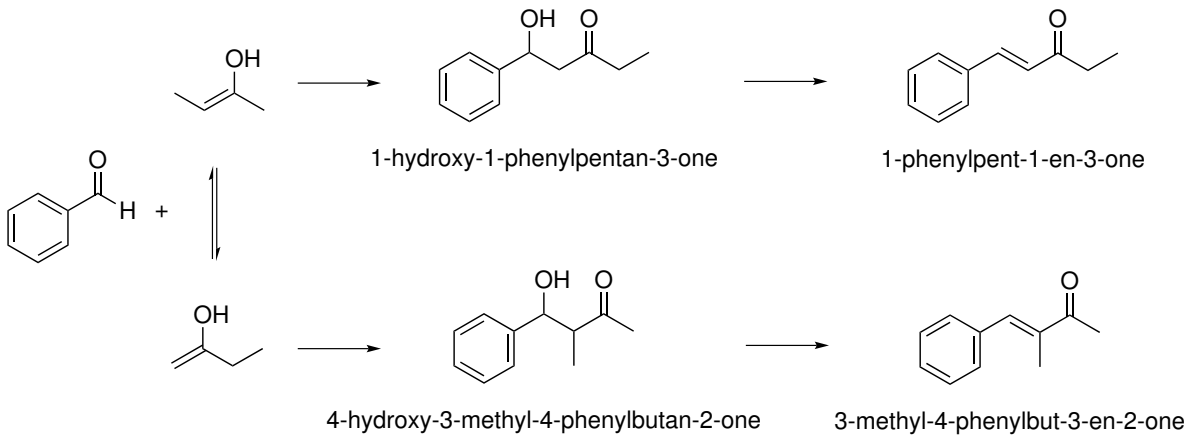

Figure 2.4: Claisen-Schmidt condensation of benzaldehyde with 2-butanone yields a pair of enones through a respective pair of ketol intermediates. [17]

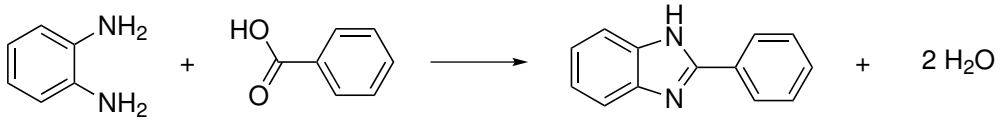

Figure 2.5: Condensation of 1,2-phenylenediamine with benzoic acid yields 2-phenylbenzimidazole. [61]

were carried out between 250°C and 300°C, where the ion product of water is roughly 10^{-11} $(\text{mol/kg})^2$. Condensation to both products occurred at each temperature tested. Interestingly, selectivity of the butenone was independent of temperature over the range tested, remaining between 10 and 15%, while selectivity of the pentenone decreased with increasing temperature. Other products included second additions and oligimerization products. As expected, addition of HCl increased the yield of butenone after 15 minutes from 0% without acid to 30%. The rate of formation of pentenone also increased slightly from 1% to 10%, as did the formation of side products.

Poliakoff et al. developed a means of synthesizing simple benzimidazoles in near- and supercritical water from a 1,2-phenylenediamine and benzoic acid. See Figure 2.5. [61]

This reaction is normally carried out under highly acidic conditions often coupled

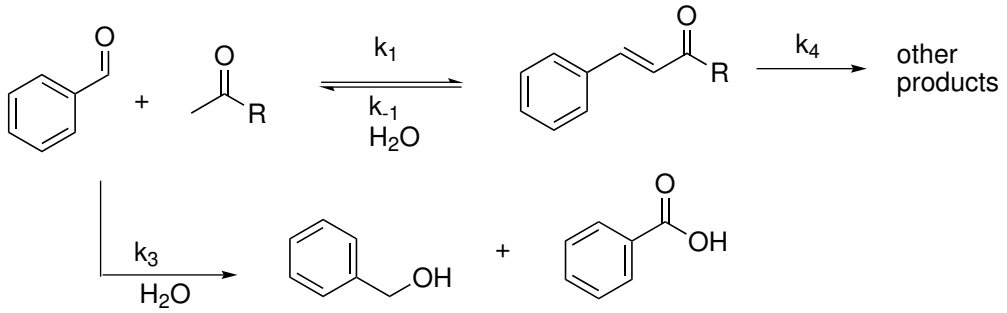

Figure 2.6: Condensation of benzaldehyde with ketones yields α, β-unsaturated ketones such as benzalacetone and chalcone. (adapted from [20])

with great thermal excitation. Reaction in HTW, the researchers found, removes the need for acid and simplifies the purification while still achieving good yields (near 90%) in reasonable reaction times (4 hours) when operating at 350°C and 21.7 MPa. 1,2-phenylenediamine was then reacted with various simple aliphatic carboxylic acids, diacids, and aromatic dicarboxylic acids at temperature ranging from 210 to 350°C for 1 to 4 hours, depending on reactant stability and reactivity. Moderate to excellent yields were achieved. [61] This work was followed by synthesis of phthalimide derivates in a 1:1 (v/v) ratio of water to ethanol between 260 and 380°C, 1240-4800 psi. [62]

Continuing with condensation reactions, Comisar and Savage [20] investigated the synthesis of benzalacetone from benzaldehyde and acetone, and the related synthesis of chalcone from benzaldehyde and acetophenone. Maximum yields achieved were 24% for benzalacetone after 5 hours at 250°C, and 21% for chalcone after 15 hours at 250°C. A reaction network, Figure 2.6, was proposed to account for the various products formed. Data was fit to the proposed model, and the relevant kinetic parameters determined. [20]

A study of the effects of pH upon this reaction was also carried out by adding HCl or NaOH to the reaction vessel. Rate acceleration was observed in both cases, but more so with added acid. At pH 4.25, after one hour at 250°C, yield of benzalacetone was 16%, compared to 6% with no added acid.

A portion of the Comisar paper treated the degradation of benzalacetone via Michael addition followed by intramolecular Meerwein-Pondorf-Verley reduction followed by retro aldol condensation to form benzaldehyde and acetaldehyde. Lu et al. were very interested in this degradation reaction and studied the related retro aldol condensation of cinnamaldehyde to benzaldehyde and acetaldehyde. [63] They found that the addition of NH_3 to the reaction mixture promoted the reaction rate.

The dehydration of 1,4-butanediol to form tetrahydrofuran is an industrially important reaction whose ease may be improved significantly by HTW. The most common process, the Reppe process, is typically carried out at temperatures above 100°C, pressures near atmospheric, and with catalysis by either mineral acids which must later be neutralized, or by aluminum silicates or ion exchange resins which must be regenerated. Use of HTW may minimize the cost of waste removal for this process. Richter and Vogel studied the reaction in HTW in a flow reactor between 300 and 400°C and achieved selectivities of nearly 100%. They showed that the correlation between Kw and reaction rate is weak. [64] Nagai et al. [65] showed that alone, the Kw of water could not explain the reactivity of 1,4-butanediol entirely. Hence, the water-induced pathway must be significant in neutral water. Hunter et al. found that the addition of CO_2 to the reaction mixture did not increase yield as significantly as one would expect from an acid-catalyzed mechanism. [21] They conducted experiments over a wide range of pH values (between 2 and 10) with the addition of HCl or NaOH at 200, 250, and 300°C, and proposed that under acidic conditions, H+ is the dominant proton-donor, but under neutral or basic conditions, H_2O serves in this role. Further, under acidic or neutral conditions, the protonated oxonium ion of tetrahydrofuran is deprotonated predominantly by water; whereas under basic conditions, OH- serves this role. [21] Of course, the exact pH of neutral water changes with temperature, as does the onset or cut-off of specific-acid catalysis for butanediol dehydration. Accounting for these effects, Hunter et al. explain kinetically why

addition of acid increases the rate more at lower temperatures than a commensurate addition of acid at higher temperatures.

2.4 Hydrolysis

Researchers studying benzoic acid ester hydrolysis in near-critical water demonstrated autocatalysis with an inflection point in a plot of the conversion of n-propyl benzoate to benzoic acid versus time. [66] The Hammett reaction constant ρ was determined to be nearly zero, signifying that the transition state of the rate-determining step maintains the charge of the ground state. This is consistent with acid-catalyzed hydrolysis of esters, and is contrary to what is expected if the reaction were base-catalyzed. Hence, the ordinary AAC2 mechanism that is normally expected for acid-catalyzed hydrolysis also dominates in near-critical water.

Eckert et al. later published a more complete study with experiments converting methoxy and ethoxy benzene derivatives to the alcohols. [67] Hydrolysis of anisole may proceed by three mechanisms: acid-catalyzed, base-catalyzed, or S_N2 addition. A Hammett plot analysis produced a positive Hammett reaction constant, ρ, which is inconsistent with an acid-catalyzed mechanism. This is in agreement with Klein et al. [68] who more carefully decoupled solvent and substituent effects in their Hammett plot analysis to determine $\rho = 1.8$. Eckert et al. basified their reaction medium to estimate the rate of the base-catalyzed pathway. With this parameter known, the rate of S_N2 addition was then determined. Nucleophilic attack by water was found to be the dominant pathway for hydrolysis of anisole in neutral HTW, mainly because the concentration of water is much greater than the concentration of hydroxide ions. The earlier analysis of Klein et al. also favored the S_N2 pathway.

The work by Klein et al. and Eckert et al. improved the physical understanding of how anisole hydrolysis proceeded in HTW. It is important to note, though, that Hammett plots only allow one to conclude whether a particular mechanism with a

particular rate-determining-step is either consistent or inconsistent with an experimentally determined ρ value. The explaining-potential of a ρ value is limited in this way because all a Hammett plot really measures is the accumulation or depletion of electron density in the transition state relative to the ground state. This is an important distinction to make because the expected ρ value for a particular mechanism changes based on which step is rate-determining.

Nitrile hydrolysis was first studied in HTW by Iyer and Klein, who showed that butyronitrile autocatalytically hydrolyzed first to butanamide and then to butyric acid. [69] Similarly, acetonitrile was shown to hydrolyze first to acetamide and then to acetic acid in SCW. [70, 71] Kinetic observables for the hydrolyses of benzonitrile, benzamide, and iminodiacetonitrile were also studied in HTW. [72, 73]

In a large study of the hydrolysis of dibenzyl ether, benzyl t-butyl ether, methyl t-butyl ether, methylbenzoate, and diphenylcarbonate in HTW, both with and without added acid or base, it was discovered that the apparent reaction order in [H+] did not exceed 0.2 for any example ether, ester, or carbonate. [74] This was contrary to the widespread notion that such hydrolysis reactions were specific-acid catalyzed in HTW, a scenario in which the apparent reaction order in [H+] is expected to be one. This result is consistent with catalysis by water molecules.

Oshima, Watanabe, and Ogawa studied the synthesis of polyorganosiloxanes from alkoxysilanes by hydrolysis and condensation without added catalyst. [75] At 300°C, an average MW of 1550 was achieved within 15 minutes. The effects of monomer to water ratio, pressure, temperature, and substrate upon MW were broadly studied. The authors believe that supercritical water could be shown to be an advantageous medium for the formation of polyorganosiloxanes. [75]

The hydrolysis of 6-aminocapronitrile followed by cyclization to form ϵ-caprolactam was studied in HTW. [76] Caprolactam finds importance as an intermediate in the production of Nylon-6. Under the proper conditions, conversion of 6-aminocapronitrile

reached 94% and yield of ϵ-caprolactam reached 90% in under 2 minutes in a flow reactor (400°C, 400 bar, 30% by volume initial concentration of starting material). The researchers studied the effect of temperature, pressure, and residence time upon yield and selectivity.

2.5 Rearrangements

The Beckmann and pinacol rearrangements occur in SCW without any added catalyst. Of the temperatures examined, Beckmann rearrangement of cyclohexanone-oxime into ϵ-caprolactam occurred fastest at 380°C, 22.1 MPa with an observed first-order rate constant of 8160 ± 750 s^{-1}. Observed first-order rate constants for pinacol rearrangement of 2,3-dimethyl-2,3-dihydroxy-butane to 3,3-dimethyl-2-butanone were determined by IR measurements to be on the order of tens of thousands of s^{-1}. The researchers attribute the observed rate enhancements for these systems to an increased local proton concentration about the substrates. A theoretical study of neopentyl and pinacol rearrangements showed that the mechanism does not involve the formation of carbocations. [77] In particular, pinacol rearrangement of the model substrates 2,3-dimethyl-2,3-butanediol and 2,3-diphenyl-2,3-butanediol proceeded by a concerted process where proton transfer was promoted by a H-bonded relay. The reaction was modeled with interaction with 12 water molecules and one hydronium molecule. [77]

A quantum mechanical/molecular mechanical method calculation with energy representation was carried out to study the thermodynamics of Beckmann rearrangement of acetone oxime in the supercritical state. [78] The activation energy was reduced by 12.3 kcal/mol if two molecules of water participated in the reaction. Also, the transition state was stabilized in comparison to the ground state by 2.7 kcal/mol with the participation of two water molecules. [78]

In their study of the rearrangment of benzil, Comisar and Savage [79] observed diphenylketene, benzophenone, benzhydrol, and diphenylmethane, but not the ex-

pected product, benzilic acid, which was presumed to react away more quickly than it was formed. It was discovered that while base catalysis is the sole mechanism for the rearrangement in the conventional water-dioxane system at 100°C, the reaction is acid, base, and water-catalyzed in HTW, depending on pH. New mechanisms for the acid- and water-catalyzed routes were posited to account for this behavior. Further, selectivities to rearrangement products and decomposition products were pH dependent. While decomposition was favored at a near-neutral pH, rearrangement rates were lowest at pH 3 and increased with increasing pH. A later study [80] of the benzil-benzilic acid rearrangement with no added catalyst tested the proposed kinetic pathways by first reacting proposed intermediates to verify an overall reaction network, and by fitting kinetic data to the proposed reaction network with favorable results.

The work of Wang et al. confirmed many of the observations of Comisar and Savage in their study of benzil rearrangement. They studied the oxidation of benzhydrol and benzoin in pure HTW. [81] After 3 hrs at 460°C, benzhydrol was nearly completely consumed (>99% conversion) to benzophenone (63% yield) and diphenylmethane (10% yield). At 440°C with no water present, pyrolysis of benzhydrol gave a 48% yield of benzophenone and a 53% yield of diphenylmethane, likely through disproportionation. The higher ratio of oxidation product to reduction product achieved in the presence of water leads the researchers to believe that oxidation of benzhydrol occurs through some mechanism other than disproportionation in HTW. Hydrogen gas was detected in some experiments. Hydrogen evolution is consistent with the proposed hydrogen-bonded 8-membered ring transition state structure shown in Figure 2.7, which was proposed by Takahashi et al. [81]

Benzoin reacted more readily than benzhydrol to form a mixture of products: benzil, benzyl phenyl ketone, benzaldehyde, benzhydrol, benzophenone, and diphenylmethane. In their studies, the researchers were careful to exclude molecular oxygen

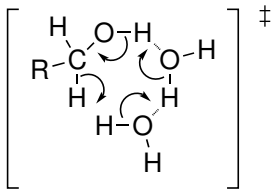

Figure 2.7: A transition state structure consisting of an eight-membered ring with two hydrogen-bonded water molecules may explain hydrogen evolution. (adapted from [81])

from their reactors by purging the water with nitrogen and sealing the reactors under nitrogen.

2.6 Hydration/Dehydration

Akiya and Savage [82] found that cyclohexanol dehydration to the alkene occurred without catalyst present. They determined that two pathways for cyclohexanol dehydration are probable in HTW: unimolecular and bimolecular elimination. Bimolecular elimination seemed to be the only mechanism at work at low temperature of 250 and 275°C. However, increasing the temperature of the system beyond 275°C allowed for the formation of methylcyclopentanes, which form by rearrangement of cyclohexyl carbocation. This suggested unimolecular elimination. Increasing the water density under supercritical conditions (T=380°C) further improved the yields of methylcyclopentanes, suggesting further enhancement of E1.

The E2 mechanisms requirement of planarity allows for only two possible transition states, the most unfavorable of which is synperiplanar elimination from the high-energy and ephemeral boat configuration. The lower energy antiperiplanar elimination from the chair structure with oxygen axial constitutes a configuration which costs roughly 0.5 kcal/mol, which is certainly manageable in HTW.

Hunter and Savage showed that addition of CO_2 to HTW could increase the reaction rates of acid-catalyzed reactions such as cyclohexanol dehydration to cyclohexene.

[52] The addition of 8 mg dry ice to cyclohexanol in saturated HTW at 250°C for 30 min increased the yield of cyclohexene from 10 ± 3% to 22 ± 2%. At 275°C, addition of 10 mg dry ice increased yields from 7 ± 3% to 18 ± 4%. [52]

The dimerization of hemiterpene alcohols prenol and 2-methyl-3-buten-2-ol to form a suite of monoterpene alcohols was carried out without added catalyst in HTW. The most promising result from this study was the formation of linalool, geraniol, nerol, lavandulol, and alpha-terpineol in 9, 10, 1, 24, and 10 % yield respectively at 450°C and 40 MPa in under five seconds. [83]

The synthesis of phthalimide derivatives was studied in a batch reactor in HTW. [62] Nucleophilic attack by an amine onto o-phthalic acid followed by ring closure yielded a substituted phthalimide plus two molecules of water. Rather than cyclization, bis-amidation may occur, but would be followed by intramolecular deamination to yield the same substituted phthalimide. Formation of an ammonium salt with any of the carboxylic acids detracted from phthalimide yield. Purification of phthalimides is normally done by recrystallization from an ethanol and water solvent system. With the intent of developing a reaction/purification process, the researchers thus chose an ethanol and water mixture as the solvent system. Various ratios of water to ethanol were tested using N-phenylphthalimide and N-benzyl-phthalimide as model nucleophiles. A one-to-one volume ratio of water to ethanol gave high purity crystals in good yields for both substrates, and was thus chosen as the solvent system for most of the further experiments with different substrates. [62]

A variety of amines were tested, all with reaction times between 5 and 12 minutes. Other functional groups (halogen, nitro) and heteroaromatics (pyridine) were found to perform poorly in this reaction due to increased salt formation with the acid, or lack of stability at reaction conditions. The researchers expect such problems to persist for other functional groups (cyano, ester, ether, etc.). Three amino acids were applied as amines 4-aminobenzoic acid, L-phenylalanine, and glycine and all were

decarboxylated in the phthalimide product. [62]

Aida et al. studied the dehydration of D-glucose in high temperature water at 40, 70, and 80 MPa. [84] Previous work elucidated the major products and reactive pathways of sugar molecules in HTW. Aida et al. added to these studies by focusing on changes in yield and selectivity due to changes in pressure at subcritical (350°C) and supercritical (400°C) temperatures. Although yields of the desired product 5-hydroxymethylfurfural never rose above 8%, it was concluded that high temperatures and pressures and short residence times increased the selectivity of 5-hydroxymethylfurfural. Short residence times are needed to prevent further reaction to 1,2,4-benzenetriol. High temperatures and pressures with long residence times, of course, increase yields of 1,2,4-benzenetriol and furfural, which is a decomposition product of 5-hydroxymethylfurfural. The researchers suggested a new mechanism for D-glucose decomposition which they feel better represents their product distribution vs time data. [84]

Aida et al. continued their work with D-fructose and compared the decomposition products of D-glucose with those of D-fructose. D-fructose gave higher yields of 5-hydroxymethylfurfural while D-glucose gave higher yields of furfural. The latter was contrary to expectations based on the current reaction pathways in the literature, so another reaction scheme was proposed. [85]

Researchers [86] have found HTW a useful medium for forming cyclic dipeptides such as cyclo(Gly-Gly) by the dehydration of linear dipeptides in HTW at 240-300°C and 20 MPa. Hydrolysis of the linear dipeptides formed amino acids. The cyclic peptides could also hydrolyze back to the linear dimer. [86]

The conversion of propylene glycol to 2-methyl-2-pentenal was studied in HTW at 300°C with and without salt additives. Without additives, the reaction yielded 1.8wt% aldehyde in two hours. In the presence of 1wt% $ZnCl_2$, 59wt% 2-methyl-2-pentenal was produced. No reaction took place with the addition of Na_2CO_3.

Presumably, the transformation begins with dehydration of propylene glycol to propionaldehyde. Aldol condensation with another propylene glycol molecule produces 3-hydroxy-2-methyl-pentanal, which itself undergoes dehydration to 2-methyl-2-pentenal. [87]

2.7 Elimination

The thermal energy of HTW makes it an attractive medium for decomposition reactions. Although total decomposition is not covered in this review, some decomposition reactions are productive of small molecules. In particular, there is a trend to use HTW for producing amino acids and organic acids from waste protein streams as from the seafood industry in Japan. [88] Dunn et al. [89] studied the decarboxylation of various aromatic carboxylic acids in contribution to the use of HTW in the purification and synthesis of aromatic diacids. Benzoic acid was the most stable aromatic acid tested. Kinetic analysis revealed that terephthalic acid and trimellitic anhydride decarboxylated with autocatalysis. The CO_2 formed during decarboxylation formed carbonic acid in solution which lowered the pH of the reaction medium and catalyzed further decarboxylation. Fu et al. studied the kinetics of the hydrothermal decarboxylation of pentafluorobenzoic acid and quinolinic acid and determined the activation energies for these processes. [90] At the temperatures investigated, 150°C or cooler, only decarboxylation products were observed; dehalogenation products were not detected.

Fraga-Dubreuil et al. studied the oxidative decarboxylation of benzoic acid to phenol over heterogenous catalysts (NiO, CuO, Carulite, MnO_2 and Al_2O_3) in HTW in a flow reactor. [91] Carulite 300 was determined to be the best catalyst of those tested for the experimental conditions explored. As much as 65% yield of phenol can be achieved at 134 minutes with this catalyst (340°C, 14 MPa, in the presence of 18 mol% NaOH), but activity decreases substantially shortly thereafter. However, after

the catalyst was regenerated with oxygen, which was fed to the reactor in the form of hydrogen peroxide, yield rebounded to a respectable 70%. Without NaOH, which forms the promoter sodium benzoate in situ, the highest yield observed was only 46%. The researchers also investigated temperature, pressure, and oxygen addition methods. One drawback of the approach is organic material adsorbs to the catalyst and oxidizes to form CO_X gases during catalyst regeneration with O_2 (H_2O_2).

The decarboxylative oxidation of benzoic acid to phenol was pursued for its potential in improving the Dow Process, which produces phenol on the industrial scale in two stages. The first converts toluene to benzoic acid; the second, benzoic acid to phenol. Recently, other researchers have produced phenol in 20% yield by direct oxidation of benzene. [91, 92]

2.8 Partial oxidation to form carboxylic acids

First studied by Holliday et al. [93], partial oxidation of alkyl aromatics to form carboxylic acids is one of the most well-studied systems in HTW. In particular, the oxidation of p-xylene to form terephthalic acid has received a great deal of research attention for its success and industrial significance. [26, 94, 95] For example, Dunn and Savage explored the effects of various process variables upon the yield and selectivity of terephthalic acid from p-xylene. [26] Of seven different catalysts tested ($MnBr_2$, $CoBr_2$, Mn/Co/Br, Mn/Ni/Zr/Br, Mn/Co/Hf/Br, Mn/(OAc)/Br, and Mn/Hf/Br), $MnBr_2$ produced the highest yield of terephthalic acid (49+/-8%). [26, 27, 95] This was a peculiar result because Mn/Co systems delivered higher yields than $MnBr_2$ alone in acetic acid reactions. Other researchers confirmed that $MnBr_2$ achieved better yield and selectivity than $NiBr_2$ and $CoBr_2$. [96]

Temperatures between 250 and 400°C were tested. At 250°C, yields were low, but many intermediates were produced. At 350°C, decarboxylation destroyed a significant portion of the terephthalic acid. The best yields were delivered at 300°C. Experiments

in a 440-mL autoclave reactor allowed use of air as the oxidant and quantification of CO and CO_2 yields. An 80% yield of terephthalic acid was demonstrated at 300°C; yields at both lower and higher (including supercritical) temperatures were much lower. [27] Osada and Savage [97] discovered that the manner of oxygen addition significantly affected p-xylene conversion and terephthalic acid selectivity. Small, quick, discrete bursts of oxygen addition lead to high selectivities (>90%) of terephthalic acid, while continuous oxygen feed did not. In their experiments, Osada and Savage also used a much higher loading of p-xylene (0.2 mol/L) than was previously used in research on this system (typically less than 0.05 mol/L).

Dunn and Savage examined the economic and environmental impact of the terephthalic acid synthesis in HTW and SCW. [28] They compared four different HTW/SCW plants with the conventional acetic acid system. The four hypothetical plants differed by reactor temperature and pressure and by the presence or absence of air separation. The HTW process (300°C) appeared to be superior to the SCW process, and competitive with the existing technology, which uses acetic acid as the reaction medium. These results were encouraging, as they demonstrated the potential feasibility of HTW in productive industry.

Additional work has been done on the oxidation of other alkyl-substituted benzenes, naphthalenes, and pyridines to the corresponding acids. [2, 91, 96] A breadth of aliphatic aromatics of varying sterics and electronics underwent oxidation to the acid derivative, showing that the synthesis was general, though usual nuances were revealed. For example, lower yields are observed for m-xylene oxidation (66%) than for p-xylene (90%) because there is no resonance stabilization of the radical intermediate at the meta position as there is for oxidation at the ortho and para positions. [2]

Partenheimer et al. used extended X-ray absorption fine structure (EXAFS) and X-ray absorption near edge structure (XANES) spectroscopies to study the coordina-

tion geometry of $MnBr_2$ solutions and explain the importance of bromide concentration for this reaction. [98] Under dilute ambient conditions in water, Mn(II) was octahedral and fully hydrated with six molecules of water. Upon introducing a solution of 1.0 m or less $MnBr_2$ to the supercritical condition, the octahedral $[Mn(II)(H_2O)_6]_2^+$ transformed into the tetrahedral $[Mn(II)(H_2O)_2(Br^{-1})_2]$. An excess of Br^{-1} ions led to more Br^{-1} ions occupying the first solvation shell and contact ion pairs with Mn, and the coordination number of water decreasing proportionally. Further, acetate deactivated the Mn catalyst through the formation of insoluble MnO. [1]

2.9 C−C Bond cleavage

Bisphenol A decomposed in HTW to form first equimolar amounts of phenol and p-isopropenylphenol. [99] The latter product, which is the desired one in this transformation, either hydrated to acetone and phenol or hydrogenated to p-isopropylphenol. Bisphenol A decomposition in HTW was first-order in bisphenol A and occurred by specific acid, specific base, and general water catalysis. A three-parameter model fit to experimental data based on a base-catalyzed mechanism portrayed the data well. Using their mechanistic understanding of this transformation, Hunter and Savage explained the reactivity observed for other biaryl groups linked by methylene bridges. [22] Savage and co-workers also modeled the decomposition of bisphenol E in HTW, which primarily produced phenol and 4-vinylphenol, the latter of which further reacted to form 4-ethylphenol. [100] Vinylphenol oligomers were also suspected.

2.10 H-D Exchange

The deuterating ability of high-temperature deuterium oxide was recognized early on [101, 102] and efforts continue to exploit its potential. Studies have focused on deuteration of 2-methyl-naphthalene, eugenol, resorcinol, and phenol. [103–105]

While it was well known that the ortho and para positions of phenol were deuterated upon heating [106], it was found that the meta position could also be deuterated in supercritical deuterium oxide. [105]

The kinetics of hexane deuteration were studied in supercritical water at 380 and 400°C with acid catalysis by DCl. In contrast with the known pathway for deuteration in magic acid, no evidence was seen for hydride abstraction in supercritical D_2O; carbocation rearrangement products were not found, nor was hydrogen gas evolution detected. Hence, it was concluded that hydride abstraction to form carbocations either does not occur at all, or is too slow to be measured by the applied experimental procedure. [107] Superacids, such as magic acid, are typically used for the deuteration of alkanes. [106]

2.11 Amidation

1-Hexanol and acetamide formed N-hexylacetamide in 75% yield after 10 minutes at 400C without catalyst by amination of 1-hexanol followed by amidation. [108] This constitutes a new method of producing amides from primary alcohols. Upon further study of the reaction mechanism, the researchers determined that yield could be increased further with the addition of ammonium acetate. [109]

2.12 Conclusions

A wide variety of transformations have been demonstrated under hydrothermal conditions. In particular, antithetical reaction pairs – such as C-C bond cleavage and C-C bond forming reactions – demonstrate the general breadth of possible reaction mechanisms. Most of the transformations studied were done without catalysts. The major exceptions being Heck coupling with a Pd catalyst in the presence of base, and aryl methyl carboxylation reactions using catalysts such as $MnBr_2$. Hence, it is

perhaps no surprise that most of these transformations feature rates and yields that are uncompetitive with traditional techniques. The general application of catalysis in conjunction with HTW could vastly improve the appeal of HTW. Our work will help fill this gap by demonstrating the potential of water-tolerant Lewis acids (WTLA), $In(OTf)_3$ in particular, in vastly improving the rates and yields of organic reactions under hydrothermal conditions.

CHAPTER III

Experimental Methods

> We are what we repeatedly do. Excellence, therefore, is not an act but a habit.
>
> *Aristotle*

This chapter describes the general method used for all experiments, including dominant variations. It covers each step of a complete experimental procedure and is written to provide the reader with the ability to essentially repeat experiments, if ever some dark possession compelled him to do so. Most, if not all, of these procedures experienced multiple revisions. What is presented below is the most robust procedure to date. Care was taken to reject data when poor experimental procedure compromised the integrity of the results. For example, early experiments were not quantified with matrix-matched calibration standards. Later, matrix-matching was found to be critical, especially for high concentration samples of some analytes ($\geq$ 5 to 8 mM substrate, depending on the compound's hydrogen-bonding ability). The early data collected without matrix-matching was rejected. To take another example, some experimenters did not thoroughly rinse their reactors with solvent during the reactor unloading process. They may have used three washes instead of eight. With this procedure, the experimenter would sometimes collect 90% or more of the initial reaction material and sometimes not. Rather than reject all of the data collected by

this procedure, we only rejected the data with mole balances that showed a loss of more than 10 mol% of the initial moles loaded, and noted for future reference that eight washes with solvent are necessary for optimal recovery.

3.1 Materials

The reactants and solvents used in this study were all commercially available and were used as received. The purity was always ≥95% and was usually ≥98%. Solvent grade was always reagent or better. The water employed, which will be referred to as "diH_2O", was deionized and treated by reverse osmosis prior to use. Appendix A contains more detailed information regarding the source and purity of individual compounds.

3.2 Catalyst solution preparation

All the WTLA catalysts used in this work are hygroscopic. Hence, the pure solid catalysts are only handled in a glovebox. Deliquescence is rapid in a humid environment, and can occur quickly in a seemingly dry environment.

For the purpose of loading 590-μL reactors with about 5 μmol catalyst, a mass of catalyst corresponding to roughly 250 to 350 μmol catalyst was weighed into a 10-mL volumetric flask in a glove box. For $In(OTf)_3$, this corresponds to about 0.12 g. Outside the glovebox, the 10-mL flask is filled to volume with di H_2O. The resulting solution concentration allows the researcher to fill each reactor with 100 to 200 μL solution to achieve the desired catalyst loading of 5 mol% relative to substrate, while maintaining a high level of accuracy.

3.3 Loading reactors

This work made use of four distinct kinds of reaction vessels. The most commonly used vessel comprised a 1/4″ Swagelok port connector sealed at both ends with 1/4″ caps. The internal volume of this vessel is estimated to be 590 μL by a geometric analysis of manufacturer-provided dimensions. Some experiments made use of a larger version of this reactor, produced with a 1/2″-port connector and two 1/2″ caps, and having a calculated internal volume of approximately 4.1 mL.

The small quartz reactors used in this study had an internal diameter of 2 mm and outer diameter of 6 mm, per the manufacturer's specifications. The 2-mm wall thickness provided a maximum allowable pressure of 2300 psig or 150 atm for a reactor of good structural integrity. This pressure was always lower than the estimated reaction pressure for experiments in this study, based on the thermophysical properties of water. The length of these capillary quartz reactors (18.8 cm or 7.4 in) was chosen to nominally match the internal volume of the 1/4″ stainless steel reactors. Swagelok's own manufacturer testing results shows that both the 1/4″ and 1/2″ reactors are manufactured to withstand temperature cycling between room temperature and 377°F (192 °C) for at least 1,100 cycles and still pass room-temperature pressure-decay tests at 4000 psig (270 atm). Our experiments were somewhat more demanding than this because we require the Swagelok tube fittings to maintain pressure while heating, at elevated temperatures and pressures, and during cooling. We find that our reactors do not last 1,100 reactions, but they will usually last for several dozen reactions. Reasons for early reactor failure include over-tightening, which deforms the ferrules that provide the high-pressure seal, mis-threading, and rounding off the hexagonal nut, both of which make it difficult for the experimenter to properly tighten the reactor.

The large quartz reactors had an inner diameter of 6.91 $\pm$ 0.03 mm and an outer diameter of 8.9 $\pm$ 0.03 mm. These dimensions and their associated errors were deter-

mined by measuring 14 different reactors 6 times each per dimension using calipers accurate to 0.01 mm. Their maximum allowable pressure was estimated as 300 psig, or 20 atm for a structurally un-compromised vessel. The pressure of saturated liquid water at 200°C is 15 atm. At 225°C, it is 25 atm. Hence, for experiments carried out at the saturated liquid condition, the maxiumum allowable pressure of quartz reaction vessels corresponds to a maximum allowable temperature. Given the thermophysical properties of saturated liquid water above its normal boiling point, the maximum allowable temperature of the 6.9-mm ID quartz reactors is about 213°C. At 213 °C, the pressure of saturated liquid water is very nearly 20 atm. There is a safety factor built into the maximum allowable pressure estimate; we were able to collect data in 6.9-mm ID quartz reactors up to 225°C. However, at 250°C, where the pressure required for saturated liquid water is almost 40 atm, the reactors uniformly failed catastrophically. Length, nominally 4 in., was chosen to match the volume of the $1/2''$ stainless steel Swagelok reactors.

The total fluid volume to be added to each reactor was determined by assuming all the reaction mixture to behave thermodynamically like water, and then choosing the total volume that achieved a 95%-full reactor at the reaction temperature, as expressed in Equation 3.1. Filling the reactors to only 95% of their nominal volume served as a safety net against reactor over-pressurization. If the reactors are too full, over-pressurization can lead to the loss of reactor material. Because there is reactor-to-reactor variation in internal volume, and because the thermodynamics of the system are somewhat different from the case of pure water, over-pressurization was a common event. For particularly problematic systems, when all other reasons for reactor leaking were ruled out by experiment, the volume added to the reactors was scaled back from 95%, usually to 90%.

$$V^{\text{total}}_{\text{room temp}} = 0.95 * V^{\text{total}}_{\text{rxn temp}} \frac{\rho_{\text{rxn temp}}}{\rho_{\text{room temp}}} \tag{3.1}$$

Some care should be taken when loading reactors. For liquid organics loaded into Swagelok reactors, water is loaded first, followed by catalyst solution, followed by liquid organic substrate. This procedure prevents contamination of the catalyst solution, and affords the opportunity to seal the reactors as soon as the organic is added. For very volatile substrates, such as anisole and 1-phenyl-1-propyne, it is critical to minimize the time between loading organic and sealing the reactor so as to minimize the loss of material due to evaporation. When needed in the reaction vessel, nonvolatile solid material, such as stainless steel powder or quartz particles, is added first. This allows the experimenter to more smoothly adjust the amount of solid material added, without time consuming revisions in cases of over-shooting a target amount.

The quartz reactors are all fashioned from a hollow tube, originally opened at both ends. One end is sealed in a 1400-K flame to form a test tube. When the vessel has cooled, reaction material is loaded. Then the test tube is sealed at the other end by a 1400-K flame at the desired length to form a closed capillary vessel.

When loading quartz reactors, catalyst solution is added first followed by water. Liquid organic is injected by syringe as a slug within the aqueous layer. This order of material addition helps ensure that only water vapor is exposed to the 1400-K flame used to seal quartz reactors. Hence, reliability in substrate and catalyst concentration is not compromised by the sealing procedure, which would otherwise volatilize, burn, or decompose the inorganic and/or organic material. When solid material is needed for experiments in the 2-mm ID capillary quartz reactors, as for the experiments with stainless steel additive, the mouth of the capillary test tube is widened in the glass shop to about 4 mm on one end. This step greatly facilitates the addition of solid material to a capillary vessel whose inner diameter is only 2 mm. The reactor's volume is unchanged by this process because the final seal is done below the widened mouth. Once the solid material is added, the remaining reaction components are

added in the same order as before.

3.4 Reaction

Reactors were heated by placing them in a stainless steel basket suspended in a hot Techne sand bath held at reaction temperature. The pores in the basket allowed hot sand to permeate through the basket and contact the reactors. The Techne sandbath is manufacturer specified to maintain constant temperature within 0.2°C. Without thermal perturbations, this performance measure is usually met. However, when reactors are first loaded into the sandbath, the temperature will drop 2 to 4°C for about 2 to 5 minutes, and will then return to set point temperature. Earlier experiments have shown that the contents of a 3/8″ stainless steel Swagelok reactor will reach the temperature of a Techne sand bath at a set-point temperature of 350°C within 2 minutes. [110, ch. 3] This heat-up time is negligible for long reaction times. It becomes slightly more important for short reaction times. All the reaction times in this study were measured from the time the reactors were added to the sand bath.

Once reaction time is reached, the entire basket containing reactors is removed from the sand bath and plunged into a bucket of cold water. The reactors rapidly cool. They are then set before a fan to dry and further cool by forced air convection. Once the reactors are dry and at ambient temperature, they are either unloaded immediately or stored in a freezer and unloaded at a later date. Very volatile substrates, such as anisole and 1-phenyl-1-propyne, are always allowed to cool in the freezer overnight before unloading. These reactors are unloaded immediately after being removed from the freezer. They do not first warm to room temperature, but are instead unloaded while still being cold. This step minimizes material loss due to volatilization.

3.5 Unloading reactors and preparing samples

The essential task in unloading reactors and preparing samples is to transport all the reaction vessel material into a known volume of solvent. For 590-μL reactors, this goal is adequately achieved if the reaction mixture is transported by syringe into a 10-mL, class A, volumetric flask, and followed by at least eight rinses of acetone. Each aliquot of acetone is allowed to contact all the internal surfaces of the reaction vessel that were exposed to substrate. To aid in dissolving the reaction material with the solvent, the reactors are stirred with each aliquot of acetone. The Swagelok reactors feature an "annular region" between the outer edge of the port connector and the inner edge of the sealing cap. This region inadvertently collects reaction material during the unloading and collection procedure, and must therefore also be rinsed with solvent. All the rinses for a reactor are collected in the same 10-mL flask, which is brought to volume with acetone and then analyzed by gas chromatography. An experiment wherein reactors were washed once, twice, thrice, ... , or eight times with acetone demonstrated that it was crucial to rinse with eight reactor-volumes of solvent to ensure complete recovery of organic substrate.

The procedure for the larger 4.1-mL reactors is almost exactly analogous, except that 10-mL volumetric flasks may no longer serve as the receiving vessel. The problems incurred are two. One, each aliquot of rinse solvent must undergo several passes to ensure complete collection since the ratio of 10 to 4.1 is small. Two, the phase behavior of a solution of approximately 30% water in acetone presents analytical problems which will be discussed in Section 3.6. In short, the use of 25- or 50-mL, class A volumetric flasks should be chosen to maintain analytical fidelity when working with 4.1-mL reactors.

During reactor unloading, the volume of material initially removed by syringe is recorded, as is the weight of the reactor before and after sample collection. These values aid in trouble-shooting analytical problems. Low volumes and mass differ-

ences can indicate that the vessel leaked during reaction. This could be due to over-pressurization, over- or under-tightening the Swagelok cap, worn threads, or even an unfortunate pattern of thermal expansion during the vessel heat-up period. Volume is never recorded for experiments with solid additives; doing so results only in clogged syringes. Volume is often not recorded for experiments with highly volatile organic substrates; these mixtures are collected cold to prevent loss of the substrate, and ice does not flow well through a syringe needle.

3.6 Preparation of calibration standards

The first step in preparing a set of calibration standards is to prepare the diluent, which matrix matches the samples. Matrix matching is necessary for two reasons related to the nature of the analytical technique, gas chromatography-flame ionization detector (GC-FID). The first reason is the behavior of solutes in binary solvent mixtures in GC. When solvents of very different polarities or boiling points are injected together onto a capillary column for gas chromatography, analyte phase partitioning occurs between three to four phases instead of the normal two phases: in this case, between stationary phase and water, between water and acetone, between stationary phase and acetone, and between acetone and mobile phase. Soon after injection, the solvent is stripped away from the analyte slug due to its own high affinity for the gas phase. Acetone leaves first, then water. However, partitioning among the solvent phases has already created a non-uniform deposition of analyte on the column. As the analyte moves through the column, these bands spread. Analyte elution produces a doublet peak. This behavior will persist for all solvent systems composed of two or more solvents with large differences in polarity or boiling point. For water at room temperature, $\epsilon = 78$; for acetone, $\epsilon = 30$. Table 3.1, showing dielectric constant and boiling point for a number of water-miscible solvents shows that there are few alternative solvent choices that would improve the chromatography. Experi-

Table 3.1: Dielectric constants of common water-miscible solvents.

solvent	boiling point (°C)	ϵ
water	100	78.0
acetone	56.2	20.7
acetonitrile	81.6	37.5
n-propanol	97.4	20.3
isopropanol	82.4	19.9
ethanol	78.5	24.6
methanol	65.0	32.7

ments with acetonitrile and n-propanol also exhibited peak splitting. Analysis with gas chromatography/mass spectrometry (GC/MS) was frequent in order to assure that doublets in GC-FID chromatographs were always single components. Non-polar analytes do not experience peak-splitting due to mismatched solvent polarities within the matrix. Only polar analytes display a propensity to partition between water and acetone, and hence, only polar analytes display doublet formation. The second reason for matrix matching is the effect of water upon the FID; the presence of water is known to suppress FID signal. This phenomenon affects both polar and non-polar analytes. Hence, rather than fix the problems of peak splitting and signal suppression due to the presence of water, the feature was matched in the standards.

Matrix matching is achieved by preparing a diluent of wet acetone that matched the water concentration in the reaction samples. For example, if a reactor contained 0.400 mL of water, and the sample was diluted to 10 mL with acetone for GC analysis, then a diluent was prepared by diluting 4 mL of water to 100 mL with acetone. This diluent is then used to dilute all the calibration standards. In this way, each calibration standard contains the same concentration of water as the reaction samples.

Once diluent is prepared, a parent standard is produced in a 10-mL, class A volumetric flask. The concentration of the parent standard should be about five times that of the highest concentration sample. It may contain multiple analytes,

as the analytical method will separate them before quantifying. Daughter standards are prepared by dilution of the parent. Generally, three generations of three siblings each are prepared. The three siblings are prepared by taking one, two, and three mL respectively of the same parent and diluting to 10 mL with diluent. Figure B.1 in Appendix B shows pictorially the relationship among all the standard solutions. A 1.7-mL aliquot of each standard solution is placed into a gas chromatography (GC) sample vial for analysis by GC.

Early in this work, experiments were carried out to validate a method of internal standardization, which could be more convenient than preparing matrix-matched calibration standards for each reaction. Some drawbacks made the use of standard calibrations more appealing. One, the presence of water was found to cause signal suppression in different compounds to different extents. Hence, the signal from ethylbenzene would not be suppressed by water as much as the signal from anisole, for example. However, the method of internal standardization relies upon the two compounds behaving similarly in the presence of changing analytical conditions. If the assumption of similar behavior is not met for a particular pair of internal standard and analyte, then the chosen internal standard will not give optimal results. Two, a well chosen internal standard for the purposes of matching signal behavior, gave inferior results compared to the method of matrix-matched calibration standards when the analyte was less than half the concentration of the internal standard. Hence, the internal standard needed to also be close to the analyte concentration for good results. These two factors, the need to carefully choose both the internal standard and its concentration, made the method of internal standardization less robust and less convenient than the method of matrix-matched calibration standards.

3.7 Analytical techniques

This section describes the analytical techniques used to quantify organic material in reaction mixtures. The basic approach was to identify compounds by GC/MS and quantify by GC-FID.

3.7.1 Gas chromatograph/mass spectrometry

An Agilent 6890N gas chromatograph with 7563 mass spectrograph equipped with a turbomolecular pump and single quadrupole mass selector was used to identify reaction species. Separation of different components was achieved by a HP-5ms column with dimension 50 m length x 0.200 mm ID x 0.32 μm film thickness. The HP-5 is a poly-siloxane column with 5% phenyl groups. Optimal linear velocity through the column (20-40 cm/s) was achieved with a flow rate of about 0.70 ccm. Constant flow was the choice mode of operation. Bernoulli's equation, Equation 3.2, explains why. Our instrument does not measure flow rate directly; it measures pressure and uses the dimensions of the column and the properties of the mobile phase to estimate flow rate. However, if constant pressure is used, as the oven warms during an analysis, density ρ will decrease. This will cause velocity v to decrease as well. However, decreasing the velocity below its optimum value will reduce peak resolution and increase peak broadening. This effect is avoided by operating in constant flow mode.

$$\frac{v^2}{2} + gz + \frac{P}{\rho} = \text{constant} \tag{3.2}$$

A typical injection was 2 μL of sample with a 20:1 split. The inlet was kept at 50°C hotter than the highest ambient-pressure boiling point of the analytes of interest, or 345°C, whichever was cooler. The oven temperature program began at 150°C less than the lowest ambient-pressure boiling point of the analytes of interest, or about 10 °C cooler than the boiling point of the least volatile solvent, whichever was cooler.

The initial oven temperature was never set less than 40 °C. Further details of oven temperature programs for various analyses are available in Appendix B.

The mass spectrograph was operated in scan mode for the purpose of compound identification. Mass fragments between 29 and 500 were counted. Lenses were auto-tuned to optimal voltages by set programs within the manufacturer's Chemstation software. All identification was carried out with a recently tuned (within one week) mass spectrograph. Compound identification was assisted by the 1998 version of the NIST/EPA/NIH Mass Spectral Library (NIST98) as distributed by Agilent Technologies, version Rev.D.03.00, November 2001. Where the library lacked a suitable structure identification, the theory of ion fragmentation patterns, in addition to the literature, was consulted. [111]

3.7.2 Gas-chromatography-flame ionization detection

An Agilent 6890 GC-FID was used for most quantification purposes. An equivalent column was used for both GC-FID and GC/MS, allowing for straightforward peak identification in the FID chromatogram once the MS chromatogram was produced. Reaction product identification was further confirmed by retention-time matching to a known sample. The method used for analysis was also equivalent to the method implemented on GC/MS. The flame ionization detector was operated at generally accepted conditions: 350 to 400°C, 40 ccm H_2 flow rate, 400 ccm air flow rate, 40 ccm make-up He flowrate, and a 10 Hz data collection rate.

On very few occasions, the Agilent 7890 GC-FID was used for quantification instead of the 6890. Operating parameters were equivalent, the main different between the two instruments being the use of N_2 as make-up gas on the 7890 instead of He as on the 6890. The data from the two instruments are treated as equivalent.

3.7.3 Analyzing the data

Determination of reactor contents was carried out by forming a calibration curve based on the GC-FID signal from the calibration standards, and applying it to GC-FID signal from the reaction samples. The calibration curve, Eqn 3.3 was the result of line fitting to a plot of concentration vs signal for each analyte in the calibration standards. No terms higher than first order were ever needed to obtain an adequate calibration curve.

$$(\text{concentration/mM}) = m * (\text{signal}/(pA * s)) + b \tag{3.3}$$

Four "best-fit" lines were determined for each analyte in each set of calibration standards:

1. linear regression
2. linear regression with intercept (term b) set to zero
3. non-linear or weighted regression
4. non-linear or weighted regression with intercept (term b) set to zero

Linear regression is the simple algorithm found in most elementary textbooks on quantitative analysis, regression, or modeling. The procedure consists in supposing values of m and b, calculating the difference ($y_{experiment} - y_{calculated}$), squaring it, and then summing all the squared errors. The best-fit line is obtained when m and b are chosen such that the sum of squared errors (SSE) is minimized. The second method is the same as the first, except that the parameter b is set to zero. Hence, the best fit line is the one obtained when m is chosen such that the SSEs is minimized. In other words, we seek to minimize the objective function in Equation 3.4. The third and fourth methods are analogous to the first and second methods, except for the

objective function that is minimized. Instead of minimizing the SSEs, these methods weigh each squared error by one over the relative percent error in the calibration standard concentration, as shown in Equation 3.5. The relative percent error is estimated by error propagation of the manufacturer-claimed error within the class A 10-mL volumetric flasks, any Hamilton syringes used in material delivery, and any pipetters used in material delivery. The relative percent error is calculated to reflect the propagation of error through the three generations of standards. Hence, the weights for all three "siblings" in a given set of standards are numerically very similar.

$$F = \sum_{i=1}^{n} \left(y_i^{experiment} - y_i^{calculated} \right)^2 \tag{3.4}$$

$$F = \sum_{i=1}^{n} w_i \left(y_i^{experiment} - y_i^{calculated} \right)^2 \tag{3.5}$$

$$\text{where } w_i = \left(\frac{1}{\text{estimated error}} \right)^2$$

The values of m and b determined by these four methods of parameter estimation are always very similar. Typically, the results from linear regression are accepted because of the method's good minimization of absolute error at moderate concentrations, and because of the method's simplicity. For low concentrations of analytes ($\leq$ 0.5 mM), it is often preferable to use one of the parameter estimates that force b to equal zero. These methods (2 and 4) control the relative errors more uniformly, as they were designed to do. Further, they force positive values of concentration for low signals. Depending on the value of b, methods 1 and 3 may offer negative concentration values for very low signals. Even though the absolute difference between the use of methods 1 or 2, for example, will only be 0.1 mM or less for low signals, positive molar yields (even if they are low) are much more pleasing.

Once the parameters m and b from Equation 3.3 are chosen, the equation is used

to compute the concentration of analyte in the reaction sample. Multiplication of this value by the dilution volume gives the total moles of analyte in the reaction vessel. The analyte concentration within the reaction vessel is then determined by dividing the total moles of analyte in the reaction vessel by its liquid volume at reaction temperature. Typically, the dilution volume is 10 mL because 10-mL volumetric flasks were used in the sample dilutions. The reactor liquid volume at reaction temperature is typically 563 μL for the 1/4″ stainless steel reactors. These relationships are expressed in the following equations, where y' is the reaction sample concentration in mM, x is the GC-FID signal in pA*s for a reaction sample, $y_{\mu moles}$ is the μmol of analyte in the reactor, DV is the dilution volume, and V_{rctr}^{T} is the liquid volume of the reactor at reaction temperature.

$$y_{\mu moles} = DV * (x * m + b) \tag{3.6}$$

$$y' = \frac{y_{\mu moles}}{V_{rctr}^{T}} \tag{3.7}$$

3.8 Additional experimental procedures

3.8.1 Particle size determination

Stainless steel powder and quartz particles were used in this study to help ascertain whether the reactor material of construction contributed to the kinetics. Two-dimensional images of these particles were measured on an Olympus SZX12 stereomicroscope equipped with an EVOLUTION LC video camera and controlled by Image-Pro Plus image analysis software on a computer. The 2D surface areas of a total of 368 particles of stainless steel powder and 298 particles of quartz were measured and then converted into estimates of 3D surface area using material bulk density and the assumption of spherical shape. The average area per unit mass of stainless steel powder particles was 27.6 ± 8.7 mm^2/mg; of quartz particles, 11 ± 0.55 mm^2/mg.

The surface areas reported in this study are the estimated 3D surface areas.

3.8.2 pH measurement

Our laboratory is not equipped to measure the pH of reaction mixtures at reaction conditions. The literature will usually provide data for the acidity or basicity of common acids and bases at various temperatures and concentrations. However, the behavior of the WTLAs in this work has not yet been documented with such thoroughness. Hence, the reported pH of acid catalyst aqueous media is the pH measured at room temperature. Measurements of pH were carried out with an Accumet pH meter. For acidic samples, the pH meter was calibrated immediately prior to use with standard buffers at pH 2, 4, and 7. After the pH meter reported stability, about six readings were taken, one every ten seconds for about one minute. These readings were averaged to give the solution pH. This procedure was repeated with three different aliquots of the aqueous acid catalyst media under study, and the results were averaged.

CHAPTER IV

Hydration of 1-Phenyl-1-Propyne

> Things are not always what they seem; the first appearance deceives many; the intelligence of a few perceives what has been carefully hidden.
> *Phaedrus*

Alkyne hydration is a means of producing synthetically useful ketones. The reaction, which comprises hydro-hydroxylation of an alkyne followed by tautomerization, was first discovered by Kucherov [112], who demonstrated the catalytic activity of mercuric salts in this reaction. Kucherov's classic procedure continues to be in use because of its reliability, but much research activity, including some work in high-temperature water, has been devoted to discovering more benign alternatives to its toxic reagent. Most of the alkyne hydration work in high-temperature water featured phenylacetylene as a model compound. Phenyl acetylene is much easier to hydrate than our choice model compound, 1-phenyl-1-propyne. Katritzky showed that phenylacetylene produces acetophone in 51% yield in near critical water without catalyst after five days at 250°C. [113] In 0.5 M H_2SO_4, 90% yield may be obtained after an hour at 280°C.[114] Microwave irradiation also promotes the transformation, providing 78% yield after 2.5 hours at 295°C. [115] Outside of high-temperature water research, efforts toward better catalysts include ruthenium(II) complexes for anti-Markovnikov hydration of terminal alkynes [116], cationic gold(I) complexes for the

addition of alcohols to alkynes [117], platinum(II) derivatives for hydration of electron rich alkynes [118], and many others.

Hintermann and Labonne's review of alkyne hydration summarizes much of the recent work in this field.[119] The authors note that there are few alkyne hydration catalysts in the first third of the periodic chart, including the lanthanides. We have found some water-tolerant Lewis acids within this region of the Mendeleev table that are respectably active toward our model alkyne hydration substrate in near-critical water. We advance research efforts toward more environmentally benign alkyne hydration reagents with our demonstration of the activity of $Sc(OTf)_3$, $Yb(OTf)_3$, $In(OTf)_3$, and $InCl_3$ in transforming 1-phenyl-1-propyne to propiophenone in high-temperature water. We further offer a comparison with Brönsted acid catalysts at the same conditions, a kinetic study, and mechanistic scenarios consistent with the experimental kinetics and previous literature on this reaction.

We designed experiments to quantify the kinetic behavior of 1-phenyl-1-propyne hydration. We began with an evaluation of different reactors and their propensity to affect kinetic measurements. We then tested a collection of Lewis and Brönsted acid catalysts to determine their effectiveness toward hydration. Having chosen a catalyst with which to conduct kinetic experiments, we determined order in catalyst and substrate, followed by the rate constant for reaction at different temperatures. This offered an appraisal of the activation energy and frequency factor. Finally, we integrated our results and their implications with current understanding of the general mechanism of alkyne hydration.

Our studies involved quantification of two species, 1-phenyl-1-propyne and propiophenone, as these were the only species detected by GC/MS for most experiments. At the lowest temperature investigated, 150°C, a small amount of partial or intermediate oxidation products were detected by GC/MS in quantities that accounted for less than 1% of the total organic reaction material. Products of aldol-type reactions

were never detected, and our mole balances for the results herein are always good; losses are never greater than 10% by mole, and our average is 7% by mole. Although the hydration of acetylene is known to proceed without catalyst at high temperatures, our experiments without catalyst for 1-phenyl-1-propyne did not yield any detectable products, not even at our highest reaction temperature of 225°C.

4.1 Effect of reactor wall material

The conscientious experimentalist may be concerned that the wall of a stainless steel reactor may catalyze a reaction in high-temperature-water, obfuscating the kinetics of reactions thus carried out. Taking due diligence, we compared reactions in 1/4″ stainless steel reactors versus reactions in 2-mm ID quartz ampule reactors. After 60 minutes at 200 °C, the stainless steel reactors produced 84 ± 8% yield while the quartz reactors produced only 21 ± 7% yield. We define yield herein as the percentage of the original moles of reactant that appear as product. The initial concentration of 1-phenyl-1-propyne was 0.142 M and the loading of $In(OTf)_3$ catalyst was 5 mol% with respect to reactant.

It is tempting to conclude from just these experiments that stainless steel catalyzes alkyne hydration in HTW. Though such a conclusion is oft rightfully made, it is not necessitated by these results alone. Two other explanations are possible: the reaction may be inhibited by quartz, or some other incidental effect may be producing these results while both stainless steel and quartz are inert. To test the hypothesis of stainless steel catalysis, we added 0, 10, 20, and 40 mg of stainless steel powder to quartz reactors. These amounts correspond to increasing the stainless steel surface area to 0, 276, 552, and 1103 mm^2 respectively. The inner surface area of a typical stainless steel reactor is about 580 mm^2. After one hour at 200°C, conversion and yield were measured, but no effect due to stainless steel was observed, as shown in Figure 4.1.

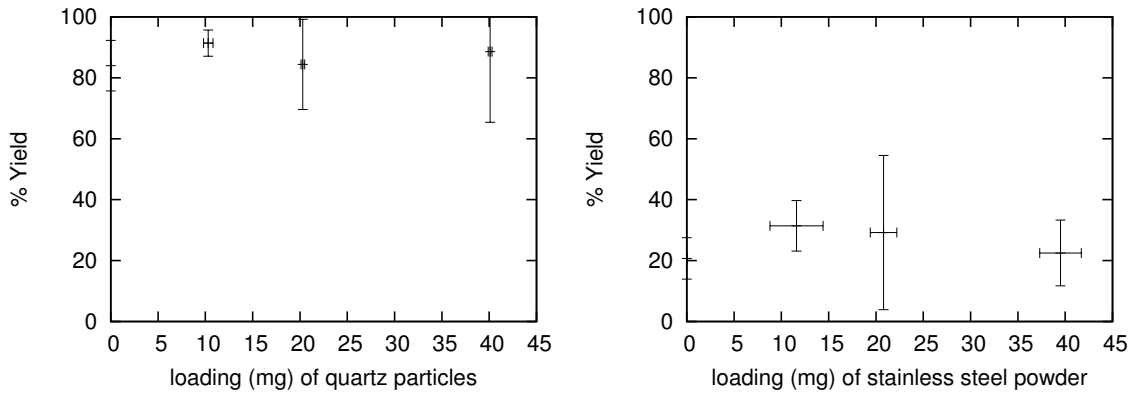

Figure 4.1: Yield of propiophenone (left) in stainless steel reactors loaded with increasing amounts of quartz and (right) in quartz reactors loaded with increasing amounts of stainless steel. Error bars depict 95% confidence intervals for the data.

Next, we tested the hypothesis of inhibition by quartz by adding 0, 10, 20, and 40 mg of quartz particles to stainless steel reactors. This corresponds to increasing the quartz surface area to 0, 110, 220, and 440 mm^2 respectively. The inner surface area of a typical quartz reactor is about 1200 mm^2. After one hour at 200°C, with the same catalyst and substrate loadings, conversion and yield were measured as before, see Figure 4.1.

The conclusion drawn was that neither did stainless steel catalyze nor did quartz inhibit alkyne hydration in HTW; rather, neither displayed any measurable effect upon the reaction rate. However, this result does not point to any positive explanation for the initial disparity observed between reaction in stainless steel and reaction in quartz. Hence, more experiments were carried out.

Stainless steel and quartz reactors of larger volume were tested. The stainless steel reactors had an inner diameter of $1/2''$ and an internal volume of 4.1 mL. The large quartz reactors had an inner diameter of 6.91 mm, and a length of approximately 109.5 mm, to afford an internal volume of 4.1 mL. The larger reactors were loaded to closely match the concentrations of substrate and catalyst used in the smaller reactors. The results from large SS and large quartz reactors are in good agreement

with each other: 70±16% yield in large SS versus 74±18% yield in large quartz from reaction at 200°C for 60 min with an initial reactant concentration of 0.156 M and 5 mol % $In(OTf)_3$ catalyst. These results are also in agreement with the 84±8% yield obtained in the smaller stainless steel reactors. Thus, we concluded that the reactor material (stainless steel or quartz) does not affect the reaction, but rather, it is the reactor diameter that is the key variable.

We now hypothesize that the rate difference between small stainless steel and quartz reactors is due to transport limitations in 2-mm ID quartz. The reactants are immiscible at room temperature; solubility of the organic substrate in water increases as the reactor heats up. The reactant must then diffuse through the aqueous phase to encounter catalyst. The constrained reactor geometry coupled with the hydrophilicity of quartz may induce increased capillary forces, which prevent sufficient transport axially in the reactor.

In response to our suspicions of diffusion limitations, we calculated the Weisz-Prater parameter [120, 121] for this reactive system at 200°C. The Weisz-Prater parameter, C_{WP} in Equation 4.1, compares measured rate constants with transport resistance to help determine whether the observed rate is kinetically controlled or diffusion limited. A value much greater than unity implies the intrusion of transport limitations upon the intrinsic reaction kinetics. The Weisz-Prater parameter was born out of heterogeneous catalysis where it is used to determine the potential effects of rate limiting pore diffusion. It is apropos to our homogeneously catalyzed reaction system; molecular diffusion through a pore to a reactive site is analogous to reagent and substrate diffusion toward each other.

$$C_{WP} = \frac{\text{observed reaction rate}}{\text{rate of diffusion}} = \frac{k_{observed}}{D/L^2} \tag{4.1}$$

We conducted a series of batch experiments with 2-mm ID quartz capillary reactors and with $1/4''$ stainless steel reactors with 'typical' loadings as described in the

Procedure. All reactions were at 200°C; reaction time was varied. The rate constant k was determined by fitting the data to a first-order rate law. We did this by linear regression, minimizing an objective function that was the sum of squared differences between the calculated and actual alkyne concentration. Rate constant k was determined to be 8.1x10^{-5} s^{-1} for 2-mm ID quartz reactors, and 6.8x10^{-4} s^{-1} for 1/4″ stainless steel reactors. We approximated the diffusivity (D) of 1-phenyl-1-propyne at reaction conditions to be 1.05x10^{-4} cm^2/s based on heuristics for the diffusion of liquids in liquids, and the general relationship among diffusivity, temperature, and viscosity for liquids. [120] For quartz reactors with a characteristic length of 189 mm (the length of the 2-mm ID quartz capillary reactors), C_{WP} was 280 at 200°C. For stainless steel reactors with a characteristic length of 4.3 mm (the radius of the 1/4″ Swagelok reactors), C_{WP} was 1.2 at 200°C. It is clear that transport within the narrow quartz reactor was slow enough to limit the observed reaction rate. The values of C_{WP} for the larger quartz and stainless steel reactors at 200°C are 1.3 and 0.75 — nearly unity. Given the similarity of the product yields from the experiments in these latter three reactors and that C_{WP} was less than or about unity, we conclude that these reactors can be used to obtain the intrinsic reaction kinetics. At 225°C, C_{WP} is 2.9 for the 1/4″ stainless steel reactors.

4.2 Catalyst screening

We chose a set of water-tolerant Lewis acids that indicated promise for organic transformations in water, and which were distinctively different from one other in terms of electronic structure. $Yb(OTf)_3$, which has demonstrated promising ability to act as a Lewis acid catalyst in water through its high yield (92%) toward a model Mukaiyama aldol reaction,[32] was selected as one of the catalysts to examine. $Sc(OTf)_3$ was found to be a good Diels-Alder, allylation, and Friedel-Crafts acylation catalyst.[33] $In(OTf)_3$ demonstrated good activity toward alkyne-aldehyde coupling

reactions.[34] Further, the behavior of these metals as judged from their hydrolysis constants and water exchange rate constants, are distinctively different. Sc and In both have low hydrolysis constants; Yb and Sc both have high water exchange rate constants.[35] Hence, without exhaustively testing every water-tolerant Lewis acid, we hoped to portray a broad van Gogh-brush stroke of catalytic activity by water-tolerant Lewis acids. We then compared the results for alkyne hydration with these catalysts with behavior from Brönsted acids. We measured the pH of the aqueous reactor material at room temperature for each catalyst.

Stainless steel (1/4″ Swagelok) reactors were loaded as described in the experimental section. The reactors were then brought to 175°C for a two-hour batch holding time, after which their contents were quantified by GC-FID as described earlier.

Results, shown in Figure 4.2, indicate that $In(OTf)_3$ is the best catalyst with $InCl_3$ being a near second. The error bars in Figure 4.2 depict one standard deviation. The 95% confidence interval for $In(OTf)_3$ is tighter than one standard deviation because many (nine) repetitions were carried out. Thus, we have a high level of confidence in concluding that $In(OTf)_3$ was the most active catalyst of those tested.

The mineral acids showed activity toward 1-phenyl-1-propyne, as was expected, but on a per mole basis, the mineral acids were less active than the In(III) complexes that were tested, even though their pH was lower.

We did not find any definite correlation between catalyst activity (as inferred from conversion and product yield) and pH. This result indicates that although the reaction may proceed through simple acid catalysis [112], the metal centers seem to play an important role as well. However, our results indicate that the metal center does not exclusively determine activity; the conversion with $In(OTf)_3$ is almost 8% greater than that with $InCl_3$. Indium triflate's greater activity over that of $InCl_3$ may be due to its slightly heightened acidity. From this brief catalyst study, we offer the possibility that for the water-tolerant Lewis acids, at least two mechanisms may

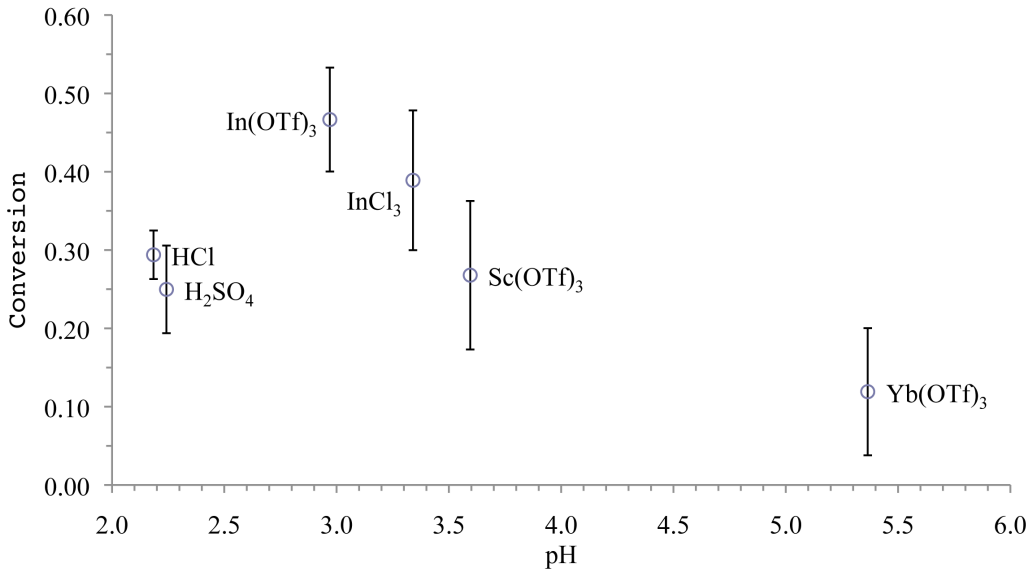

Figure 4.2: Conversion of 1-phenyl-1-propyne to propiophenone after 2 h at 175°C with 5 mol% catalyst loading based on addition of starting material.

contribute: one that is Brönsted acid catalyzed, and one that is Lewis acid catalyzed. We discuss possible mechanisms in more detail in a subsequent section.

4.3 Reaction order in $In(OTf)_3$ catalyst

We chose $In(OTf)_3$ as the catalyst to carry forward in our kinetic study. To determine the reaction order in catalyst, we carried out a set of experiments wherein catalyst concentration was changed while holding water and substrate loadings constant at the typical values described in the procedure. Reaction time was chosen such that conversion would be approximately 30%. These experiments were carried out at 175°C in 1/4″ SS reactors. For our data analysis, we calculated the pseudo-first-order rate constant, k′, from the experimental observables of conversion (X) and time (Equation 4.2).

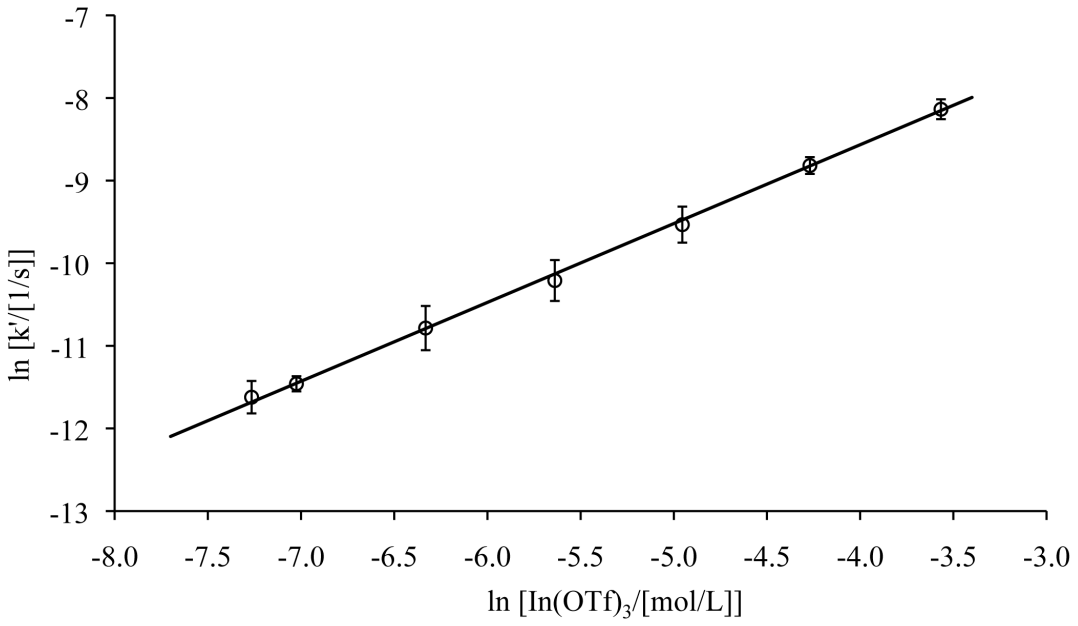

Figure 4.3: Influence of $In(OTf)_3$ catalyst concentration on pseudo-first-order rate constant.

$$k' = \frac{-\ln(1-X)}{t} = kC_a^{\alpha-1}C_{Catalyst}^{\gamma} \tag{4.2}$$

$$\ln k' = \ln k + (\alpha - 1)\ln C_a + \gamma \ln C_{Catalyst} \tag{4.3}$$

In these experiments, changes in the pseudo-first-order rate constant can be attributed solely to the changes in the catalyst concentration since the alkyne concentration and temperature were fixed. According to Equation 4.3, a log-log plot of k′ versus $C_{Catalyst}$ should provide a straight line, with slope equal to γ, the reaction order in catalyst.

Figure 4.3 shows the pseudo-first-order rate constant k plotted against the initial catalyst concentration on log-log coordinates. Weighted linear regression of these data gave a slope of 0.95 – unity, for all practical purposes. Hence, we conclude that the reaction is first order in catalyst.

4.4 Temporal variation of conversion

We collected conversion data at various reaction times for four different temperatures: 150°C, 175°C, 200°C, and 225°C. Reactions carried out at 250°C completed so rapidly that we could not collect accurate rate data given the reactor heat-up time of approximately 2 minutes. Reactions were performed in 1/4″ stainless steel reactors with an initial concentration of 0.142 M 1-phenyl-1-propyne and 7.13 mM $In(OTf)_3$ catalyst (5 mol % loading). Figure 4.4 shows the experimental results. The reaction is very slow at 150°C; the conversion is below 50% even after 1000 minutes. In contrast, the reaction is much faster at 225°C; a conversion greater than 60% was obtained after only 10 minutes. We used the integral method to verify that the reaction was first order in alkyne. Plots of $\ln(1 - X)$ versus time were linear, even for the high conversion data that permit discrimination between different reaction orders. To estimate numerical values for the rate constants, we fit concentration-vs-time data at each temperature to the differential equation for reaction in a constant-volume batch reactor, Equation 4.4.

$$\frac{dC_{alkyne}}{dt} = -kC_{catalyst}C_{alkyne} \tag{4.4}$$

We determined the values of k at each temperature with the software Scientist; we performed parameter estimation upon the ordinary differential equation with unweighted least squares analysis. Table 4.1 reports the values for k at each temperature along with the computed standard error.

Having obtained the rate constant at four different temperatures, we determined the activation energy and frequency factor for the transformation in HTW using a method of least squares in Scientist™. The activation energy, 21.4 ± 0.6 kcal/mol, is in excellent agreement with the value of 22 kcal/mol determined by Noyce and Schiavelli for reaction in warm concentrated sulfuric acid solution. [122] The frequency factor,

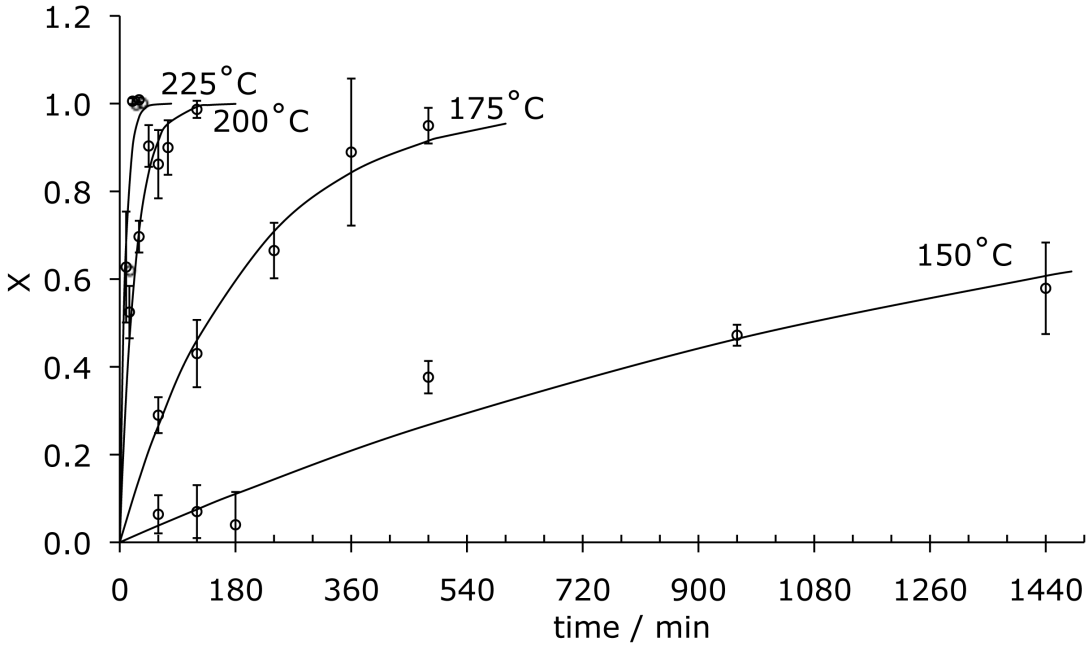

Figure 4.4: Temporal variation of alkyne conversion at different temperatures. Discrete points are experimental results. Smooth curves are from a kinetics model first-order in alkyne.

Table 4.1: Second-order rate constant k (L mol^{-1} s^{-1}) with standard error for each temperature.

T (°C)	k L mol^{-1} s^{-1}	std error in k L mol^{-1} s^{-1}
150	0.00152	0.00010
175	0.01202	0.00066
200	0.0960	0.0053
225	0.270	0.027

$10^{8.8\pm0.3}$ L mol^{-1} s^{-1}, is also a reasonable value for a second-order reaction in solution.

4.5 Discussion of mechanism

Alkyne hydration is known to proceed via simple electrophilic addition with rate-determining protonation and general acid catalysis in warmed concentrated sulfuric acid solution (see Figure 4.5). [122–125] Our experiments with mineral acids indicate that this route is plausible in HTW conditions as well, with a far lower acid concentration than what is needed for reaction at room temperature or slightly above. The metal catalysts we experimented with demonstrated a higher activity than the mineral acids. Although our pH measurements were at room temperature, not at reaction conditions, if the relative order of acidity of our catalysts remains the same at reaction conditions, then Brönsted acid catalysis alone cannot explain the order of reactivity. Hence, another mechanism may be important for the metal-catalyzed experiments.

Alkyne hydration via Kucherov synthesis with mercuric salts (Figure 4.6) is known to proceed through a mercuric complex with the alkyne, which draws electron density away from the triple bond to incite attack by water. [106] Deprotonation yields an enol, which tautomerizes to the ketone final product. The Kucherov synthesis results in the Markovnikov product, as does our reaction. It is possible that the metal catalysts used in the present experiments complex with the alkyne substrate in a similar manner to allow attack by water.

4.6 Conclusions

The hydration of 1-phenyl-1-propyne proceeds readily in HTW with Lewis acid catalysis. Of the four water-tolerant Lewis acid and two Brönsted acid catalysts studied, $In(OTf)_3$ is the most active. The reaction rate law appears to be first order in

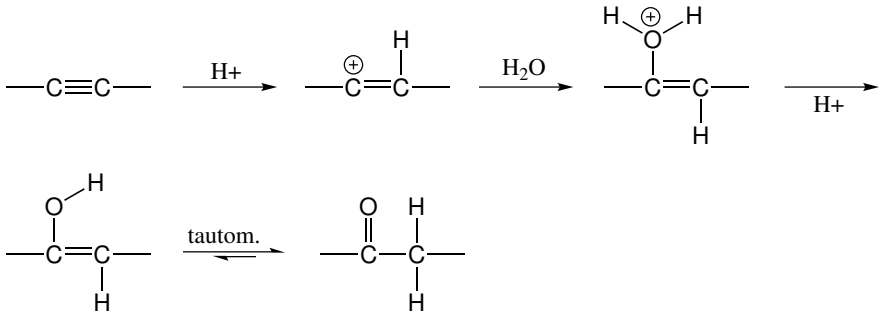

Figure 4.5: Alkyne hydration by electrophilic addition of a proton to an alkyne.

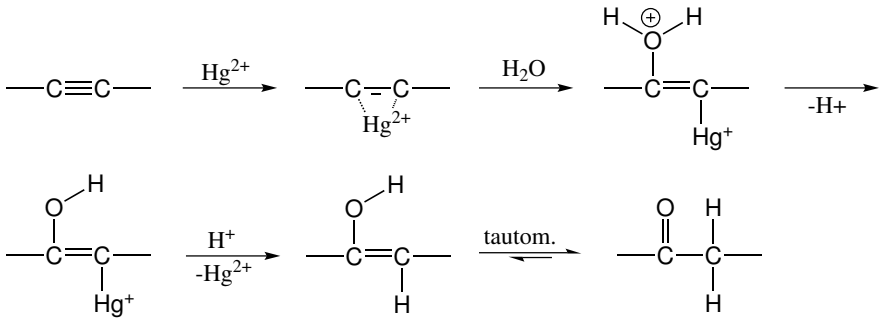

Figure 4.6: Alkyne hydration by dihydro-oxo-biaddition.

substrate and first-order in catalyst. There is evidence for no effect upon the reaction due to stainless steel or quartz reactor walls. However, transport limitations are likely a limiting effect in capillary quartz reactors, especially at high temperatures, 200°C or higher. We suspect that hydration occurs through simple nucleophilic addition with an intermediate vinyl cation and/or through metal-assisted nucleophilic addition. This study does not resolve these two possibilities, but offers circumstantial evidence for both. This work represents the first demonstration of catalysis by water-tolerant Lewis acids in high-temperature water. It is also the first demonstration of alkyne hydration to be catalyzed by the metal triflates we tested.

CHAPTER V

Activity Toward Alkyne Hydration

> The weight of evidence for an extraordinary claim must be proportioned to its strangeness.
>
> *Laplace*

Once the kinetics of hydration for one alkyne were well studied, we sought to test other alkynes to develop a sense of the method's practical applicability. Hence, a series of experiments were conducted to determine the relative reactivity of different alkynes. This chapter is structured such that data, observations, and interpretations for each tested alkyne are presented first, followed by integrating conclusions and remarks. The different alkynes tested are divided into two unbalanced groups: aromatic and aliphatic. By "aromatic", I mean that the alkyne functionality is one carbon removed from an aromatic ring; I do not mean that the alkyne is part of a (4n+2)-electron ring system. We tested more alkyne examples in the aromatic group than in the aliphatic group toward hydration.

5.1 Aromatic alkynes

Any alkyne may be hydrated by the Kucherov method, which proceeds through the mechanism depicted in Figure 4.6. Some activated alkynes may hydrate by simple electrophilic addition, as depicted in Figure 4.5. These include acetylenic ethers,

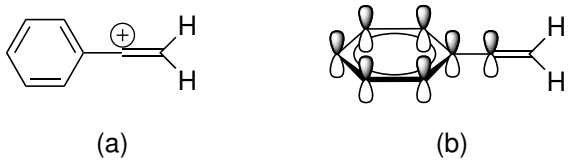

Figure 5.1: (a) A carbocation intermediate is formed in the electrophilic addition to an alkyne. (b) A carbocation beside an aromatic ring is stabilized by hyperconjugation.

thioethers, and ynamines, [106] as well as phenylacetylenes. The increased reactivity of phenylacetylenes toward hydration is due to their ability to stabilized the carbocation formed as part of the mechanism for electrophilic addition. The carbocation is stabilized by an electron delocalization phenomenon called hyperconjugation stabilization. In this case, hyperconjugation stabilization is the ability of the aromatic pi cloud to donate electron density to the empty sp^2 orbital of the vinyl carbocation, as shown in Figure 5.1

5.1.1 Phenylacetylene

Phenylacetylene, Figure 5.2, is just one methyl group shorter than our original substrate for alkyne hydration work. At 200°C, it is completely converted to acetophenone in under 30 minutes. At 150°C, 80.7±1.7% yield acetophenone is achieved after one hour with a catalyst loading of 8.1 mM and an initial phenylacetylene loading of 162 mM. Based on this data, we calculate a second order rate constant k at 150°C was .057±0.003 L s^{-1} mol^{-1}, where the reported error is the 95% CI. In the absence of catalyst, hydration to the ketone is very slow. Katritzky et al. report 1.3% yield of acetophenone after 6 hours at 150°C; and 50.8% yield after 5 days at 250°C. [113] The use of $In(OTf)_3$ greatly accelerates this tranformation.

There is one nuance that arose in the study of this reaction that merits some discussion. An impurity was detected by GC in both "pure" starting material and in reaction mixtures. By GC/MS, the molecular weight of this impurity was determined

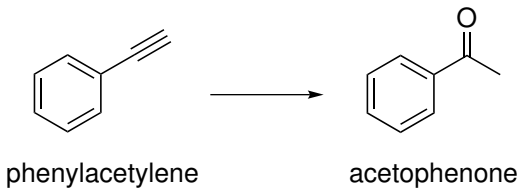

Figure 5.2: Phenylacetylene hydrates to form acetophenone.

to be 204 amu, which would correspond to a dimer of phenylacetylene. In fact, phenylacetylene is known to dimerize and trimerize. Katritzky et al. report 3.9% yield 1-phenylnaphthalene at 150°C after 6 hours. [113] In our experiments, the quantity of dimer is too low to definitively identify by GC/MS. However, if it is the 1-phenylnaphthalene, we estimate its production to be about 0.5% yield after 1 hour at 150°C. This is roughly in agreement with Katritzky et al. [113]

5.1.2 4-Ethynyltoluene

The hydration of 4-ethynyltoluene yields 4-methylacetophenone, as shown in Figure 5.3. After 30 minutes at 150°C with a catalyst loading of 6.5 mM and an initial 4-ethynyltoluene loading of 140 mM, 4-methylacetophenone is produced in 39.2±1.9% yield. Based on this datum, we calculate a second order kinetic rate constant of 0.052±0.004 L s^{-1} mol^{-1}, where the reported error is the 95% CI. Without catalyst, the rate is very slow. We increased the temperature to 175°C and the reaction time to two hours to measure a yield of p-methylacetophenone of 11.9±2.4%, giving an estimated first order rate constant of 2.72±0.51 x10^{-5} s^{-1} for the uncatalyzed reaction. Since the catalyzed rate of hydration is much faster than the rate due to only the hydrothermal environment, we assume that we are measuring the rate of WTLA-catalyzed hydration within the error of our technique.

A small amount of dimer of 4-ethynyltoluene was detected in most of the reaction samples, though not in pure starting material samples. Without catalyst at 175°C, 2.2±0.2% dimer was formed, compared to 0.31±0.42% yield dimer in the catalyzed

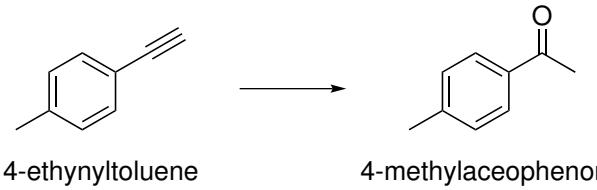

Figure 5.3: 4-ethynyltoluene hydrates to form 4-methylacetophenone.

reactions at 150°C after 30 minutes. Note that the percent yields reported for dimer are educated estimates based on calibrations for 1-phenylnaphthalene.

5.1.3 4-(tert-butyl)-Phenylacetylene

For the hydration of 4-(tert-butyl)-phenylacetylene at 150°C, Figure 5.4, the formation of dimer becomes a more significant fraction of the total alkyne conversion. The kinetic route toward dimerization cannot be neglected. In these experiments, our catalyst loading was 8.2 mM and our initial loading of alkyne substrate was 0.20 M. We collected a slightly larger data set than for the previous two alkynes, and modeled the kinetics with the set of differential equations shown in Equation 5.1, where C_A, C_B, C_D, and C_{WTLA} are the concentrations of alkyne, ketone, dimer, and WTLA ($In(OTf)_3$), respectively. Constants k_H and k_D denote the kinetic rate constants for hydration and dimerization respectively. We chose to model the dimerization process as second-order in alkyne. Hydration remains second-order overall; first-order in substrate and first-order in catalyst.

$$\begin{aligned} \frac{dA}{dt} &= -k_H C_{WTLA} C_A - k_D C_A^2 \\ \frac{dB}{dt} &= k_H C_{WTLA} C_A \\ \frac{dD}{dt} &= k_D C_A^2 \end{aligned} \tag{5.1}$$

We used Scientist to solve the differential equations numerically using the Runge-

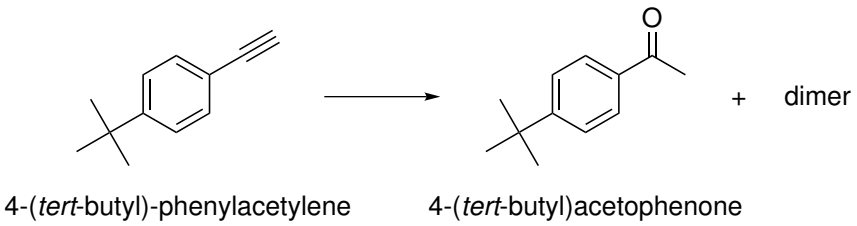

Figure 5.4: 4-(tert-butyl)-Phenylacetylene hydrates to form 4-(tert-butyl)-acetophenone.

Kutta method and to perform parameter estimation using a least squares fit of the model to the collected data set. The resulting parameter estimates determine k_H to be 0.0012±0.0002 L s^{-1} mol^{-1}, and k_D to be 2.8±1.6x10^{-8} L s^{-1} mol^{-1}, where the errors represent a 95% CI. The experimental data, depicted with points and 95% CIs, along with the model fit in lines, appear in Figure 5.5.

5.1.4 4-Ethynylbenzyl alcohol

The reaction of 4-ethynylbenzyl alcohol to p-acetylbenzyl alcohol presented some challenges. In addition to the expected alkyne and ketone, three additional compounds appeared in the GC/MS data. Further, precise quantification was difficult because the product p-acetylbenzyl alcohol was not commercially available.

GC/MS identified three compounds in the reaction mixtures aside from the starting material and product; these compounds have molecular weight 130, 134, and 148 as determined by their mass spectra. One of these compounds, the one with molecular weight 130, was also detected in the starting material. For the MW130 peak, the library-suggested structure of 4-ethynylbenzaldehyde carried a match quality to a library spectrum of 83%. The expected fragmentation pattern from 4-ethynylbenzaldehyde matches the main features in the experimental MS. Loss of the aldehyde hydrogen yields a peak at m/z 129; β-cleavage of the aldehyde yields a peak at m/z 101 with loss of HC≡O:$^+$. Hence, the impurity with MW 130 can be ascribed to 4-ethynylbenzaldehyde with confidence. The estimated concentration

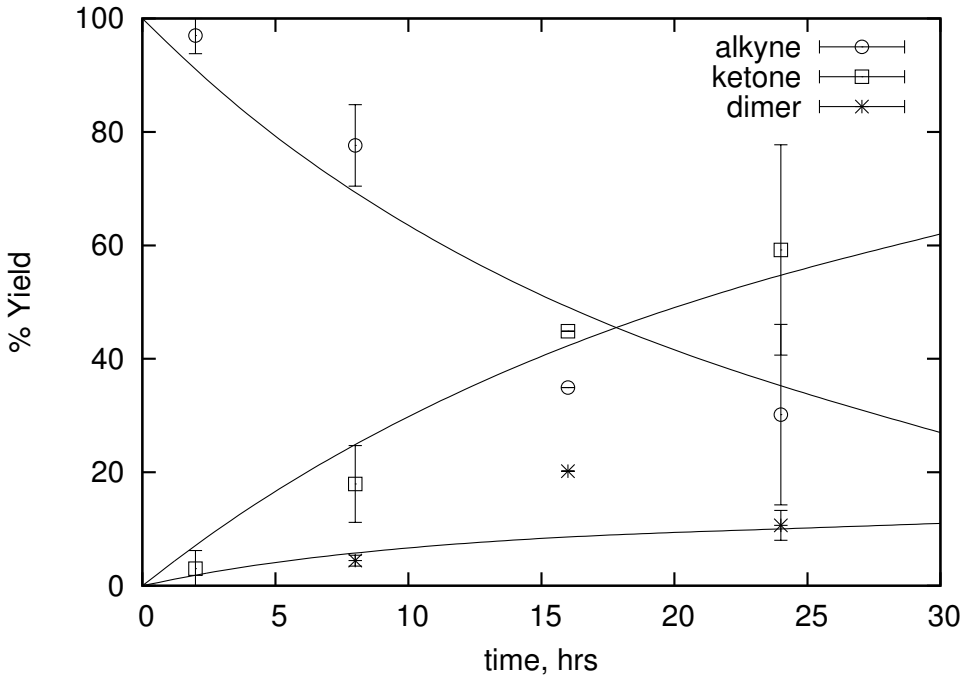

Figure 5.5: Conversion of 4-tert-butyl-phenylacetylene (circles) to 4-tert-butyl-acetophenone (squares) at 150° C with formation of alkyne dimer (stars). Error bars represent 95% confidence intervals. Data at 16 hours represent a single datum and thus do not have error bars.

of the 4-ethynylbenzaldehyde impurity in unreacted samples of the starting material mixed with water and catalyst suggest a concentration of about 4% based on the MW130 peak's area percentage relative to that of the starting material. Such a level is significantly higher than the total % impurities reported in the certificate of analysis for the starting material (0.8%, see App. A), but still within the range of anticipated uncertainty given the analytical techniques used for this reaction system.

Alkyne 4-ethynylbenzaldehyde would be expected to hydrate under our reaction conditions to form 4-acetylbenzaldehyde, which has molecular weight 148. Our library does not contain an entry for 4-acetylbenzaldehyde. However, analysis of the expected fragmentation pattern for this compound is in excellent agreement with experimental spectra: loss of the aldehyde hydrogen yields a peak at m/z 147; β-cleavage of the aldehyde yields a peak at m/z 119 with loss of $HC{\equiv}O{:}^{+}$, α-cleavage of the ketone bond to the ring yields m/z 105 with loss of $H_3C{-}C{\equiv}O{:}^{+}$, and α-cleavage of the ketone bond to the methyl group yields m/z 133 with loss of $H_3C\cdot$. Hence, we assign the peak with MW 148 to p-acetylbenzaldehyde.

The peak corresponding to a compound with molecular weight 134 was assigned to 4-methylacetophenone based on matching spectra with the NIST database (NIST chemical webBook), and also based on ruling out other reasonable structures. For example, it cannot be 4-ethylbenzaldehyde because its MS lacks significant features of the 4-ethylbenzyaldehyde fragmentation pattern (m/z 134 as the strongest ion, and m/z 105 with 45% abu relative to 134); nor can it be p-vinylbenzyl alcohol for it lacks m/z 105 as the strongest ion. [126, 127]

Previous work in HTW shows that benzyl alcohol may form benzaldehyde and toluene. [115] Katritzky et al. show that at 250°C, benzyl alcohol forms dibenzyl ether, benzaldehyde, and toluene in 10, 9, and 4% yield respectively after one day. The pathway is explained by disproportionation of the CH_2OH moiety to CH_3 and CHO. It is reasonable to speculate that a similar pathway takes place here to provide 4-

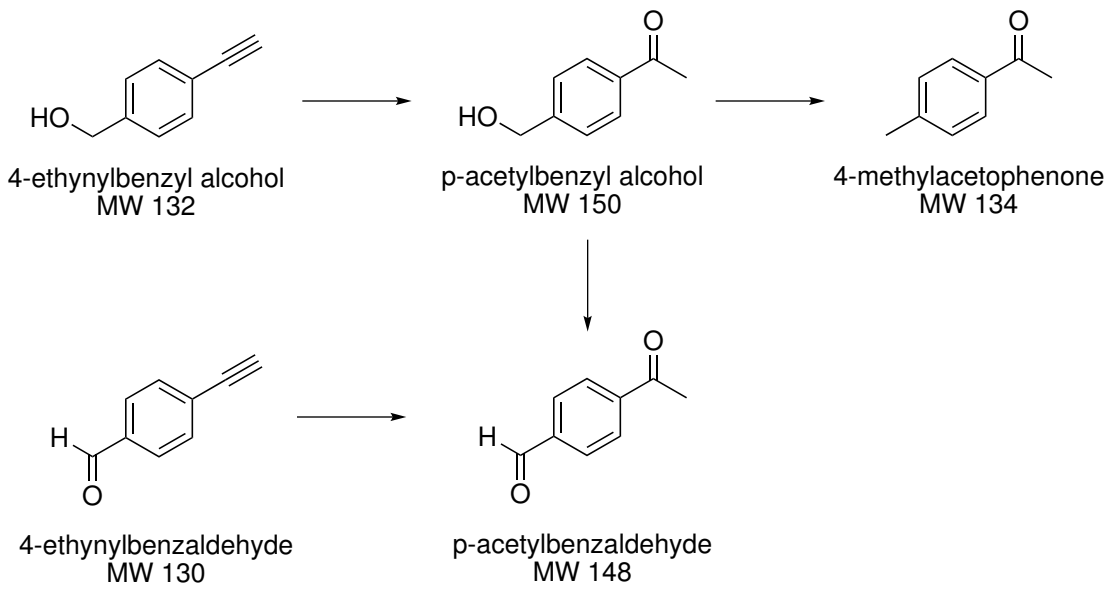

Figure 5.6: Pathways of impure 4-ethynylbenzyl alcohol with $In(OTf)_3$ catalyst in HTW.

methylacetophenone and p-acetylbenzaldehyde in low yields, as depicted in Figure 5.6. Note than unlike the preceding examples, 4-ethynylbenzyl alcohol did not dimerize.

The product p-acetylbenzyl alcohol was not commercially available. Hence, we needed an alternative method by which to quantify our experimental results. The literature in FID shows that the FID response factor for any given compound can be modeled as a linear combination of response factors for the comprising functional groups. In other words, a sort of Benson-Group-Increment-Method exists for FID response factors. By this point in our research, we had already performed alkyne hydration experiments for many different alkynes. Our research database includes calibration parameters for many alkyne-ketone pairs. We used this data to form a correlation between the calibration parameters of alkynes and of ketones. We then tested the correlation against the known pairs of alkyne-ketone calibration parameters. Among the monosubstituted phenyl alkynes, the ability to predict the ketone calibration parameters was very good. No more than 7% error was incurred for 10 mM concentrations (this high concentration corresponds to a typical reaction sample

of complete conversion), and was less for lower concentrations. The average error in this method was computed as 3%, based on the correlation's ability to compute the concentration of ketone given the alkyne calibration used in developing the correlation. This level of uncertainty should be tolerable for our purposes. Hence, we used this correlation to predict the calibration parameters of p-acetylbenzyl alcohol given the calibration parameters of 4-ethynylbenzyl alcohol. Further details regarding our correlation are available in the Appendix.

A true kinetic mechanism would be based upon the pathways illustrated in Figure 5.6. Applying such a mechanism to our own data set, however, is impractical because the side products are present in low quantities, and because of significant peak overlap between 4-ethynylbenzaldehyde and 4-methylacetophenone. Thus, we chose to model the reaction with a lumped "side component" term, C, that represented the quantities of 4-methylacetophenone, 4-ethynylbenzaldehyde, and p-acetylbenzaldehyde summed together. This greatly simplified the kinetic model while still affording a respectable estimate of the rate of hydration – the latter being our main goal in this study. Hence, Equation 5.2 was used to model the kinetics. Since C was taken to be the sum of the concentration of all three side components together; C_0, the initial concentration of lumped side components, was taken to be the initial concentration of 4-ethynylbenzaldehyde impurity in the reaction system. Hydration rate constant k_H was computed as 0.076±0.006 L s^{-1} mol^{-1}. The data set with 95% confidence and the model fit are depicted in Figure 5.7.

$$\begin{aligned} \frac{dA}{dt} &= -k_H C_{WTLA} C_A - k_2 C_A \\ \frac{dB}{dt} &= k_H C_{WTLA} C_A \\ \frac{dC}{dt} &= k_2 C_A \end{aligned} \tag{5.2}$$

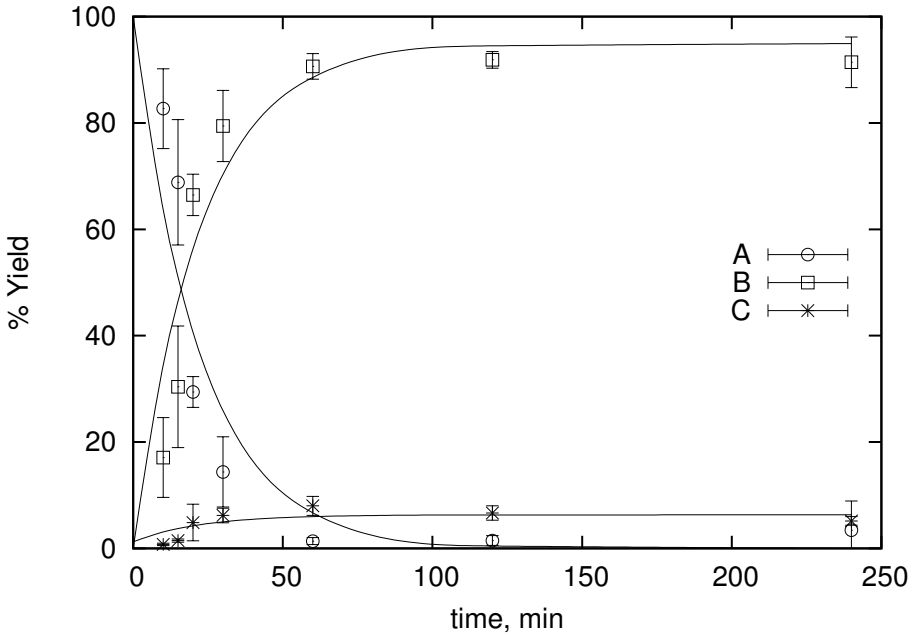

Figure 5.7: Conversion of 4-ethynylbenzyl alcohol (circles) to p-acetylbenzyl alcohol (squares) at 150° C with lumped side components (stars). Error bars depict 95% confidence intervals.

Upon close inspection of Figure 5.7, a peculiar feature is visible. The formation of ketone product and the depletion of alkyne starting material both follow a sigmoidal curve. Sigmoidal curves implicate autocatalysis. To our knowledge, an autocatalyzed alkyne hydration mechanism is nowhere described in the literature. Thus, it would be very interesting to repeat these kinetic experiments in an autoclave reactor, with higher concentrations and at a lower temperature so that this strange feature could be studied with greater precision.

Curiosity compelled us to model the reaction data we have with an autocatalysis term in addition to the second-order WTLA catalysis term, Equation 5.3. Analysis produced the data fit depicted in Figure 5.8. The fit is good. Yet, we maintain that the extraordinary postulate of autocatalysis will need extraordinary evidence. More questions are raised by autocatalysis than are answered, particularly regarding the mechanism of autocatalysis. Hence, we will accept the second-order rate constant for hydration of 4-ethynylbenzyl alcohol to serve the purposes of this work. We leave the

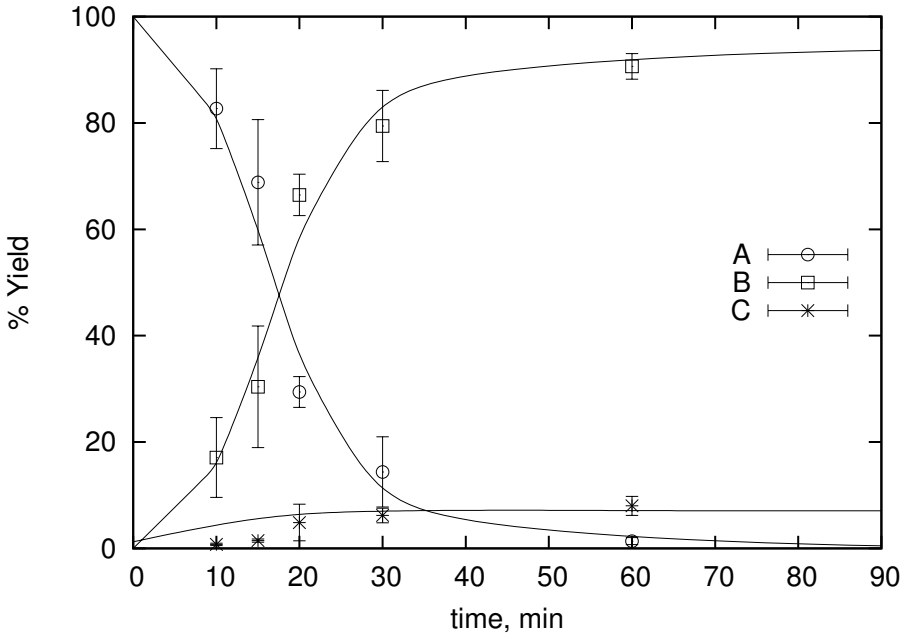

Figure 5.8: Conversion of 4-ethynylbenzyl alcohol (circles) to p-acetylbenzyl alcohol (squares) at 150° C with lumped side components (stars). Error bars depict 95% confidence intervals. Data fit to second-order and autocatalytic pathways.

exploration of potential autocatalysis to future studies.

$$\begin{aligned} \frac{dA}{dt} &= -k_1 C_{WTLA} C_A - k_2 C_A - k_3 C_A C_B \\ \frac{dB}{dt} &= k_1 C_{WTLA} C_A + k_3 C_A C_B \\ \frac{dC}{dt} &= k_2 C_A \end{aligned} \tag{5.3}$$

5.1.5 4-Ethynylbenzonitrile

At 175°C with a 2-hr reaction time, an $In(OTf)_3$ loading of 10.3 mM, and a 4-ethynylbenzonitrile loading of 0.22 M, an average 3.4% yield of p-acetylbenzonitrile was achieved. However, an average of 59% of the initial moles of substrate loaded could not be accounted for. Reaction at 150°C provides analogous results. Reaction

for three hours produces 2% yield of the ketone, but presents a 47% molar loss of the starting material. This trend continues with time: 4% yield and 66% material loss at 7 hours; 2% yield and 74% material loss at 12 hours.

GC/MS showed the formation of two compounds which help explain these results: one with MW 254 and one with MW 381. Given the formation of dimer and trimer in other alkyne hydration experiments, we assigned these peaks to the dimer and trimer of the alkyne starting material, p-cyanophenylacetylene, which has molecular weight 127. Higher order oligomers were not observed by GC/MS. However, this does not rule out their presence; high molecular weight species may not volatilize well enough for GC analysis.

Other possible causes for the systemic loss of material were ruled out. Reactors loaded to be just 40% full at reaction conditions showed material losses on par with reactors loaded in the typical fashion, 95% full at reaction conditions. The integrity of the calibration parameters are ensured by good molar recoveries of "$t = 0$" reaction samples, wherein the reactor is loaded with material as for a reaction, but instead of reaction at 150°C, the $t = 0$ reactor is kept refrigerated, and is then unloaded and analyzed with all the other reaction samples. The average recovery of 4-ethynylbenzonitrile from $t = 0$ reactors was 96%. Hence, we conclude that alkyne hydration is a subordinate reaction pathway for 4-ethynylbenzonitrile, and that oligomerization predominates.

With hydration being a minor pathway, we could not offer kinetic rate constants with accuracy. However, an order-of-magnitude computation places the rate constant at 0.0001 L s^{-1} mol^{-1}, assuming that all of the catalyst is available for hydration. This may not be the case. A closer study of the dimerization and trimerization processes would be needed to check this assumption.

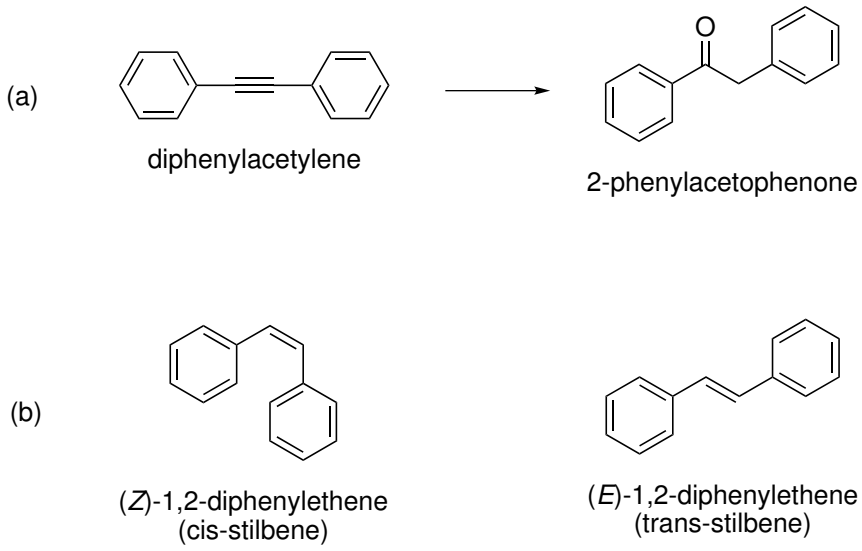

Figure 5.9: (a) Hydration of diphenylacetylene to 2-phenylacetophenone. (b) Impurities cis- and trans-stilbene are present in low concentrations.

5.1.6 Diphenylacetylene

The hydration of diphenylacetylene to 2-phenylacetophenone, Figure 5.9, proceeds more slowly than does the hydration of 1-phenyl-1-propyne. After five hours at 200°C with a catalyst loading of 12 mM $In(OTf)_3$ and an initial diphenylacetylene concentration of 240 mM, 24% 2-phenylacetophenone is produced. Raising the temperature to 225°C greatly increases the rate to achieve 94% yield after 12 hours. No side products were formed in significant yield. However, both isomers of stilbene were identified – both in the reaction samples and in samples of unreacted material. Stilbene levels were quantified and are presented in Table 5.1 as percents of the total organic material added to the reactor with errors denoting one standard deviation from the mean. The observed average level of each stilbene increases with temperature and time, but so does the spread in the data. Many of the uncertainty levels place the measurement within error of zero. Hence, for practical purposes we cannot claim the stilbenes as reaction side-products with confidence.

We modeled the system simply as A $\longrightarrow$ B, with a reaction order of one in alkyne

Table 5.1: Stilbene levels present in reaction mixtures, in terms of mol% with respect to the amount of added starting material. Column 'n' represents the number of replicates for each experiment. Error represents one standard deviation from the calculated mean. For this data set, the average concentration of catalyst was 11 mM, and the average initial concentration of diphenylacetylene was 220 mM.

T (°C)	time (hrs)	n	cis-stilbene	trans-stilbene
–	0	4	0.02±0.02	0.05±0.03
200	5	4	0.036±0.008	0.084±0.005
225	3	4	0.7±0.6	1.3±1
225	12	3	2.0±2	2.5±2

and one in catalyst. The results of model fitting against the collected data set are shown in Figure 5.10 in terms of percent yield of 2-phenylacetophenone vs. time. Attempts to model the kinetics with stilbene production terms resulted in unphysical rate constants, or rate constants well within error of zero. The computed specific rate of hydration of diphenylacetylene at 200°C was 0.0016 ± 0.0006 L s^{-1} mol^{-1}. At 225°C, the computed specific hydration rate was 0.012 ± 0.002 L s^{-1} mol^{-1}.

Some side-products were detected for this reaction by GC/MS. These include 1,2-diphenyl-2-propen-1-one, benzil (shown in Figure 5.11), and a yet unidentified compound of MW 168. Signal from these compounds was so small that they were completely ignored in the quantitation.

5.1.6.1 Diphenylacetylene hydration in the presence of salt

The low volatility of diphenylacetylene made it very attractive for application in additional studies of hydration. We wanted to test the effect of added salt upon the rate of hydration. If the reaction proceeded through a carbocation intermediate, we would expect that decreasing the dielectric constant of the reaction medium would destabilize the carbocation, and therefore would decrease the reaction rate. An easy way to decrease the dielectric constant of water is to simply add a salt, such as LiCl.

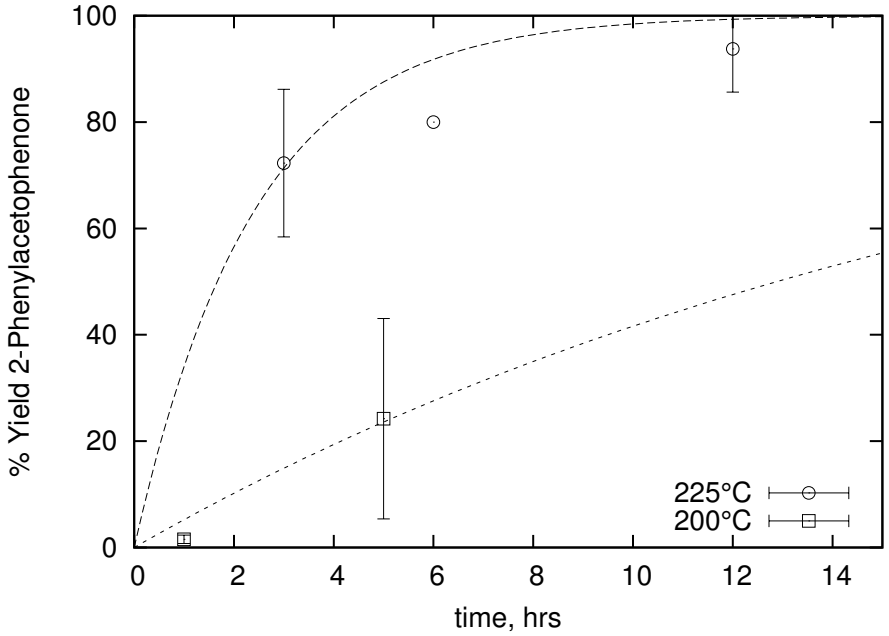

Figure 5.10: Diphenylacetylene hydrates to form 2-phenylacetophenone.

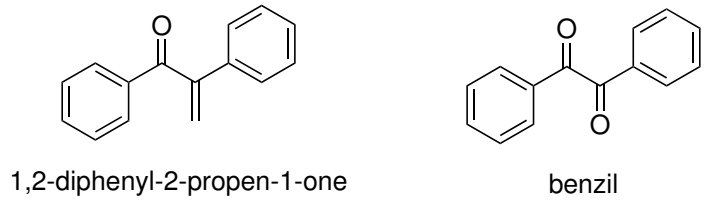

Figure 5.11: Diphenylacetylene hydration results in some side-products.

Table 5.2: The effect of LiCl salt upon the hydrolysis of diphenylacetylene. All data were collected at 225°C with a 3-hr batch holding time. Reported errors represent standard deviations.

[LiCl]/M	% Conversion	% Yield of 2-phenylacetophenone
0	75±11	74±14
0.20	13±3	14±2
2.0	0±0.3	1±0.4

We conducted experiments at two different levels of LiCl loading, 0.2 and 2.0 M, against a condition with no added salt. These experiments were conducted in replicates of three to five experiments for each condition, using 1/4″ Swagelok reactors at 225°C with a batch holding time of 3 hrs. Loading of $In(OTf)_3$ catalyst was the same 5 mol% relative to substrate for all experiments. The calibration standards for these experiments were matrix matched to the LiCl concentration in the reaction samples, as well as to the water concentration.

Our results, found in Table 5.2, show that the rate of diphenylacetylene hydration is greatly suppressed by the presence of LiCl. A concentration of 0.2 M LiCl will reduce the the yield of 2-phenylacetophenone from 74% to only 14%. In the presence of 2.0 M LiCl, the reaction is practically halted.

Hence, we consider this experiment as evidence consistent with an elimination pathway.

5.1.6.2 Diphenylacetylene hydration in methanol

Some hydration preparations may also add alcohols if present and in the absence of water. We wanted to test whether $In(OTf)_3$ would also prepare a methyl ether if methanol is used as the solvent/reagent instead of water.

We carried out experiments in methanol in the same 1/4″ Swagelok reactors with no added water. However, no efforts were made to ensure that the added methanol

Table 5.3: Hydration of diphenylacetylene in methanol. "Ketone" denotes 2-phenylacetophenone, and "ether" denotes 1-methoxy-1,2-diphenylethane.

Temperature (°C)	time hrs	% X	% Yield ketone	% Yield ether
200	5	38	14	16
225	6	90	66	0

was dry. The substrate and $In(OTf)_3$ catalyst loadings were about 0.19 and 0.01 M respectively, analogous to other diphenylacetylene experiments in water. Additional conditions, and the experimental results, are found in Table 5.3. The data at 200°C represents averages for two experiments; while the data at 225°C represents a single reaction. Because of the increased pressure of methanol at its saturation condition, relative to water, experiments with methanol were difficult to carry out in Swagelok reactors. Since the ether was not commercially available, we estimated its calibration parameters with those of 2-phenylacetophenone. We estimate the error accrued by this method to be about 6%.

At 200°C, the ether was formed in 16% yield, as identified by GC/MS. Ketone 2-phenylacetophenone was also formed in about the same amount, 14% yield. At 225°C, no ether is recovered at all. As for reaction in water, reaction in methanol led to some side-products in low yields: mainly benzil and trans-2-methoxystilbene, shown in Figure 5.11. Other peaks were present, but were in too low concentration to offer a reliable mass spectrum. As future work, experiments at temperature lower than 200°C could be worth exploring in an attempt to increase the selectivity for the ether.

5.2 Aliphatic alkynes

5.2.1 5-Decyne

We wanted to better understand the generality of alkyne hydration in HTW with WTLA catalysis, so we included an aliphatic alkyne, 5-decyne, in our list of substrates for hydration. The hydration of 5-decyne to 5-decanone is illustrated in Figure 5.12. We collected reaction samples at different times at 225°C by the typical experimental method. We found that, although 5-decanone was produced in good yield, we also produced roughly 21 other products. Some of the structures identified by GC/MS as plausible matches for these many side products include decadienes, substituted menthenes, 3- and 4-decyne, decahydronaphthalene, alkyl-substituted cyclopentenes and cyclohexenes, and indenones. Their low concentration and weak signal precluded precise identification. Based on GC-FID signals, we estimate that all these side-products together represent about 12 mol% of the initial material loaded to the reactor at the longer reaction times (12 to 24 hours).

The reaction is slower than the aromatic-stabilized hydration reactions. We modeled the reaction with the same equations used for 4-ethynylbenzaldehyde in Equation 5.2, except with term 'C' representing the lumped sum of all the side-products together, by our best estimate. We estimate the kinetic rate constant for hydration of 5-decyne to be $0.0040 \pm .0002$ L s^{-1} mol^{-1}. The fit of our estimate to the kinetic model is shown in Figure 5.12.

5.3 Discussion

Our discussion of the mechanism of alkyne hydration should begin with the evidence from Chapter IV. Our studies of 1-phenyl-1-propyne gave evidence for both possible mechanisms presented in Figures 4.5 and 4.6. We found that the activation energy for hydration with $In(OTf)_3$ was roughly the same as the activation energy for

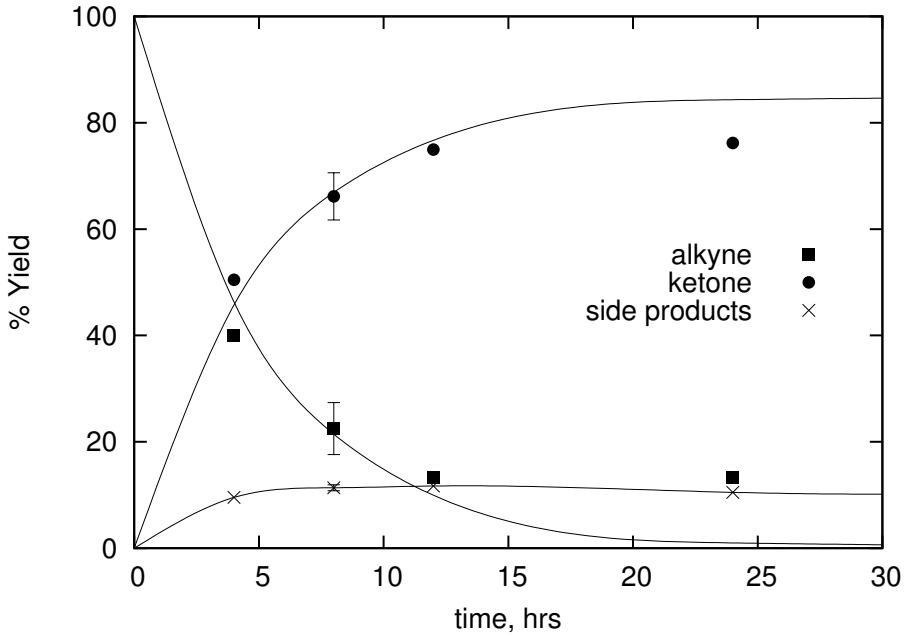

Figure 5.12: Aliphatic 5-decyne hydrates to form 5-decanone as the major product, and a myriad of other minor alkyl compounds, lumped together as "side products". The error bars on the 8-hr datum represent one standard deviation. The other points represent single experiments. Reactors were loaded to contain 220 mM 5-decyne and 11 mM $In(OTf)_3$ at the reaction temperature, 225°C.

hydration in 50% sulfuric acid solution. If the mechanism of reaction at two different conditions is the same, then the activation energy for the two conditions will be the same. The converse of this statement is not necessarily true. That is, if the activation energies for two different conditions are the same, the mechanism is not necessarily the same, even though it often is. At the very least, the agreement among activation energies is consistent with electrophilic addition. Our plot of %yield vs pH for the different catalysts tested, Figure 4.2, shows that the reactivity of $In(OTf)_3$ cannot be explained entirely by pH alone, suggesting catalysis by Lewis acid behavior.

As part of Chapter V, we tested diphenylacetylene hydration in the presence of methanol and in the presence of LiCl salt. A full carbocation is very reactive. It would be expected to form a bond with any nucleophile present in solution. We noted that 1-chloro-1,2-diphenylethane was not observed, although the rate with LiCl was very slow. However, diphenylacetylene hydration in methanol did produce some 1-methoxy-1,2-diphenylethane. Other alkyl groups may also combine with a carbocation. We only observed dimerization of the phenylacetylenes; product ketone was never observed to couple with the starting material, though product and starting material were both present only in low concentrations, especially compared with the concentration of water.

Some of the substrates in this study were chosen because they form a series of alkynes with increased steric hindrance. Table 5.4, which organizes the hydration rate constants determined as part of this study, shows that phenylacetylene hydrates faster than 1-phenyl-1-propyne, which hydrates faster than diphenylacetylene. Prima facia, one might suppose that this ordering of reactivity supports a metal-catalyzed route, which presumably would be more sensitive to steric hindrance. However, previous researchers have found that hydration of phenylacetylene is almost 30 times faster than 1-phenyl-1-propyne under purely Brönsted catalyzed conditions. [125]. This behavior was explained by considering the difference in rehybridization energy.

Table 5.4: Second-order kinetic rate constants the the hydration in water of all the alkynes tested as part of this study.

Alkyne	T (°C)	k (L s^{-1} mol^{-1})
4-tert-butyl-phenylacetylene	150	0.0013±0.0002
4-ethynyltoluene	150	0.052±0.004
phenylacetylene	150	0.057±0.003
4-ethynylbenzyl alcohol	150	0.086±0.006
1-phenyl-1-propyne	150	0.0015±0.0001
	175	0.0120±0.0007
	200	0.096±0.005
	225	0.27±0.03
diphenylacetylene	200	0.0016±0.0006
	225	0.012±0.002
5-decyne	225	0.0040±0.0002

For phenylacetylene, C_{sp}–H rehybridizes to C_{sp^2}–H in the transition state. This is easier than the corresponding change necessary for 1-phenyl-1-propyne, wherein C_{sp}–C rehybridizes to C_{sp^2}–C in the transition state. [125] With $In(OTf)_3$ catalysis in HTW at 150°C, phenylacetylene hydrates 38 times faster than 1-phenyl-1-propyne.

Lastly, the ease of hydration of all the aromatic alkynes compared to hydration of 5-decyne also supports the formation of a vinyl carbocation. However, it is not inconsistent with Lewis-acid catalysis. Aromatic rings may also stabilize the complexation of an alkyne with indium.

5.4 Conclusions

If we look more closely at the mechanistic pathways debated here, we see that the primary difference is the formation of a full vinyl carbocation in the pathway for electrophilic addition, as against the formation of a 3-centered carbocation in the pathway for dihydro-oxo-biaddition, wherein a positive charge is shared among two carbons and a metal complex. The rate determining step of these two pathways is so

similar in nature, varying only in degree and not in kind, that it is no wonder that the supporting data collected confounds then.

As future work, data may be collected to improve our estimates for the hydration of phenylacetylene and 4-ethynyltoluene, and further data may be collected with electron-withdrawing substituents attached to phenylacetylene. A Hammett analysis plot may then be used to distinguish between the electrophilic addition mechanism, which would give a negative Hammett reaction constant less than -3, and the dihydro-oxo-biaddition mechanism, which would give a negative Hammett reaction constant of lower absolute value, between 0 and 3. Based on the current data, we hypothesize that both mechanisms may be at work.

CHAPTER VI

Anisole Hydrolysis

Destitutus ventis, remos adhibe

If the wind will not serve, take to the oars.

6.1 Introduction

The hydrolysis of aryl alkyl ethers is an important transformation due to its use in the deprotection of alcohols. Protection is used to mask a functional group, such as an alcohol, from reactions desired elsewhere on the molecule. The formation of a methyl ether in place of a hydroxy group is one example of protection. Later on in a multi-step synthesis, the protection ether must be removed to present the alcohol anew. Most recipes for this transformation call for the use of chlorinated solvents and strong Lewis acids, such as BF_3 or BCl_3. New methods are continuously developed with improvements in selectivities, yields, reaction times, simplicity, and/or cost. For example, researchers developed a boron-trichloride tetra-n-butylammonium iodide system for readily deprotecting methyl-, ethyl-, and benzylnaphthyl ethers at low temperatures (-78°C warmed to rt) over 1-2 hours. [128] Notably, benzyl ethers are selectively cleaved in the presence of methyl ethers, and basic functional groups are well tolerated with additional equivalents of BCl_3. [128] In another deprotection study, lithium-ethylenediamine in a THF-mediated cold system successfully depro-

tected sterically hindered alkyl ethers such as 2,6-di-tert-butyl-anisole, a feat the boron-trichloride tetra-n-butylammonium iodide system failed to accomplish. [129] However, the reagent was so aggressive that reduction of the aromatic ring often reduced yields. [129] Chakraborti et al. explored aryl alkyl cleavage by thiolates that were generated in situ by reaction of base with PhSH. [130] Others researched ionic liquids of 1-n-butyl-3-methylimidazolium bromide and p-toluenesulfonic acid (or some other Bronsted acid) at 115°C over 12 to 48 hours. [131] Research efforts have also focused on merely comparing the behavior of deprotection reagents. For example, the study by Hwu et al. compared the behaviour and effectiveness of two different alkali organoamides ($NaN(SiMe_3)_2$ and $LiN(i{-}Pr)_2$) under similar conditions. [132] Konieczny et al. focused efforts on demonstrating the extent to which $BF_3 \cdot SMe_2$ can selectively cleave allyl or methyl phenyl ethers depending on reaction conditions and the ether's position on the ring. [133]

Research in HTW has shown that anisole may hydrolyze to form phenol without any added catalyst. [67, 68] If it could be made practical, ether hydrolysis in HTW could avoid the use of chlorinated solvents and strong Lewis acids. Together, the work of Klein et al. [68] and Patrick et al. [67] show that the reaction in HTW and in SCW is most likely S_N2, catalyzed by water. Both authors determine a positive Hammett analysis constant for the reaction, corroborating their mechanistic assignment.

To correct for the possible interaction of metal and substrate, the Savage lab carried out experiments in quartz capillary reactors. These experiments were all carried out by Stephanie Fraley in the summer of 2006, who was then an undergraduate student research assistant, under the guidance of Craig Comisar, who was then a graduate student research assistant in the Savage laboratory. In the following account, Fraley's experimental results are reanalyzed, interpreted, and integrated with the literature concerning anisole hydrolysis in HTW. Later, the results of this study will be integrated with insight gained from experiments with WTLA catalysis.

6.2 Anisole hydrolysis without added catalyst

Reactions were carried out by the applicable general procedure described in chapter 3. Reactions were executed in quartz capillary reactors (6-mm outer diameter, 2-mm inner diameter, internal volume approximately 590 μL). Reactors were loaded at room temperature such that the expansion of water at reaction conditions rendered them 95% full at the reaction temperature; the thermophysical properties of the system were approximated as the thermophysical properties of water, and steam tables were used to estimate the liquid density at reaction conditions. Each reactor was first loaded with deionized, distilled water and then loaded with 10 μL of anisole. Reactors were heated in a Techne sand bath and cooled by forced convection with air at ambient conditions. After thermal quenching, reactors were snapped open, unloaded, and rinsed with acetone (Aldrich, reagent grade) into a 10-mL class A volumetric flask, which was then diluted to volume with acetone.

Analysis of the product stream was carried out by GC/MS and GC-FID. GC/MS was used to verify the contents of the product stream, and GC-FID was used to quantify the components. Gas chromatography was carried out on a 6890 Agilent system equipped with an HP-5 (GC-FID) or HP-5ms (GC/MS) capillary column (50 m x 0.2 mm x 0.33 μm) and split/splitless injector. Standardization was achieved for the FID by preparing calibration standards for each analyte.

Reactions were carried out at different times at 350, 365, 380, and 400°C. Since the critical temperature of water is 374°C, the last two temperatures are within the supercritical regime. The subcritical experiments in this work are all carried out at the saturation condition of water, and thus have a defined water density. In supercritical water, the water density may be altered by the pressure. The 380°C experiments were carried out with a water density of 0.40 g/mL; the 400°C experiments, 0.20 g/mL. The experiments were carried out without replication except for one condition (69 hrs, 365°C) at which 3 replicates were done. At 350°C, no products other than phenol

were formed. At 365°C and above, side products were formed: benzene and benzyl alcohol. At 400°C, toluene and benzaldehyde were also formed.

The data are plotted in Figure 6.1 as % yield of phenol and % recovery of anisole. Figure 6.1 also shows the result of data fitting, which will be explained further. In supercritical water at 380°C with a water density of 0.4 g/mL, a maximum of 48% yield was achieved after 24 hours. If near-critical water is used instead, and the reaction temperature is lowered to 365°C, 80% yield of phenol is achieved after 24 hours. Lowering the temperature another 15°C causes the rate to slow dramatically, achieving only 58% yield at 65 hours. Increasing the temperature to 400°C increased the rate of conversion of anisole, but decreased the phenol yield due to thermal degradation reactions. Hence, the optimal temperature for anisole hydrolysis in HTW is 365°C; this temperature gives the best yield by maximizing hydrolysis rates while keeping decomposition rates low. At 400°C, a significant fraction of the original starting material decomposed or over oxidized to form benzene, benzaldehyde, benzyl alcohol, and toluene, in that order of abundance.

Based on the experimental data, 365°C achieves the best yield in short times. Higher temperatures promote greater thermal degradation products. Lower temperatures have significantly slower kinetics. Previously, the HTW literature on anisole hydrolysis neglected reaction at 365°C. In fact, researchers generally neglected a study for the optimum temperature altogether.

In order to determine the reaction kinetics, we fit the experimental "%yield of phenol", "%recovery of anisole", and "%yield of by-products" data to a system of rate equations, shown in Equation 6.1, where A is anisole concentration, B is phenol concentration, D is the total concentration of all side-products, and W is water concentration. Expressing the rate of hydrolysis with a 2.79-order in water will be corroborated by evidence later in this section. Since each decomposition product was found in relatively low yield, we chose to lump them together. Figure 6.1 shows that

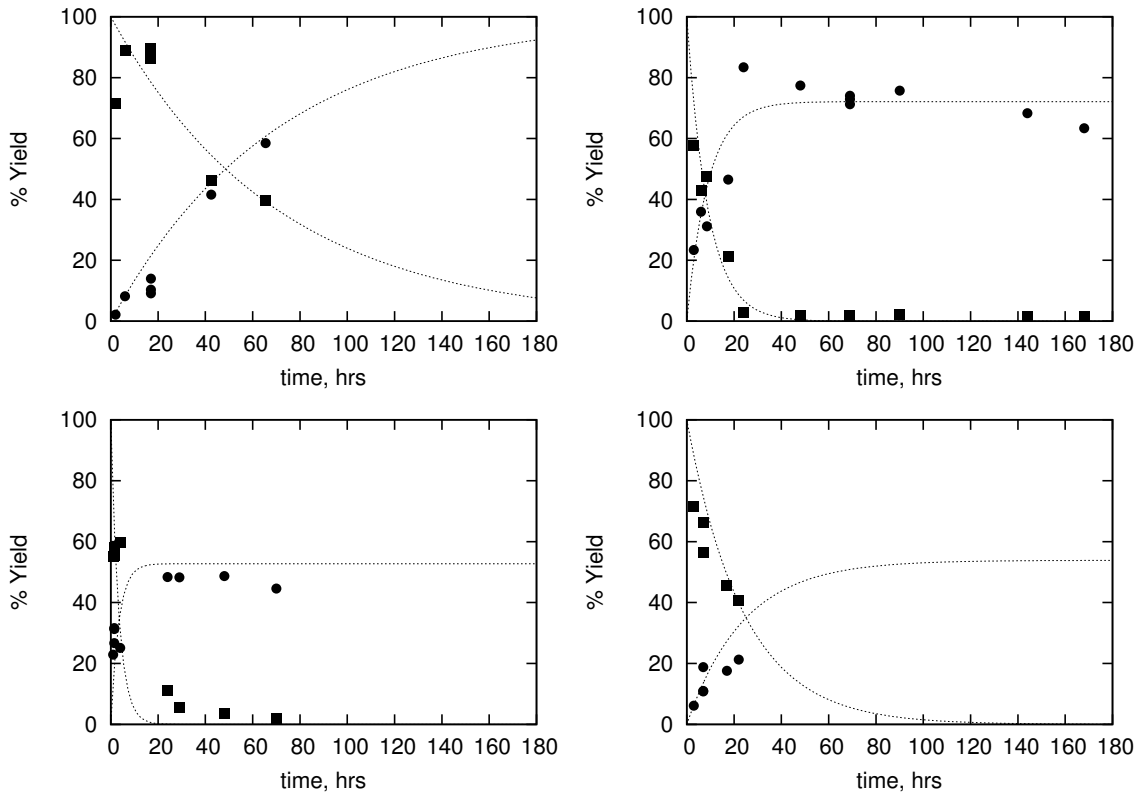

Figure 6.1: Hydrolysis of anisole to phenol. Circles represent %yield of phenol; squares represent %anisole unreacted. Dashed lines represent fit to model equations 6.1, with k_D equal to zero for reaction at 350 and 400°C, as no decomposition products were detected at these conditions. (a) top left, 350°C. (b) top right, 365°C. (c) bottom left, 380°C. (d) bottom right, 400°C.

the result of data fitting was generally good.

$$\begin{aligned} \frac{dA}{dt} &= -kC_W^{2.79}C_A - k_D C_A \qquad (6.1) \\ \frac{dB}{dt} &= kC_W^{2.79}C_A \\ \frac{dD}{dt} &= k_D C_A \end{aligned}$$

(6.2)

We tested the effect of water density in the supercritical regime, at 380° C, and found a strong relationship. This is consistent with literature results from the Klein lab. [68] One beautiful aspect of supercritical water is the ability to change water density and hence water concentration, without changing temperature. For this data set collected at 380° C, we calculated the pseudo-first-order hydrolysis rate constant k_H, and plotted it against water concentration on log-log coordinates in Figure 6.2. Alongside our data, we plotted the analogous data from the Klein lab. [68] We used the data fitting software Scientist™ to estimate, with nonlinear regression, the slope of the line formed by our data set to be 2.5 ± 0.2. Similarly, we estimated the slope formed by the data set from Klein et al. to be 2.8 ± 0.1. Given the scatter in our data, we judge these results to be in good agreement.

The two data sets are slightly offset from one another, likely due to the difference in experimental apparatus. Klein's experiments were conducted in 1/4″ stainless steel reactors, while the Fraley data set was obtained with 2-mm quartz capillary reactors. Experiments were not conducted assuring that anisole hydrolysis reactions in these two vessels is commensurate. Further, since the experiments were also conducted in different labs, there may be systematic error in reaction temperature, as different equipment was used to heat the reactors in the two studies. Many other experimental variables may explain the systematic deviation. However, in each set of experiments,

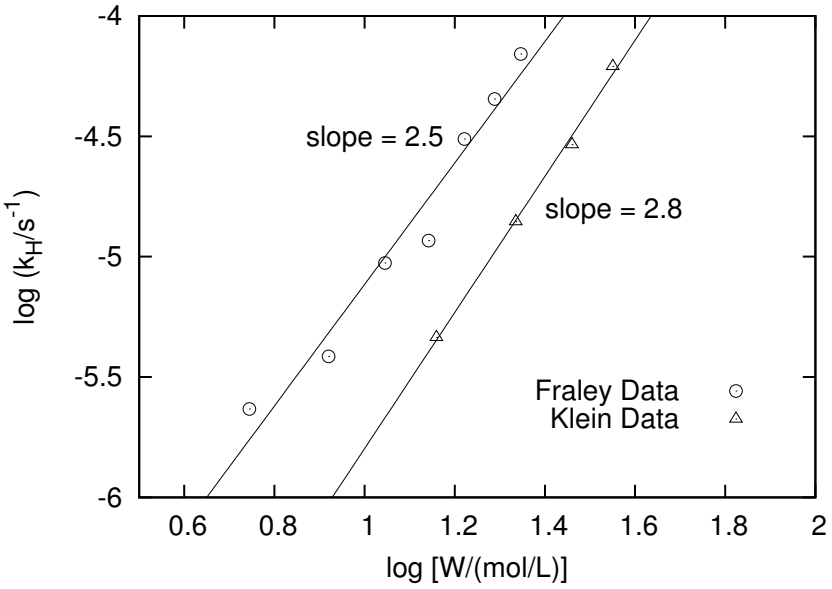

Figure 6.2: Hydrolysis rate constant k_H vs water concentration at 380° C. Data from Klein et al. were taken from reference [68].

it is only the water density that is being varied. Hence, the slope of each line still offers order in water, largely decoupled from other experimental factors.

This result suggests that hydrolysis of anisole is almost third order in water. We supposed that this should also be the case for subcritical water. We combined our data with the other literature data for anisole hydrolysis in HTW, and plotted all on an Arrhenius plot, with rate constant k first order in anisole and 2.79-order in water, according to the published Klein data. [68] The agreement among all the data was good, as shown in Figure 6.3. This strongly supports the notion that anisole hydrolysis is almost third order in hot water, when the S_N2 mechanism predominates over the acid- and base-catalyzed mechanisms. From the Arrhenius plot, we determine activation energy to be 41 kcal/mol and frequency factor to be $10^{5.1}$ s^{-1} $M^{-2.79}$.

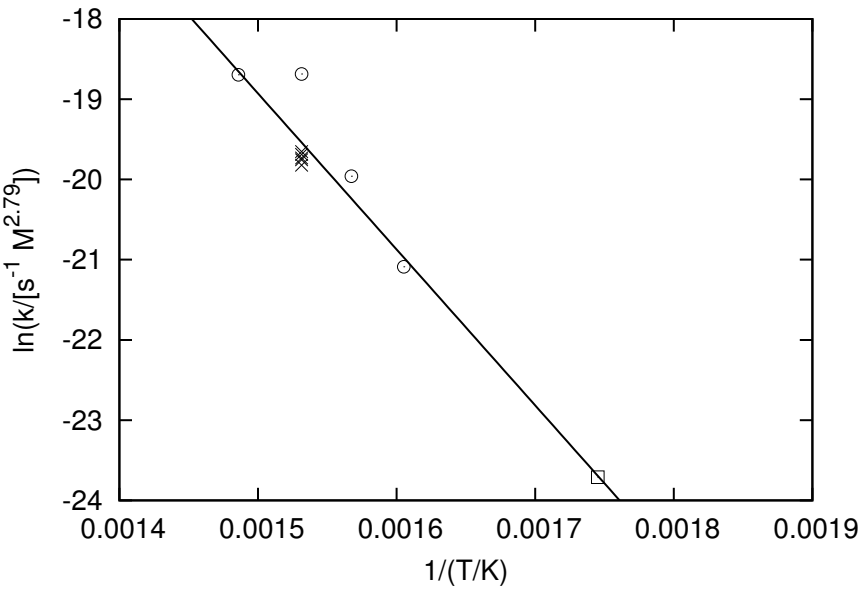

Figure 6.3: Arrhenius plot for hydrolysis of anisole to phenol. Data is taken from three labs: Patrick et. al. [67] (square), Klein et al. [68] (Xs), and Fraley (circles).

6.3 Conclusions regarding uncatalyzed anisole hydrolysis in HTW

Given the data presented thus far for anisole hydrolysis, there seems to be three factors that are most important in determining the optimal conditions of uncatalyzed anisole hydrolysis in HTW. Since order in water concentration is almost three, conditions should be chosen to maximize water density. However, the activation energy for this system is also quite large, 41 kcal/mol, indicating that high temperatures are necessary for adequate rates. For saturated liquid water below the critical point, as temperature increases, water density decreases. However, the temperature dependence is exponential while the water density dependence is of a third power, so higher temperatures will generally increase the reaction rate ... at least until decomposition reactions become important. We hypothesize that a temperature near 365°C would best optimize uncatalyzed anisole hydrolysis in HTW due to the relatively high water

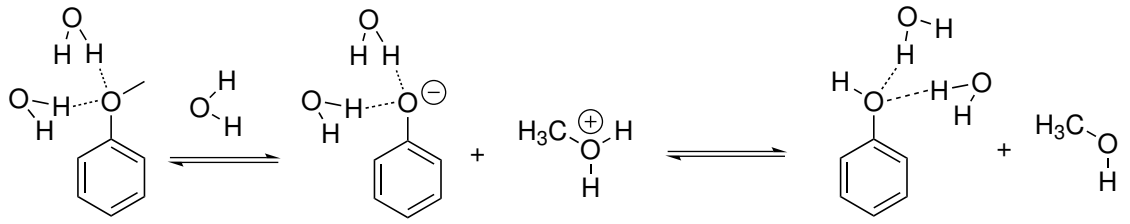

Figure 6.4: The S_N2 hydrolysis of anisole in HTW may proceed through a phenoxide anion that is stabilized by hydrogen bonding with water molecules.

density (compared to the supercritical conditions), high temperature, and low rate of decomposition.

However, there are drawbacks to reaction at this condition. First, the temperature is very high. Since the deprotection of aryl methyl ethers is a reaction of interest to the pharmaceutical and fine chemical industry, a high temperature of 365°C would preclude many application with thermally labile moieties. Second, the pressure required to maintain a saturated liquid condition for water at 365°C is almost 200 atm. Third, decomposition at this temperature is not negligible. Lastly, and perhaps most importantly, the rate is still slow. After 24 hours, only 83% yield is achieved. Longer reaction times only result is lower yields, perhaps due to decomposition reactions. Other methods proceed at milder conditions with better selectivity and shorter reaction times. [128, 133]

The generality of the rate law describing anisole hydrolysis as almost third order in water leads us to posit a mechanism for anisole hydrolysis in HTW (including sub- and super-critical conditions) that may account for this data. We suggest that the most likely role played by water is to stabilize the incipient phenoxide anion, as shown in Figure 6.4.

6.4 Anisole hydrolysis catalyzed by water-tolerant Lewis acids

We supposed that since the customary procedure for aryl alkyl ether hydrolysis involved the use of a Lewis acid, that perhaps a water-tolerant Lewis acid could

improve the reactivity of anisole toward hydrolysis in near critical water. A survey of four different WTLAs alongside mineral acids in HTW at 275°C was carried out in 1/4″ stainless steel reactors. Each experiment was replicated two to seven times, and the resulting 95% confidence intervals recorded. The room temperature pH of each aqueous solution was measured with an Accumet pH meter calibrated with standard buffer solutions at pH 2, 4, and 7. As our lab lacks the equipment to measure pH at reaction conditions, room temperature pH is offered instead, as an estimate of the relative acidity of the reaction media tested.

Figure 6.5 shows percent yield of phenol after 2 hours and 45 minutes at reaction temperature for the different acid catalysts tested. For each experiment, the initial loading of anisole was 160 mM and catalyst loading was 8.0 ± 0.3 mM. Error bars represent 95% confidence. The results demonstrate that indeed WTLA are successful in catalyzing anisole hydrolysis. Some of the WTLAs tested – namely, $In(OTf)_3$ and $Sc(OTf)_3$ were superior to a commensurate loading (by mole) of mineral acids HCl and H_2SO_4. These results were promising, and inspired us to continue studying anisole hydrolysis catalyzed by $In(OTf)_3$.

We began by confirming reaction order in substrate and in catalyst. The analytical procedure for these analyses is exactly analogous to that described for 1-phenyl-1-propyne hydration. To recapitulate the methodology in brief, initial rates are measured for substrate loadings that differ greatly. Here, almost four orders of e were spanned in anisole concentration, from 8.2 to 650 mM. If the reaction is first order, then the rate will not change if substrate concentration changes. Figure 6.6 shows the result of the pseudo-first-order analysis in anisole, where k' (s^{-1}) is the pseudo first order rate constant in substrate, and the the mean concentration of anisole, A (mol/L), is found by taking the arithmetic mean of anisole concentration before and after the reaction. Note that anisole concentration before reaction is calculated based on the amount of anisole added to the reactors (10 μL). Each experiment was repli-

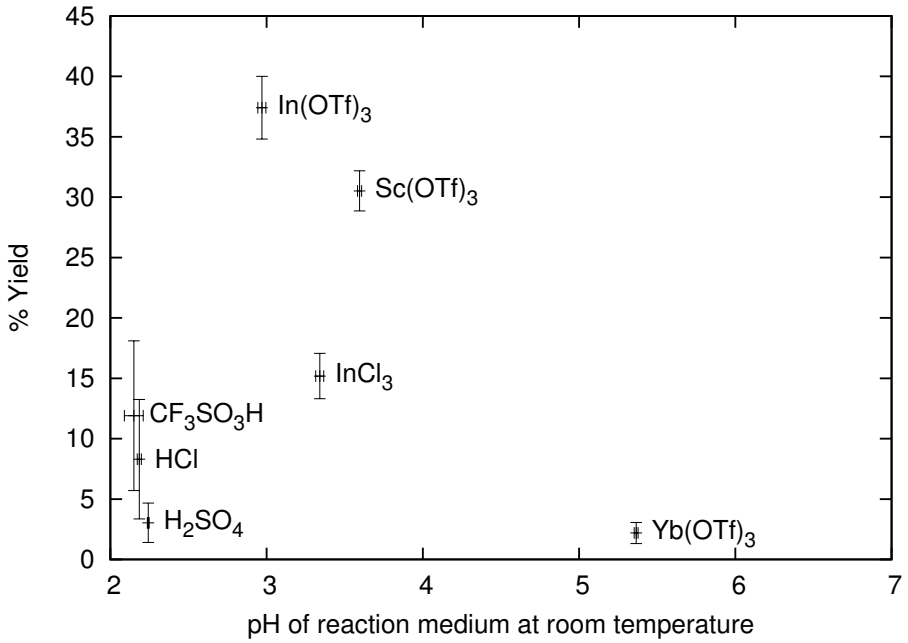

Figure 6.5: Anisole hydrolysis to phenol at 250°C and 2.75 hours; comparison of yield using different catalysts. Initial anisole loading was 160 mM, and catalyst loading was 8.0±0.3 mM.

cated 2 to 8 times, with the average number of replicates being 4.2 per datum. The error bars shown signify 95% confidence intervals in both $\ln(k')$ and $\ln\left(\left[\overline{A}\right]\right)$ The slope of zero indicates that the reaction is first order in substrate.

To find order in catalyst, a similar analysis was carried out, wherein catalyst concentration is varied by almost four orders of e, from 1.8 to 65 mM, and the effect upon rate is measured by calculating the pseudo first order rate constant k′. The concentration of catalyst is assumed to be constant over the period of reaction, and to be given by the amount added to the reactor. Anisole concentration is held constant at 160 mM for all of these experimental runs. Experiments were conducted in replicates of two to eight per datum, with the average number of replicates being 4.4. A slope of unity would indicate that the reaction is first order in catalyst. The experimentally determined slope from Figure 6.7 is 1.33 ± 0.08.

Armed with knowledge of order in substrate and in catalyst, we proceeded to collect data at different times for different temperatures to determine activation energy

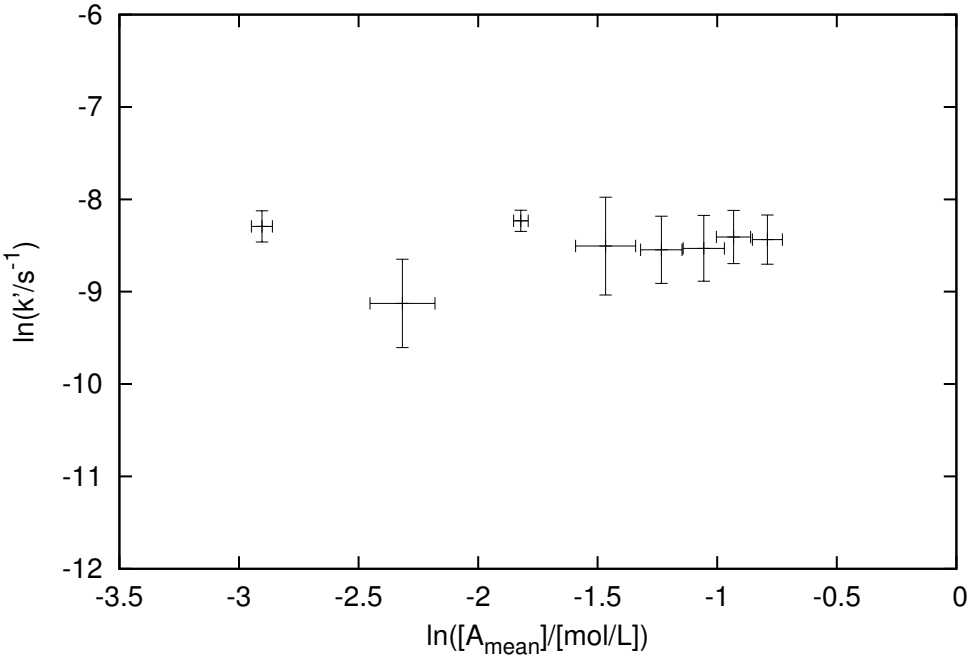

Figure 6.6: Pseudo-first-order plot for substrate in anisole hydrolysis at 275°C with catalysis by $In(OTf)_3$. Catalyst loading was 8.2 mM. Error bars represent 95% confidence intervals.

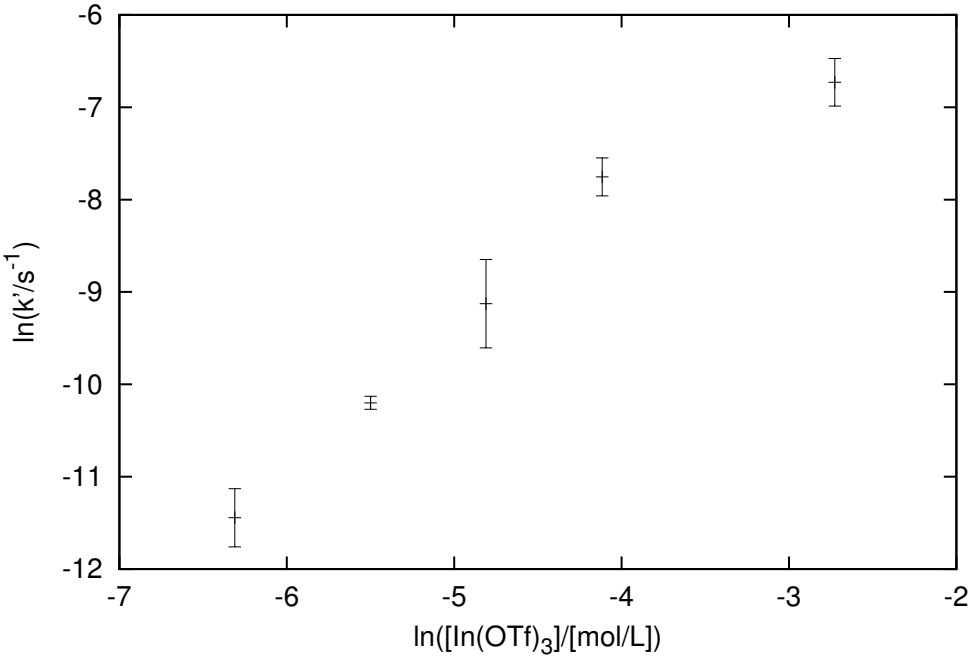

Figure 6.7: Pseudo-first-order plot for catalyst in anisole hydrolysis at 275°C with $In(OTf)_3$. Initial loading of anisole was 160 mM. Error bars represent 95% confidence intervals.

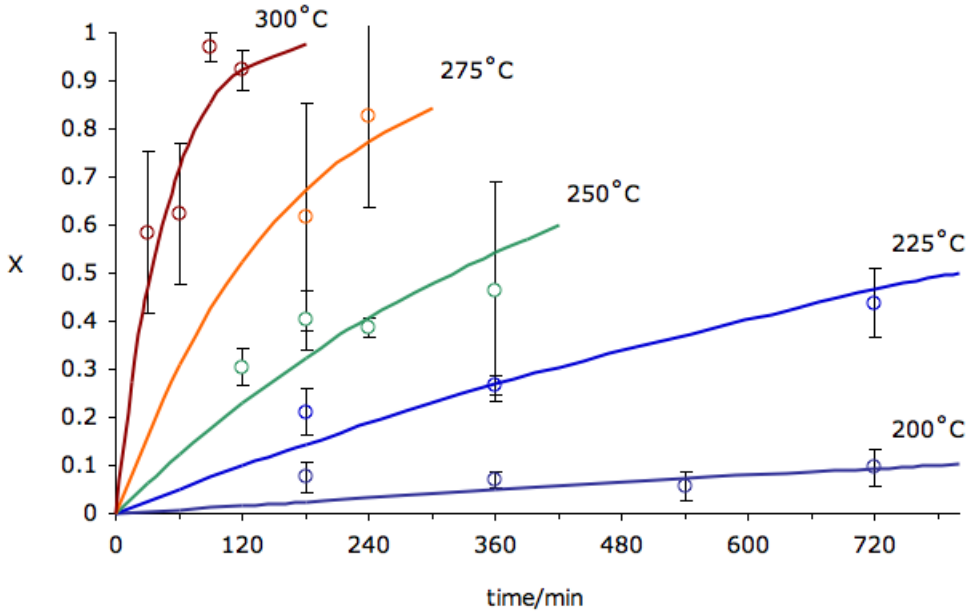

Figure 6.8: Kinetics of anisole hydrolysis at different temperatures with $In(OTf)_3$ catalyst, represented as conversion vs time. Error bars represent 95% confidence intervals.

and frequency factor for $In(OTf)_3$-catalyzed anisole hydrolysis. We performed a series of many experiments with anisole hydrolysis with 160 mM initial anisole loading and 5 mol% $In(OTf)_3$ catalyst at temperatures 200, 225, 250, 275, and 300 °C. The results of our study are depicted in Figure 6.8

We could now determine the activation energy and frequency factor for this reaction with an Arrhenius plot. We plotted the natural log of k against inverse temperature in Kelvin to arrive at Figure 6.9. The activation energy was determined to be 31 kcal/mol; the frequency factor, $10^{10.6\pm0.5}$ s^{-1} L mol^{-1}.

6.4.1 Conclusions regarding anisole hydrolysis with $In(OTf)_3$ catalysis

We have now studied anisole hydrolysis under HTW conditions, and under WTLA catalyst in HTW. We calculated the pseudo-first order rate constant k (s^{-1}) at 365°C for HTW hydrolysis, and compared it to the pseudo-first order rate constant at 300°C for $In(OTf)_3$ catalyzed hydrolysis in HTW. These values are shown in Table 6.1. Com-

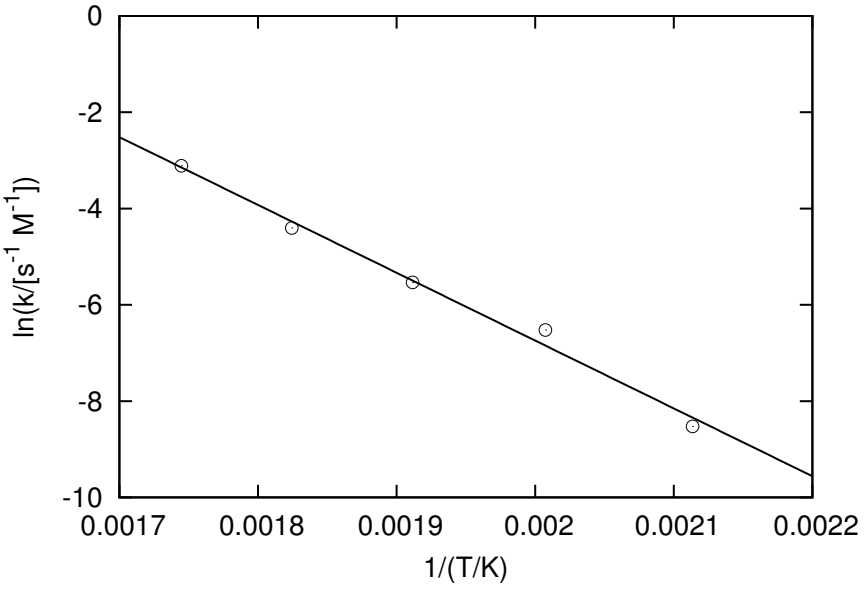

Figure 6.9: Arrhenius plot for anisole hydrolysis with $In(OTf)_3$ catalyst in HTW.

pared to the uncatalyzed route in HTW, anisole hydrolysis with $In(OTf)_3$ catalysis in HTW is much faster. We further calculated the pseudo-first order rate constant for the hydrolysis of anisole to phenol using a more conventional technique that recently appeared in the literature. The method uses 6 equivalents of $BF_3 \cdot SMe_2$ catalyst in CH_2Cl_2. [133] Our estimate of k for this method is based on the single datum presented in the literature and reproduced in Table 6.1. Our method of using $In(OTf)_3$ catalyst in HTW compares favorably to the $BF_3 \cdot SMe_2$ method. This demonstrates that the use of WTLAs in HTW could offer rates and yields that are comparable to those provided by conventional techniques.

Last, we note that the activation energy determined for $In(OTf)_3$ catalyzed anisole hydrolysis was 31 kcal/mol, while the uncatalyzed method for anisole hydrolysis in HTW gave an activation energy of 41 kcal/mol. Hence, the use of $In(OTf)_3$ catalyst lowers the energy barrier by about 10 kcal/mol. This is the generally expected outcome for a catalyzed reaction.

Table 6.1: Comparison of anisole hydrolysis rate among different methods. The rates reported are pseudo-first order hydrolysis rates. Method A is the HTW method. Method B is the HTW with WTLA method described above. Method C is a $BF_3 \cdot SMe_2$ in CH_2Cl_2 taken from recent literature. [133] Catalyst $BF_3 \cdot SMe_2$ was loaded at 6 equivalents with respect to the ether.

Method	Temperature (°C)	time (hrs)	Phenol % yield	k (s^{-1})
A	365	24	83	0.000 032±0.000 003
B	300	2	88	0.000 35±0.000 03
C	0	3	80	0.000 15±

CHAPTER VII

Additional Experiments in Ether Hydrolysis

> There is conservation of pain. You can either work a little more and think a little less or think a little more and work a little less.
>
> A good mathematician is a lazy mathematician.
>
> *Alexey G. Stepanov*

In this chapter, we build upon the results in the previous chapter regarding hydrolysis of ethers in HTW. This chapter includes four main studies. First, we discuss the confounding influence of additive upon the reaction. Second, we present results for the hydrolysis of a number of related ethers and draw some general conclusions regarding reactivity. Third, work towards a Hammett analysis plot provides some insight into the mechanism of hydrolysis. Last, we present some initial data regarding hydrolysis in methanol.

7.1 Effect of stainless steel or quartz additive

Our first experiments with anisole hydrolysis in HTW focused on testing the behavior of the reaction toward two different reactor materials, so as to better direct the choice of reaction vessel. We performed the reaction in 2-mm capillary quartz reactors, 6.9-mm quartz reactors, and 1/4″ stainless steel reactors at 225°C with a

batch holding time of 5 hours, or 300 minutes. The results of this study are shown in Table 7.1. We note 12% yield of phenol in the 1/4″ stainless steel reactors, 10% yield in the 2-mm ID quartz reactors, and 22% yield in the 6.9-mm ID quartz reactors. Only the data for the large quartz reactors seem significantly different from the other two groups. In tune with the results from 1-phenyl-1-propyne hydration in different reactors, reaction could be faster in the larger-ID vessels. Regarding the conversion data, the estimated error is so large that any statement regarding the effect of reactor choice is cast in doubt.

We decided to repeat these experiments at more aggressive reaction conditions. We reacted anisole at 250°C for 4.25 hours (256 minutes) in 1/4″ stainless steel and 2-mm ID quartz reactors. We used typical loadings of anisole and $In(OTf)_3$ catalyst: 0.17 M and 8.9 mM respectively. The reactions were repeated to give a total of 5 experiments in 1/4″ stainless steel and 3 experiments in 2-mm ID quartz. We could not carry out reaction in 6.9-mm ID quartz vessels due to the vessel's mechanical properties. Briefly, if the pressure is too high, the large quartz reactors will fail catastrophically due to their larger ratio of ID to wall thickness as compared to the capillary quartz reactors. As the temperature of water rises, the pressure must also rise in order to keep water in the liquid phase; e.g., maintain water at its saturated condition. At 200°C, the reactor pressure is 15 atm; at 225°C, it is 25 atm; at 250°C, it is almost 40 atm – the 6.9-ID quartz reactors consistently explode at 250°C, but are usually good at 225°C.

The results, shown in Table 7.2, show that anisole hydrolysis proceeds more rapidly in capillary quartz reactors than in 1/4″ stainless steel reactors. Given the results from Chapter IV, this behavior was unexpected. For 1-phenyl-1-propyne hydration, experiments demonstrated the lack of any effect upon rate due to the presence of stainless steel or quartz. Further, the differences in rate between quartz capillary reactors and the other three reaction vessels tested were attributed to mass transport

Table 7.1: Comparison of anisole conversion and phenol yield for anisole hydrolysis in quartz and stainless steel reactors, 590-μL in volume, and 4.1 mL in volume. Reactions were carried out at 225°C for 5 hours. Anisole loading was 0.167 M and catalyst loading was 8.87 mM, approximately 5 mol% relative to anisole. The column labelled 'n' indicates the number of experiments in each data set.

Reactor Material	n	%Conversion of Anisole			%Yield of Phenol		
		μ	σ	95% CI	μ	σ	95% CI
1/4″ SS Swagelok	13	22.9	1.4	3.1	11.9	0.8	1.7
2-mm ID quartz	12	12.1	16.8	12.5	9.7	10.0	7.4
7-mm ID quartz	4	38.2	9.3	12.0	22.0	1.6	2.1

Table 7.2: Comparison of phenol yield from anisole hydrolysis in quartz and stainless steel reactors. Reactions were carried out at 250°C for about 4.25 hours, or 256 minutes. Anisole loading was 0.167 M and catalyst loading was 8.87 mM, approximately 5 mol% relative to anisole. Reactor volume was 590 μL. The column labelled 'n' signifies the number of experiments conducted within each data set.

Reactor Material	n	%Yield of Phenol		
		μ	σ	95% CI
1/4" SS Swagelok	5	33	5	6
2-mm ID quartz	3	64	5	7

limitations, with the capillary reactors exacerbating the ease of transport. Here, the observed rate is faster in the more constrained reactor.

These results inspired a more thorough experimental investigation. Reactions were carried out at at 250°C for 2.75 hours (165 minutes) in the 1/4″ SS reactors. The temperature and time were chosen to achieve roughly 50% conversion within a convenient time frame in the 1/4″ stainless steel reactors. This would allow easy detection of both rate acceleration and rate deceleration effects, should they exist. Next, experiments were conducted at the same temperature and time, but with 10, 20, and 40 mg of stainless steel powder added to the reactors. Next, a similar set

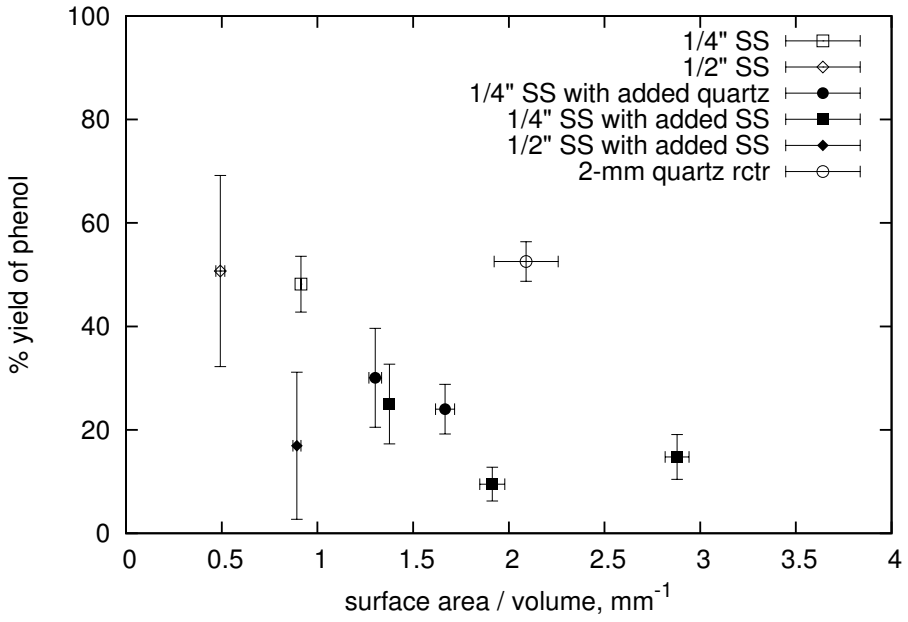

Figure 7.1: Percent yield of phenol vs surface area/volume after 2.75 hrs at 250° C. Error bars represent a 95%CI.

of experiments were conducted with 20 and 40 mg of quartz particles added to the reactors. Fourth, we collected data in 1/2″ SS reactors with the same concentration of anisole and catalyst as the smaller 1/4″ reactors to better test the effect of the vessel surface area to volume ratio. Fifth, we performed experiments in 2-mm quartz reactors. Sixth, we performed experiments with enough stainless steel added to a 1/2″ reactor to make the ratio of total surface area to volume equal to that of a 1/4″ reactor. Each set of experiments was performed in replicates of 2 to 9, with the average number of replicates per set being four to five.

In order to present all of these data on a single plot, Figure 7.1, we chose the abscissa to represent the ratio of total surface area (the surface of the reactor plus the estimated surface area of the additive) to reactor volume. The plot seems to show a trend, but the variance in the data is very large.

One possible interpretation of the data in Figure 7.1 is that there is no correlation between added stainless steel and conversion – that is, no effect upon the reaction.

One may draw a horizontal line across the figure passing through many of the error bars. In statistical analysis, this interpretation is called the "null hypothesis". It is the hypothesis that there is no significant difference among the populations studied. Tools have been developed for the statistical consideration of the null hypothesis. Our data set contains populations differing in one factor: the surface area to volume ratio. There are more than two groups in the entire study; in fact, there are seven groups of data in all (discounting the groups consisting of single data points). Hence, the one-way, or single factor, ANOVA (analysis of variance) seemed best suited to test the null hypothesis for our data set.

One-way ANOVA compares the means of multiple groups and tests whether their means are insignificantly different (in other words, the same) based on the variance in the data. ANOVA achieves this by comparing the between-group mean-square variance (MS_B) to the within-group mean-square variance (MS_W). The between-group mean-square variance is found by taking the sum of squared error of the average of each group with the average of group averages and dividing by the degrees of freedom. The within-group mean-square variance is found by taking the sum of squared errors of each datum with its group's average, and dividing by the degrees of freedom. The F ratio is simply the ratio of the between-group mean-square variance to the within-group mean-square variance. The F ratio is then compared to the F distribution at a desired level of significance, α. For our work, we always made the comparison at the 1% significance level ($\alpha = 0.01$). We performed our ANOVA calculations in Excel but without using the Excel Data Analysis Toolpak. Many statisticians strongly discourage the use of Excel for advanced statistical calculations because of many known bugs. [134, 135]

Our data from the ANOVA tests are found in Table 7.3. Our first ANOVA test comprised the entire data set of Figure 7.1, excepting those groups consisting of only a single datum. We performed a one-way ANOVA on both the conversion data and

Table 7.3: Results from one-way ANOVA using data set described by Figure 7.1.

Data set	Data type	MS_B	MS_W	F	F_{crit}	p-value
All	% X	663	153	4.3	3.7	0.004
	% Yield	1104	37	30	3.7	$1x10^{-9}$
1/4″ Swagelok rctr with added SS	% X	1101	56	20	7.6	0.0004
	% Yield	2111	14	153	7.6	$3x10^{-8}$
1/4″ Swagelok rctr with added quartz	% X	1712	192	8.9	6.4	0.004
	% Yield	989	34	29	6.4	$8x10^{-6}$

the yield data. Both values of F (based on conversion and based on yield) are larger than the critical value of F. This means that we should reject the null hypothesis at a significance level of 0.01. The p-value is the probability (ranging from zero to one) of making the Type I error, the error of rejecting the null hypothesis when in fact it is true. Since our p-values are very small, we can reject the null hypothesis with a very small probability of erring. Hence, we reject the null hypothesis for the entire data set.

ANOVA will determine whether or not all the groups follow from the same population. But if the null hypothesis is rejected, ANOVA will not directly determine *which* groups are from a different population. We know that the groups are different, but we have not yet shown that stainless steel additive exerts an effect upon the reaction, or that the quartz additive has an effect upon the reaction. Hence, we repeat a one-way ANOVA considering only the three data sets wherein different amounts of stainless steel were added to the 1/4″ reactors. Again, we reject the null hypothesis. Stainless steel additive must have an effect. Finally, we repeat the one-way ANOVA with the three data sets wherein different amounts of quartz are added to the 1/4″ reactors. We reject the null hypothesis; quartz also has an effect upon the reaction. Note again that the p-values for all of these tests are very small, signifying a low probability of committing a Type I error.

Given the results of the ANOVA calculations and their respective p-values, and given the earlier comparisons in the different reaction vessels, the conclusion of surface effects is inescapable. Is the suppression of hydrolysis by stainless steel or quartz a general phenomenon?

We tested the effect of stainless steel additive with another aryl-methyl ether substrate: 2-methoxynaphthalene. Because the rate of hydrolysis for 2-methoxynaphthalene is much faster than the rate for anisole, these reactions were carried out at a lower temperature: 200°C rather than 250°C. The batch holding time for these experiments was 1.75 hrs (105 min). Typical substrate and catalyst loadings were used; each reactor contained about 0.17 M 2-methoxynaphthalene and 8.2 mM $In(OTf)_3$ catalyst. We varied the amount of stainless steel powder added to each reactor (0, 11, 20, or 40 mg) and performed replicate experiments to achieve between 4 and 7 experiments per level.

The data are summarized in Figure 7.2, which plots conversion of 2-methoxynaphthalene against the ratio of total surface area (reaction vessel plus SS additive) to volume. The error bars in yield represent 95% confidence intervals. The error bars in SA/Vol represent 95% confidence intervals based on the weight of SS powder added to the reactors.

The trend seen in Figure 7.2 is consistent with the behavior found with anisole. Since we observe rate inhibition by SS additive with two hydrolysis substrates: anisole and 2-methoxynaphthalene, we believe that the effect is likely to be general to hydrolysis with $In(OTf)_3$ catalyst.

We performed one more test regarding the additive inhibition phenomenon to see if the effects persist in the presence of large catalyst loadings. We loaded reactors with 50 mol% catalyst (about 81 mM $In(OTf)_3$), the same concentration of 2-methoxynaphthalene as in previous experiments (0.16 M), and either 0 or 40 mg stainless steel powder. The results, shown in Table 7.4, show that the inhibitory

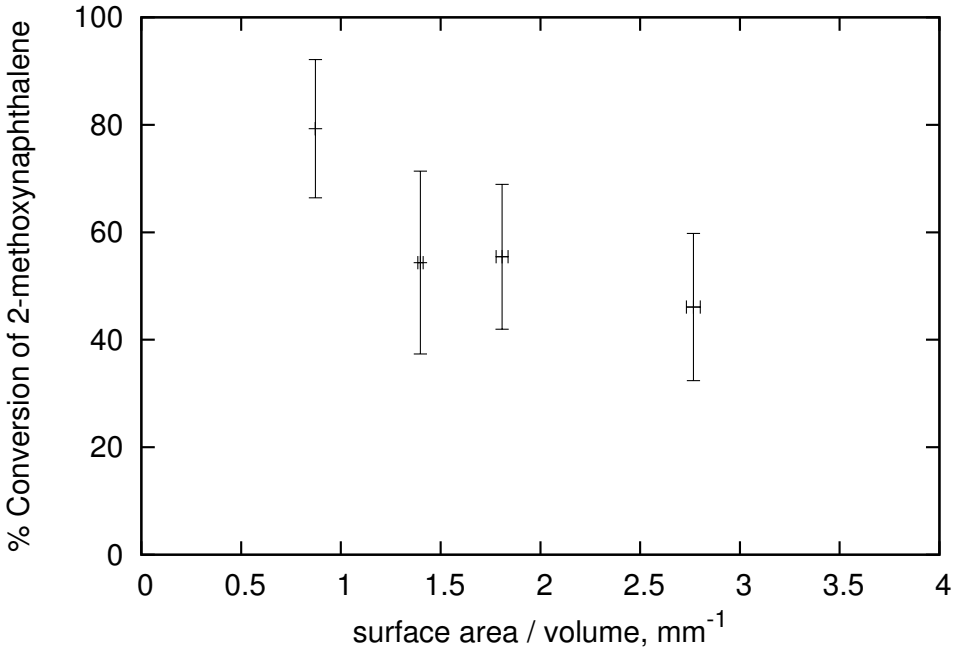

Figure 7.2: Conversion of 2-methoxynaphthalene vs surface area/volume after 1.75 hrs at 200°C. Error bars in yield and SA/Vol ratio both depict 95% confidence intervals. Reactors were loaded with 0.17 M 2-methoxynaphthalene, 8.2 mM $In(OTf)_3$, and (from the left-most datum to the right-most) 0, 11, 20, or 40 mg stainless steel powder.

Table 7.4: Hydrolysis of 2-methoxynaphthalene to 2-naphthol in the presence of 50 mol% catalyst with and without 40 mg of SS additive. Reaction temperature and time are 200°C for 15 minutes. Reactors were loaded with 0.16 M 2-methoxynaphthalene and 81 mM $In(OTf)_3$ catalyst. Each value represents the average for five experiments. The reported errors represent 95% confidence intervals.

SS added mg	SA/Vol mm^{-1}	% Conversion of 2-methoxynaphthalene	% Yield of 2-naphthol
0	0.87	24±5	20±8
37.8±4.2	2.6±0.2	29±9	21±4

effect of added stainless steel is overcome by this high catalyst loading. Hydrolysis of 2-methoxynaphthalene in the presence of 50 mol% $In(OTf)_3$ proceeds just as quickly with or without 40 mg of added stainless steel powder.

The experimental evidence we have collected for the inhibition of reactions with $In(OTf)_3$ suggests an adsorption interaction between $In(OTf)_3$ and the surface. Since both stainless steel and quartz show inhibition, we do not think that catalyst deactivation is likely. It would be very strange for both surfaces to cause deactivation. However, both surfaces are mildly reductive. Quartz is composed of a crystal of silicon dioxide; the surface of stainless steel is largely chromium oxide. Both of these surfaces may provide the diffuse electron density that indium desired to fill its empty orbital. For this to occur, indium must prefer the surface to interaction with water, a hard base. This is conceivable because indium is a soft acid and is expected to prefer softer bases. The hypothesis of adsorption also makes sense in light of the data of Table 7.4. Once enough catalyst is added to the reactor to occupy all the adsorption sites, reaction inhibition is no longer observed. If the rate of adsorption is slow, we would not observe reaction inhibition in 1-phenyl-1-propyne hydration, which is much faster than anisole hydrolysis.

Our hypothesis of adsorption may be tested by computational methods. The

binding energy of the catalyst to surface, relative to the interaction potential between the catalyst and water, would help corroborate our interpretation of the data.

As for our kinetic data in Chapter VI,

7.2 Reactivity of analogous substrates

There are two essential pathways by which ether hydrolysis may occur. One pathway is formation of an oxonium ion followed by elimination. This mechanism is depicted in Figure 7.3. In the figure, the oxonium cation is formed by protonation, and the mechanism is acid-catalyzed. The second pathway is characterized by nucleophilc substitution. A base arrives to remove the methyl group from oxygen directly. The base may be any compound with an appropriate lone pair of electrons, such as hydroxide ion, water, or methoxide ion. A third mechanism, (c) in Figure 7.3, is offered by workers in the field. [67] This is an S_N2 mechanism with water serving as the base instead of the hydroxide ion representing the base in mechanism (b). Hence, mechanisms (b) and (c) are fundamentally similar. Or mechanism (b) is really the same as mechanism (c) except that b allows for the regeneration of the base catalyst, hydroxide.

Regardless of the details of these two essential mechanisms, they can be used to predict changes in reactivity resulting from changes in substrate structure. When under rate-determining protonation, the acid-catalyzed mechanism will be promoted by electronic effects that stabilize a positive charge. Similarly, the base-catalyzed or S_N2 mechanism will be accelerated by electronic features that stabilize the negative charge accumulating upon the substrate in the rate-determining step.

Once the reactivity of anisole was relatively well understood, we sought to test the applicability of aryl alkyl ether hydrolysis in HTW more broadly. We tested four different compounds toward hydrolysis in HTW under catalysis with $In(OTf)_3$: ethyl phenyl ether, 1-methoxynaphthalene, 2-methoxynaphthalene, and diphenyl ether.

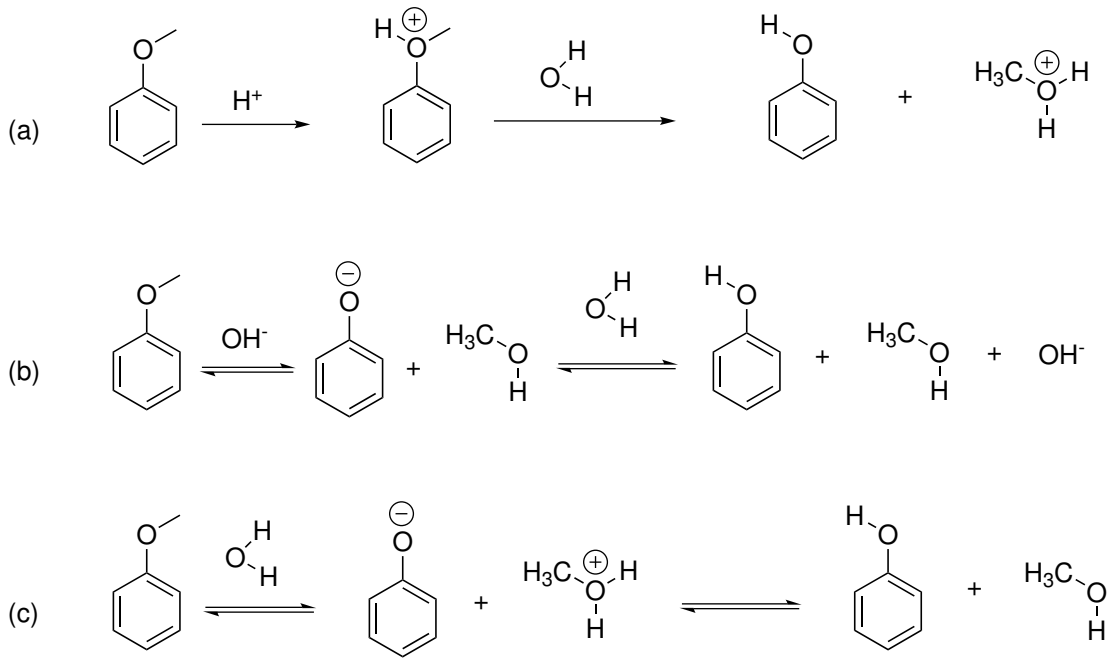

Figure 7.3: Mechanisms.

These data are shown in Table 7.5 along with analogous anisole data, in order of decreasing reactivity.

At similar conditions, hydrolysis of methoxynaphthalene is up to 2000 times faster than hydrolysis of anisole. Hydrolysis of naphthalene-derived ethers is thought to proceed by an acid-catalyzed mechanism in supercritical water without added catalyst. [136] If acid-catalysis is at work here as well, then the rate enhancement relative to anisole could be explained by the stabilization of the oxonium cation offered by the larger π cloud in naphthalene as compared to benzene. Historically, the 1-position on naphthalene is found to be more kinetically favored for substitution reactions than is the 2-position. This is because substitution at 2 places a carbocation at 1, and carbocations at the 1-position are somewhat better stabilized than those placed in the 2-position because they benefit more from the delocalization among both fused rings. In hydrolysis, then, an oxonium ion near the 2-position is expected to be better stabilized than an oxonium ion near the 1-position. The relative kinetics for 1- and 2-methoxynaphthalene are consistent with these expectations.

Table 7.5: Comparison of rate among different ethers.

Ether	Temperature (°C)	mol% $In(OTf)_3$	k ($s^{-1}M^{-1}$)
2-Methoxynaphthalene	200	5	0.03
1-Methoxynaphthalene	200	5	0.008
ethyl phenyl ether	250	5	0.006
diphenyl ether	350	20	0.0002
anisole	200	5	0.00028
	225	5	0.0018
	250	5	0.0044
	275	5	0.12
	300	5	0.43

Hydrolysis of ethyl phenyl ether is slower than hydrolysis of anisole. This relationship is also seen in non-catalyzed hydrolysis of anisole and phenetole. [67] The researchers accept an S_N2 mechanism for their results, and attribute the rate retardation in ethyl phenyl ether to electron-donating effects, and the destabilization of a negatively charged transition state structure. However, this slight rate suppression may also be due to simple steric hindrance effects. Further, the error in our data does not allow for unambiguous kinetic rate distinction between anisole and phentole.

Diphenyl ether was by far the most difficult to hydrolyze substrate in this study. The bond between oxygen and the carbon of a benzene ring is a very strong bond. Much higher temperatures and catalyst loadings were required to achieve a small yield of phenol from diphenyl ether. Part of our interest in diphenyl ether hydrolysis stemmed from the potential application of water tolerant Lewis acid catalyzed hydrolysis reactions for the purpose of waste water treatment, as diphenyl ether is often used as a model compound for such studies. Further, the Ar-O-Ar bonds of diphenyl ether are often used to mimick similar bonds in lignin for the purpose of studying biomass depolymerization. Unfortunately, the rate of diphenyl ether hydrolysis in this study was not found to be competitive with other examples in the literature.

7.3 Future work

Some interesting questions were left unanswered, or partially unanswered. I present some work toward what could become additional projects related to hydrolysis.

7.3.1 Hammett analysis

Hammett analysis plots are often used to garner evidence regarding the mechanism. The procedure involves the identification of a series of substituted benzene rings that undergo the same reaction as the unsubstituted parent compound. If electron-donating substituents in the para position are found to accelerate the reaction, it is deduced that the transition state accumulated positive charge relative to the ground state structure. Similarly, if electron-withdrawing substituents in the para position accelerate the reaction, then the transition state must involve the accumulation of negative charge.

We began experiments toward a Hammett analysis plot for anisole hydrolysis with p-hydroxy-anisole (MEHQ), which is converted to hydroquinone (HQ). We performed experiments at 300°C, a condition for which we already have kinetic data for anisole hydrolysis. Reactors were loaded in the typical fashion; substrate and catalyst concentration were about 0.21M and 9.4 mM respectively. Three and four experiments each were performed at 15 and 30 minutes respectively. Yield of HQ is computed and plotted in Figure 7.4 along with the respective 95% confidence intervals for each datum. The data were fit to a hydrolysis rate equation that is first order in $In(OTf)_3$ catalyst and first order in substrate, MEHQ. The result of this data fitting is also plotted in Figure 7.4, along with the analogous kinetic data from anisole hydrolysis at 300°C.

The nominal value for the rate constant for MEHQ hydrolysis (0.046 ± 0.006 $s^{-1}M^{-1}$), is somewhat faster than the analogous rate constant for anisole hydrolysis to

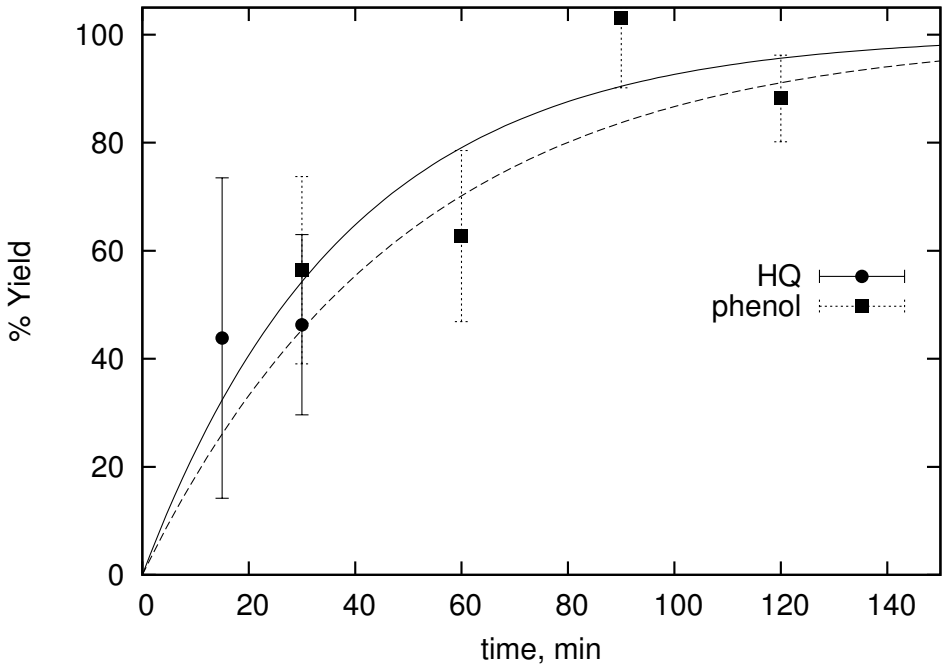

Figure 7.4: Yield of hydroquinone from monomethyl ether hydroquinone at 300°C (filled circles), shown with data fit (solid line), along with yield of phenol from anisole hydrolysis at 300°C (squares), shown with data fit (dashed line). Error bars depict 95% confidence intervals for the data.

phenol ($0.043\ s^{-1}M^{-1}$). However, these figures are within error. From this experiment alone, we can only say the the addition the electron-donation hydroxy group *may* slightly accelerate hydrolysis. Additional experiments with the compound, as well as p-hydroxybenzaldehyde, etc., could greatly aid in distinguishing between the two possible mechanisms for this reaction in HTW with WTLA catalysis.

7.3.2 Hydrolysis in methanol

Experiments showed that, for the same temperature, reaction in methanol was about three times faster than reaction in water for 1-methoxynaphthalene hydrolysis. Quartz reactors (2-mm ID) were loaded with Gas analysis demonstrated the production of hydrogen by the reaction. The production of hydrogen was interesting because it is consistent with the observations of other researchers regarding the behavior of secondary alcohols in the presence of HTW. [81] The researchers propose a 4-membered hydrogen-bonded cyclic transition state structure to explain the production of small amounts of hydrogen from secondary alcohols in HTW. [81] We see hydrogen production in high temperature methanol with no water present. These initial experiments were interesting, but were not pursued further because neither the current Swagelok reactors, nor the quartz reactors were practical for the collection and analysis of a pressurized sample. Data simply cannot be obtained consistently with the equipment in use when the course of the reaction pressurizes the vessel with hydrogen.

7.4 Conclusions and future work

The experimental evidence we have gathered points to an acid-catalyzed mechanism of hydrolysis. The velocity of 2-methoxynaphthalene hydration relative to 1-methoxynaphthalene hydration indicates that a positive charge may be forming upon the oxygen in the transition state, as in acid catalysis. Experiments with other

substrates to form a Hammett analysis plot would further help to accept or refute the acid-catalyzed route.

CHAPTER VIII

Conclusions

> The beautiful thing about science is that it shall forever patiently wait for you to discover the truth.
>
> *Jeffrey. W. Weber*

The catalytic role of WTLAs, specifically of $In(OTf)_3$, were critical to the success of hydration and hydrolysis. WTLAs have never before been applied to a HCW reaction medium. We hope that our work here will inspire further investigations of their utility in HTW. In addition to such work, efforts are needed to elucidate the mechanism by which WTLAs act in HTW organic reactions. For example, our work showed that $In(OTf)_3$ was more active toward hydration and hydrolysis than was $InCl_3$, but the literature suggests that the metal hydrate is the active species, and that the hydrate forms almost immediately upon acquaintance with water. [34, 35] At least, this is the picture drawn for reaction in room-temperature or warm water. Work investigating the mechanism of catalysis should help resolve these apparent inconsistencies.

Aside from a few key examples [2, 26], the early studies in HTW featured reactions that were of worthy proof-of-concept interest, but which languished in robustness compared to traditional techniques. Often, the HTW reactions featured long reaction times, poor yields, a lack of selectivity, and application to only the more labile ex-

amples within a functional group. Our work in hydration and hydrolysis offers yields that are competitive with traditional techniques. Hydration of 1-phenyl-1-propyne proceeds just as readily in HTW at 200°C as in warm sulfuric acid. [124] Anisole hydrolysis at 300°C is also competitive with reaction in $CHCl_3$ with BF_3. [133] Our work with WTLAs in HTW, therefore, helps bring the reaction medium to a position where it can seriously be considered among other technologies.

The literature contains many examples of the reactor wall being held accountable for changes in reaction kinetics and pathways for HTW reactions. Researchers often see a difference between yield and conversion data collected with stainless steel reactors, and the same data collected with capillary quartz reactors. [80, 81, 137] Other researchers, citing the possibility of stainless steel catalysis, simply perform their experiments in quartz capillary reactors out of a sense of safety. [138, 139] Still others provide no reason at all for their choice, which is perhaps just as remiss as providing an uncorroborated hypothesis. [107] No matter the rigor applied, the guiding philosophy in these investigations is the same: The experimental details are less important than collecting the data.

My work for 1-phenyl-1-propyne hydration breaks with this philosophy. We collected data in both reactor types, and observed a difference in apparent reactivity, but rather than latching onto the hypothesis of stainless steel catalysis, and treating it as if it were a given theory, we proceeded to study the effects of added stainless steel and added quartz to the reactors. We found that the difference in reactivity was not due to wall catalysis (or inhibition) at all. Our standing hypothesis is that the difference was due to diffusion limitations.

Had we applied the same pattern of thought to this work as previous researchers, we would have collected a large database of highly flawed experimental work. Agnosticism applied to the experimental details would have led to false certainties with data collection and interpretation. False certainties are worse than ignorance with

respect to scientific progress. We hope that this work inspires more careful attention to experimental details. Objective scientific conclusions can only be derived from objective experimental techniques.

APPENDICES

APPENDIX A

Material Source and Purity

Many chemicals were used as part of this study. The manufacturer and stated purity are noted for each chemical used, as well as lot numbers, where available. Each chemical is listed in alphabetical order. For pure chemicals, the supplier, purity, and Lot numbers (if available) immediately follow the chemical name. Thereafter, key physical properties are noted in the following order: molecular formula, formula weight, melting point (°C), boiling point (°C), specific gravity, and the vapor pressure at 25°C in torr. Finally, the CAS number and other names and/or abbreviations are provided if appropriate.

p–tert-butyl-acetophenone $C_{12}H_{16}O$, MW 176.25, bp 253.1, ρ 0.939±0.06, 0.0186 torr. CAS 943-27-1; 1-[4-(1,1-dimethylethyl)phenyl]-ethanone.

4-acetylbenzonitrile Sigma-Aldrich, 99%, Lot S21081-438. C_9H_7ON, MW 145.16, mp 56-59, bp 293±23, 0.00174 torr. CAS 1443-80-7.

p-acetylbenzyl alcohol $C_9H_{10}O_2$, MW 150.17, mp 54, bp 301±25, ρ 1.114±0.06, $4.71x10^{-4}$ torr. CAS 75633-63-5, 1-[4-(hydroxymethyl)phenyl]-ethanone.

anisole Sigma-Aldrich, 99%. C_7H_8O, MW 108.14, mp -37, bp154, ρ 0.995.

benzyl alcohol Sigma-Aldrich, ≥99%, Lot 02416CT. C_7H_8O, MW 108.14, mp -15, bp 205, ρ 1.045, 0.158 torr. CAS 100-51-6, BnOH.

benzyl ether Sigma-Aldrich, 99%, Lot 24805CA. $C_{14}H_{14}O$, MW 198.27, mp 1.5-3.5, bp 298, ρ 1.043, 0.00444 torr. CAS 103-50-4, BnOBn.

p-cresol Sigma-Aldrich, 99%, Lot 00225PZ. C_7H_8O, MW 108.14, mp 32-35, bp 202, ρ 1.034, 1 torr. CAS 106-44-5, 4-methylphenol.

5-decanone Alfa Aesar, 99%, Lot B20548. $C_{10}H_{20}O$, MW 156.27, bp 204, ρ 0.8115 at 24°C, 0.211 torr. CAS 820-29-1.

5-decyne Alfa Aesar, 98%. $C_{10}H_{18}$, MW 138.25, mp -73, bp 177-178, ρ 0.770, 1.28 torr. CAS 1942-46-7.

4-tert-butyl-4-ethynylbenzene Sigma-Aldrich, 96%, Lot MKBB4636. $C_{12}H_{17}$, MW 158.24, bp 211±19, ρ 0.877, 0.273 torr. CAS 772-38-3, 4-tert-butyl-phenylacetylene.

4-ethynylbenzonitrile Sigma-Aldrich, 97% (Certificate of Analysis reports purity (HPLC) as 99.9%), Lot 75869KJ. C_9H_5N, MW 127.14, mp 156-160, bp 230±23, 0.0666 torr. CAS 3032-92-6.

4-ethynylbenzyl alcohol Sigma-Aldrich, 97% (Certificate of Analysis reports purity (GC) as 99.2%), Lot MKBB5767. C_9H_8O, MW 132.16, mp 40-44, bp 240±23, 0.0216 torr. CAS 20602-04-7.

4-ethynyltoluene Aldrich, 97%, Lot 1430258 (Certificate of Analysis reports purity (GC area %) as 99.8%. C_9H_8, MW 116.16, bp 168-170, ρ 0.916, 2.62 torr. CAS 766-97-2, p-tolylethyne, 1-ethynyl-4-methylbenzene.

hexanophenone Sigma-Aldrich, 99%, Lot MKAA3377. $C_{12}H_{16}O$, MW 176.26, mp 26-28, bp 265, ρ 0.958, 0.00940 torr. CAS 820-29-1.

hydroquinone Sigma-Aldrich, $\geq$ 99%, Lot CY04622BX. $C_6H_6O_2$, MW 110.11, mp 172-175, bp 285, ρ 1.275$\pm$0.06, 0.00157 torr. CAS 123-31-9; 1,4-benzenediol; 1,4-dihydroxybenzene; HQ.

indium(III) chloride Sigma-Aldrich, anhydrous powder, $\geq$99.999% trace metals basis, $\leq$100 ppm H_2O. $InCl_3$, FW 221.18, ρ 3.46. CAS 10025-82-8, indium trichloride.

indium trifluoromethanesulfonate Sigma-Aldrich. $In(CF_3SO_3)_3$, FW 562.03. CAS 128008-30-0, Indium triflate, $In(OTf)_3$.

4-methoxyphenol Sigma-Aldrich, 99% ($\leq$2% hydroquinone dimethyl ether), Lot 03527LN. $C_7H_8O_2$, MW 124.14, mp 54-56, bp 243, ρ 1.109$\pm$0.06, 0.0211 torr. CAS 150-76-5, 4-hydroxyanisole, hydroquinone monomethyl ether, MEHQ.

4-methylacetophenone Fluka, $\geq$96.0% (GC), Lot 01521BJ. $C_9H_{10}O$, MW 134.18, mp 22-24, bp 220-223, ρ 1.004. CAS 122-00-9, p-acetyltoluene.

p-methylanisole Sigma-Aldrich, 99%, Lot MKBC3826. $C_8H_{10}O$, MW 122.16, mp -32, bp 174, ρ 0.969, 1.65 torr. CAS 104-93-8.

phenol Sigma-Aldrich, 99%. C_6H_6O, MW 94.11, mp 40-42, bp 182, ρ 1.071.

phenylacetylene C_8H_6, MW 102.133, mp -45, bp 142-144, ρ 0.93, 7.02 torr. CAS 536-74-3.

phenyl ethyl ether Sigma-Aldrich, 99%. $C_8H_{10}O$, 122.16, mp -30, bp 170-172, ρ 0.967, 2.01 torr. CAS 103-73-1, ethoxy benzene, EtOPh.

6-phenyl-2-hexyne Alfa Aesar, 99%, Lot I6875A. $C_{12}H_{14}$, MW 158.24, bp 240$\pm$19, ρ 0.922$\pm$0.06, 0.0596 torr. CAS 34298-75-4.

1-phenyl-1-propyne Sigma-Aldrich, 99%, 673-32-5. C_9H_8, MW 116.16, bp 185, ρ 0.928.

propiophenone Sigma-Aldrich, 99%, 93-55-0. $C_9H_{10}O$, MW 134.18, mp 17-19, bp 218, ρ 1.009.

quartz particles Sigma-Aldrich. M_r 60.08, sand 40-150 mesh.

scandium trifluoromethanesulfonate Sigma-Aldrich, 99%. $Sc(CF_3SO_3)_3$, FW 492.16. CAS 144026-79-9, Scandium triflate, Scandium(III) trifluoromethanesulfonate, Trifluoromethanesulfonic acid scandium(III) salt, $Sc(OTf)_3$.

stainless steel powder Alfa Aesar. 100 mesh, type 316-L.

sulfuric acid Sigma-Aldrich, 0.1 N standard solution in water. H_2SO_4

ytterbium(III) trifluoromethanesulfonate Sigma-Aldrich, 99.99%. $Yb(CF_3SO_3)_3$, FW 620.25. CAS 54761-04-5, Ytterbium triflate, $Yb(OTf)_3$

APPENDIX B

Detailed Analytical Methods

B.1 Methods for gas chromatography

A slightly different method was used for the gas chromatographic analysis of each reaction mixture. Presented below are the key features of each GC method, listed in alphabetical order of the organic starting material.

B.1.1 Hydration of 1-phenyl-1-propyne to propiophenone

HP-5 column (50m x 0.20 mm, 0.33 m film thickness), constant flow = 0.7 mL/min, (oven temperature ramp R, to stable temperature T C, for t min) = (∅, 80, 5), (10, 200, 1), (50, 250, 5).

B.2 Preparation of calibration standards

A single method of preparing calibration standards was used for the quantification of analytes by liquid-sampling gas chromatography. This method is explained in Chapter III. and depicted pictorially in Figure B.1. Many of the research assis-

tants who contributed to this research found the cartoon more illuminating that the explanatory prose. Hence, it is included here.

The variations upon this procedure were of three kinds. One, the more dilute sibling could be used to prepare the next generation of standards, if the limit of detection for the compound allowed. Hence, instead of standard '3', standard '4' could be diluted to prepare standards 5 through 7; or instead of standard '6', standard '7' could be diluted to prepare standards 8 through 10. Two, the concentration of analyte added to the parent standard would be increased to assure that all the reaction samples were within the range of the concentrations of the calibration standards. Typically, the concentration of the parent standard was chosen such that the concentration of starting material in standard '3' would approximate the initial concentration of starting material in each reactor. The main product was to the parent standard to be of approximately the same concentration as the starting material. Three, if the reaction featured side products for which quantification was desired, only about $n * 0.9\mu$mol of the material was loaded in the parent solution, where n is the number of μmol of organic substrate loaded to each reactor. This provided satisfactory results for quantifying minor products.

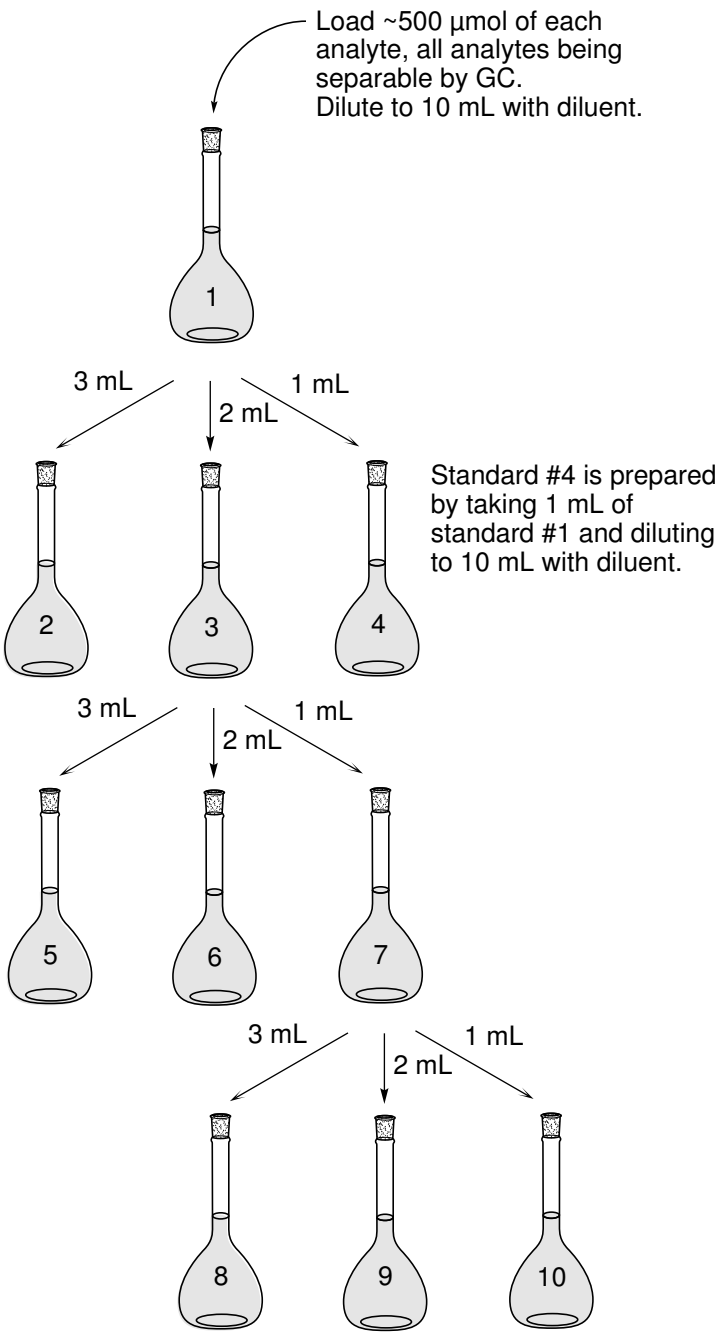

Figure B.1: Cartoon depicting the scheme used for the preparation of calibration standards.

BIBLIOGRAPHY

BIBLIOGRAPHY

[1] Yongsheng Chen, John L. Fulton, and Walter Partenheimer. The structure of the homogeneous oxidation catalyst, $Mn(II)(Br^{-1})_x$, in supercritical water: An X-ray absorption Fine-Structure study. *Journal of the American Chemical Society*, 127(40):14085–14093, October 2005.

[2] Eduardo Garcia-Verdugo, Eleni Venardou, W.Barry Thomas, Keith Whiston, Walter Partenheimer, PaulA. Hamley, and Martyn Poliakoff. Is it possible to achieve highly selective oxidations in supercritical water? Aerobic oxidation of methylaromatic compounds. *Advanced Synthesis & Catalysis*, 346(2-3):307–316, 2004.

[3] George A. Olah. *Friedel-Crafts and Related Reactions.* Interscience Publishers, New York, 1963. 4 v. in 6.

[4] R. B. Woodward and Harold Baer. The reaction of furan with maleic anhydride1. *Journal of the American Chemical Society*, 70(3):1161–1166, March 1948.

[5] Darryl C. Rideout and Ronald Breslow. Hydrophobic acceleration of Diels-Alder reactions. *Journal of the American Chemical Society*, 102(26):7816–7817, December 1980.

[6] S. Narayan, J. Muldoon, M. G. Finn, V. V Fokin, H. C Kolb, and K. B Sharpless. On water: unique reactivity of organic compounds in aqueous suspension. *Angew. Chem. Int. Ed*, 44:32753279, 2005.

[7] Yousung Jung and R. A. Marcus. On the theory of organic catalysis on water. *Journal of the American Chemical Society*, 129(17):5492–5502, May 2007.

[8] Frank E. Anderson and John M. Prausnitz. Mutual solubilities and vapor pressures for binary and ternary aqueous systems containing benzene, toluene, m-xylene, thiophene and pyridine in the region 100-200C. *Fluid Phase Equilibria*, 32(1):63–76, October 1986.

[9] Huaping Chen and Jan Wagner. An apparatus and procedure for measuring mutual solubilities of hydrocarbons + water: Benzene + water from 303 to 373 K. *Journal of Chemical & Engineering Data*, 39(3):470–474, July 1994.

[10] Karen Chandler, Brandon Eason, Charles L. Liotta, and Charles A. Eckert. Phase equilibria for binary aqueous systems from a Near-Critical water reaction apparatus. *Industrial & Engineering Chemistry Research*, 37(8):3515–3518, 1998.

[11] James S. Brown, Jason P. Hallett, David Bush, and Charles A. Eckert. LiquidLiquid equilibria for binary mixtures of water + acetophenone, + 1-Octanol, + anisole, and + toluene from 370 k to 550 k. *Journal of Chemical & Engineering Data*, 45(5):846–850, 2000.

[12] Sundaresh Ramayya, Andrew Brittain, Carlos DeAlmeida, William Mok, and Michael Jerry Antal Jr. Acid-catalysed dehydration of alcohols in supercritical water. *Fuel*, 66(10):1364–1371, October 1987.

[13] Preshious Reardon, Sean Metts, Chad Crittendon, Pat Daugherity, and Edith J. Parsons. Palladium-Catalyzed coupling reactions in superheated water. *Organometallics*, 14(8):3810–3816, 1995.

[14] Karen Chandler, Fenghua Deng, Angela K. Dillow, Charles L. Liotta, and Charles A. Eckert. Alkylation reactions in Near-Critical water in the absence of acid catalysts. *Industrial & Engineering Chemistry Research*, 36(12):5175–5179, December 1997.

[15] Karen Chandler, Charles L. Liotta, Charles A. Eckert, and David Schiraldi. Tuning alkylation reactions with temperature in near-critical water. *AIChE Journal*, 44(9):2080–2087, 1998.

[16] Michael B. Korzenski and Joseph W. Kolis. Diels-Alder reactions using supercritical water as an aqueous solvent medium. *Tetrahedron Letters*, 38(32):5611–5614, August 1997.

[17] Shane A. Nolen, Charles L. Liotta, Charles A. Eckert, and Roger Glaser. The catalytic opportunities of near-critical water: a benign medium for conventionally acid and base catalyzed condensations for organic synthesis. *Green Chemistry*, 5(5):663–669, 2003.

[18] J. S Brown, R. Gläser, C. L Liotta, and C. A Eckert. Acylation of activated aromatics without added acid catalyst. *Chemical Communications*, 2000(14):12951296, 2000.

[19] Naoko Akiya and Phillip E. Savage. Roles of water for chemical reactions in High-Temperature water. *Chemical Reviews*, 102(8):2725–2750, 2002.

[20] Craig M. Comisar and Phillip E. Savage. Kinetics of crossed aldol condensations in high-temperature water. *Green Chemistry*, 6(4):227–231, 2004.

[21] Shawn E. Hunter, Carolyn E. Ehrenberger, and Phillip E. Savage. Kinetics and mechanism of tetrahydrofuran synthesis via 1,4-Butanediol dehydration in

High-Temperature water. *The Journal of Organic Chemistry*, 71(16):6229–6239, 2006.

[22] Shawn E. Hunter and Phillip E. Savage. Kinetics and mechanism of p-Isopropenylphenol synthesis via hydrothermal cleavage of bisphenol A. *The Journal of Organic Chemistry*, 69(14):4724–4731, July 2004.

[23] Jianli Yu and Phillip E. Savage. Decomposition of formic acid under hydrothermal conditions. *Industrial & Engineering Chemistry Research*, 37(1):2–10, January 1998.

[24] E. Garcia-Verdugo, Z. Liu, E. Ramirez, J. Garcia-Serna, J. Fraga-Dubreuil, J. R Hyde, P. A Hamley, and M. Poliakoff. In situ generation of hydrogen for continuous hydrogenation reactions in high temperature water. *Green Chemistry*, 8(4):359–364, 2006.

[25] Shawn E. Hunter and Phillip E. Savage. Recent advances in acid- and base-catalyzed organic synthesis in high-temperature liquid water. *Chemical Engineering Science*, 59(22-23):4903–4909, 2004.

[26] Jennifer B. Dunn and Philip E. Savage. Terephthalic acid synthesis in High-Temperature liquid water. *Industrial & Engineering Chemistry Research*, 41(18):4460–4465, 2002.

[27] Jennifer B. Dunn and Phillip E. Savage. High-Temperature liquid water: A viable medium for terephthalic acid synthesis. *Environmental Science & Technology*, 39(14):5427–5435, July 2005.

[28] Jennifer B. Dunn and Phillip E. Savage. Economic and environmental assessment of high-temperature water as a medium for terephthalic acid synthesis. *Green Chemistry*, 5(5):649–655, 2003.

[29] Yu. E. Gorbaty and A. G. Kalinichev. Hydrogen bonding in supercritical water. 1. experimental results. *The Journal of Physical Chemistry*, 99(15):5336–5340, April 1995.

[30] M. Uematsu and E. U. Franck. Static dielectric constant of water and steam. *Journal of Physical and Chemical Reference Data*, 9(4):1291–1306, 1980.

[31] E. W. Lemmon, M. O. McLinden, and D. G. Friend. Thermophysical properties of fluid systems. In *NIST Chemistry WebBook, NIST Standard Reference Database Number 69, Eds. P. J. Linstrom and W. G. Mallard*. National Institute of Standards and Technology, Gaithersburg MD, 20899, 2008.

[32] W. L. Marshall and E. U. Franck. Ion product of water substance, 0 to 1000 C, 1 to 10,000 bars: New international formulation and its background. *Journal of Physical and Chemical Reference Data*, 10(2):295–304, 1981.

[33] Francesco Fringuelli, Ferdinando Pizzo, and Luigi Vaccaro. $AlCl_3$ as an efficient lewis acid catalyst in water. *Tetrahedron Letters*, 42(6):1131–1133, February 2001.

[34] S. Kobayashi, S. Nagayama, and T. Busujima. Lewis acid catalysts stable in water. correlation between catalytic activity in water and hydrolysis constants and exchange rate constants for substitution of inner-sphere water ligands. *J. Am. Chem. Soc*, 120(32):8287–8288, 1998.

[35] Shu Kobayashi and Iwao Hachiya. Lanthanide triflates as Water-Tolerant lewis acids. activation of commercial formaldehyde solution and use in the aldol reaction of silyl enol ethers with aldehydes in aqueous media. *The Journal of Organic Chemistry*, 59(13):3590–3596, July 1994.

[36] S. Araki, S. J Jin, Y. Idou, and Y. Butsugan. Allylation of carbonyl compounds with catalytic amount of indium. *Bulletin of the Chemical Society of Japan*, 65(6):1736–1738, 1992.

[37] Iwao Hachiya and Shu Kobayashi. Aqueous reactions with a lewis acid and an organometallic reagent. the scandium trifluoromethanesulfonate-catalyzed allylation reaction of carbonyl compounds with tetraallyltin. *The Journal of Organic Chemistry*, 58(25):6958–6960, December 1993.

[38] Ganapathy S. Viswanathan and Chao-Jun Li. A highly stereoselective, novel coupling reaction between alkynes and aldehydes. *Tetrahedron Letters*, 43(9):1613–1615, February 2002.

[39] Paolo Crotti, Valeria Di Bussolo, Lucilla Favero, Mauro Pineschi, and Marco Pasero. Metal Salt-Catalyzed addition of lithium enolates of ketones to 1,2-Epoxides. an efficient route to -Alkyl--Hydroxy ketones. *The Journal of Organic Chemistry*, 61(26):9548–9552, January 1996.

[40] Ji Zhang, Peter G. Blazecka, and Timothy T. Curran. Lewis and Brönsted acid catalyzed Friedel-Crafts hydroxyalkylation of mucohalic acids: a facile synthesis of functionalized γ-aryl γ-butenolides. *Tetrahedron Letters*, 48(14):2611—2615, April 2007.

[41] Libing Yu, Depu Chen, and Peng George Wang. Aqueous aza Diels-Alder reactions catalyzed by lanthanide(III) trifluoromethanesulfonates. *Tetrahedron Letters*, 37(13):2169—2172, March 1996.

[42] S. Kobayashi. Rare earth metal trifluoromethanesulfonates as water-tolerant lewis acid catalysts in organic synthesis. *Synlett*, (9):689–701, 1994.

[43] Phillip E. Savage. Organic chemical reactions in supercritical water. *Chemical Reviews*, 99(2):603–622, February 1999.

[44] R. C. Crittendon and E. J. Parsons. Transformations of cyclohexane derivatives in supercritical water. *Organometallics*, 13(7):2587–2591, July 1994.

[45] Robert Thornton Morrison and Robert Neilson Boyd. *Organic Chemistry Second Edition*. Allyn and Bacon, Inc, second edition, 1966.

[46] T Sato, G Sekiguchi, T Adschiri, and K Arai. Non-catalytic and selective alkylation of phenol with propan-2-ol in supercritical water. *Chemical Communications (Cambridge, England)*, (17):1566–1567, September 2001. PMID: 12240384.

[47] T. Sato, G. Sekiguchi, T. Adschiri, and K. Arai. Regioselectivity of phenol alkylation in supercritical water. *Green Chemistry*, 4(5):449–451, 2002.

[48] Takafumi Sato, Gaku Sekiguchi, Tadafumi Adschiri, and Kunio Arai. Ortho-Selective alkylation of phenol with 2-Propanol without catalyst in supercritical water. *Industrial & Engineering Chemistry Research*, 41(13):3064–3070, June 2002.

[49] Takafumi Sato, Gaku Sekiguchi, Motofumi Saisu, Masaru Watanabe, Tadafumi Adschiri, and Kunio Arai. Dealkylation and rearrangement kinetics of 2-Isopropylphenol in supercritical water. *Industrial & Engineering Chemistry Research*, 41(13):3124–3130, June 2002.

[50] Takafumi Sato, Gaku Sekiguchi, Tadafumi Adschiri, and Kunio Arai. Control of reversible reactions in supercritical water: I. alkylations. *AIChE Journal*, 50(3):665—672, 2004.

[51] T. Sato, Y. Ishiyama, and N. Itoh. Non-catalytic anti-Markovnikov phenol alkylation with supercritical water. *Chemistry Letters*, 35(7):716–717, 2006.

[52] Shawn E. Hunter and Phillip E. Savage. Acid-Catalyzed reactions in carbon Dioxide-Enriched High-Temperature liquid water. *Industrial & Engineering Chemistry Research*, 42(2):290–294, January 2003.

[53] Jon Diminnie, Sean Metts, and Edith J. Parsons. In situ generation and heck coupling of alkenes in superheated water. *Organometallics*, 14(8):4023–4025, 1995.

[54] Liz U. Gron and Amanda S. Tinsley. Tailoring aqueous solvents for organic reactions: Heck coupling reactions in high temperature water. *Tetrahedron Letters*, 40(2):227–230, January 1999.

[55] Liz U Gron, Jeanna E LaCroix, Cortney J Higgins, Karen L Steelman, and Amanda S Tinsley. Heck reactions in hydrothermal, sub-critical water: water density as an important reaction variable. *Tetrahedron Letters*, 42(49):8555–8557, December 2001.

[56] R. Zhang, F. Zhao, M. Sato, and Y. Ikushima. Noncatalytic heck coupling reaction using supercritical water. *Chemical Communications*, 34(42):1548–1549, 2003.

[57] Rong Zhang, Osamu Sato, Fengyu Zhao, Masahiro Sato, and Yutaka Ikushima. Heck coupling reaction of iodobenzene and styrene using supercritical water in the absence of a catalyst. *Chemistry (Weinheim an Der Bergstrasse, Germany)*, 10(6):1501–1506, March 2004. PMID: 15034894.

[58] Tuomo Leikoski, Juha Kaunisto, Martti Alkio, Olli Aaltonen, and Jari Yli-Kauhaluoma. Unusual nazarov cyclization in Near-Critical water. *Organic Process Research & Development*, 9(5):629–633, 2005.

[59] S. Hirano, T. Hiyama, and H. Nozaki. Acid-catalyzed cyclization of cross-conjugated dienone moiety to cyclopentenones. *Tetrahedron Letters*, 15(15):1429–1430, 1974.

[60] S. Hirano, S. Takagi, T. Hiyama, and H. Nozaki. Abnormal nazarov reaction. a new synthetic approach to 2, 3-disubstituted 2-cyclopentenones. *Bulletin of the Chemical Society of Japan*, 53(1):169–173, 1980.

[61] L. M Dudd, E. Venardou, E. Garcia-Verdugo, P. Licence, A. J Blake, C. Wilson, and M. Poliakoff. Synthesis of benzimidazoles in high-temperature water. *Green Chemistry*, 5:187192, 2003.

[62] J. Fraga-Dubreuil, G. Comak, A. W Taylor, and M. Poliakoff. Rapid and clean synthesis of phthalimide derivatives in high-temperature, high-pressure H_2O/EtOH mixtures. *Green Chem.*, 9:1067–1072, 2007.

[63] Xiuyang Lu, Zhun Li, and Fei Gao. Base-Catalyzed reactions in NH_3-Enriched Near-Critical water. *Industrial & Engineering Chemistry Research*, 45(12):4145–4149, June 2006.

[64] T. Richter and H. Vogel. The dehydration of 1, 4-butanediol to tetrahydrofuran in supercritical water. *Chemical Engineering & Technology*, 24(4):340343, 2001.

[65] Y. Nagai, N. Matubayasi, and M. Nakahara. Hot water induces an acid-catalyzed reaction in its undissociated form. *Bulletin of the Chemical Society of Japan*, 77(4):691–697, 2004.

[66] Heather P. Lesutis, Roger Gläser, Charles L. Liotta, and Charles A. Eckert. Acid/base-catalyzed ester hydrolysis in near-critical water. *Chemical Communications*, (20):2063–2064, 1999.

[67] Heather R. Patrick, Kris Griffith, Charles L. Liotta, Charles A. Eckert, and Roger Glaser. Near-Critical water: A benign medium for catalytic reactions. *Industrial & Engineering Chemistry Research*, 40(26):6063–6067, December 2001.

[68] Michael T. Klein, Yves G. Mentha, and Lori A. Torry. Decoupling substituent and solvent effects during hydrolysis of substituted anisoles in supercritical water. *Industrial & Engineering Chemistry Research*, 31(1):182–187, January 1992.

[69] Sadasivan D. Iyer and Michael T. Klein. Effect of pressure on the rate of butyronitrile hydrolysis in high-temperature water. *The Journal of Supercritical Fluids*, 10(3):191–200, August 1997.

[70] P. Krammer, S. Mittelstädt, and H. Vogel. Investigating the synthesis potential in supercritical water. *Chemical Engineering & Technology*, 22(2):126–130, 1999.

[71] Eleni Venardou, Eduardo Garcia-Verdugo, Stephen J. Barlow, Yuri E. Gorbaty, and Martyn Poliakoff. On-line monitoring of the hydrolysis of acetonitrile in near-critical water using raman spectroscopy. *Vibrational Spectroscopy*, 35(1-2):103–109, June 2004.

[72] A. Kramer, S. Mittelstädt, and H. Vogel. Hydrolysis of nitriles in supercritical water. *Chemical Engineering & Technology*, 22(6):494–500, 1999.

[73] P. G Duan, X. Wang, and L. Y Dai. Noncatalytic hydrolysis of iminodiacetonitrile in Near-Critical WaterA green process for the manufacture of iminodiacetic acid. *Chemical Engineering & Technology*, 30(2):265–269, 2007.

[74] Craig M. Comisar, Shawn E. Hunter, Ashley Walton, and Phillip E. Savage. Effect of pH on ether, ester, and carbonate hydrolysis in High-Temperature water. *Industrial & Engineering Chemistry Research*, 47(3):577–584, February 2008.

[75] Takuya Ogawa, Jun Watanabe, and Yoshito Oshima. Catalyst-free synthesis of polyorganosiloxanes by high temperature & pressure water. *The Journal of Supercritical Fluids*, 45(1):80–87, May 2008.

[76] C. Yan, J. Fraga-Dubreuil, E. Garcia-Verdugo, P. A Hamley, M. Poliakoff, I. Pearson, and A. S Coote. The continuous synthesis of ϵ-caprolactam from 6-aminocapronitrile in high-temperature water. *Green Chemistry*, 10(1):98–103, 2008.

[77] S. Yamabe, N. Tsuchida, and S. Yamazaki. Theoretical study of the role of solvent H_2O in neopentyl and pinacol rearrangements. *Journal of Computational Chemistry*, 28(9):1561–1571, 2007.

[78] Hideaki Takahashi, Kohsuke Tanabe, Masataka Aketa, Ryohei Kishi, Shin ichi Furukawa, and Masayoshi Nakano. Novel quantum mechanical/molecular mechanical method combined with the theory of energy representation: free energy calculation for the beckmann rearrangement promoted by proton transfers in the supercritical water. *The Journal of Chemical Physics*, 126(8):084508 (10 pages), February 2007. PMID: 17343459.

[79] Craig M. Comisar and Phillip E. Savage. The benzil-benzilic acid rearrangement in high-temperature water. *Green Chemistry*, 7(11):800–806, 2005.

[80] Craig M. Comisar and Phillip E. Savage. Benzil rearrangement kinetics and pathways in High-Temperature water. *Industrial & Engineering Chemistry Research*, 46(6):1690–1695, March 2007.

[81] P. Wang, H. Kojima, K. Kobiro, K. Nakahara, T. Arita, and O. Kajimoto. Reaction behavior of secondary alcohols in supercritical water. *Bulletin of the Chemical Society of Japan*, 80(9):18281832, 2007.

[82] Naoko Akiya and Phillip E. Savage. Kinetics and mechanism of cyclohexanol dehydration in High-Temperature water. *Industrial & Engineering Chemistry Research*, 40(8):1822–1831, April 2001.

[83] Yutaka Ikushima and Masahiro Sato. A one-step production of fine chemicals using supercritical water: an environmental benign application to the synthesis of monoterpene alcohol. *Chemical Engineering Science*, 59(22-23):4895–4901, November 2004.

[84] Taku Michael Aida, Yukiko Sato, Masaru Watanabe, Kiyohiko Tajima, Toshiyuki Nonaka, Hideo Hattori, and Kunio Arai. Dehydration of d-glucose in high temperature water at pressures up to 80 MPa. *The Journal of Supercritical Fluids*, 40(3):381–388, April 2007.

[85] Taku Michael Aida, Kiyohiko Tajima, Masaru Watanabe, Yuki Saito, Kiyoshi Kuroda, Toshiyuki Nonaka, Hideo Hattori, Richard Lee Smith Jr., and Kunio Arai. Reactions of d-fructose in water at temperatures up to 400 C and pressures up to 100 MPa. *The Journal of Supercritical Fluids*, 42(1):110–119, August 2007.

[86] Muhammad Faisal, Nobuaki Sato, Armando T. Quitain, Hiroyuki Daimon, and Koichi Fujie. Hydrolysis and cyclodehydration of dipeptide under hydrothermal conditions. *Industrial & Engineering Chemistry Research*, 44(15):5472–5477, July 2005.

[87] Ziyue Dai, Bunpei Hatano, and Hideyuki Tagaya. Catalytic dehydration of propylene glycol with salts in near-critical water. *Applied Catalysis A: General*, 258(2):189–193, February 2004.

[88] Nobuaki Sato, Armando T. Quitain, Kilyoon Kang, Hiroyuki Daimon, and Koichi Fujie. Reaction kinetics of amino acid decomposition in High-Temperature and High-Pressure water. *Industrial & Engineering Chemistry Research*, 43(13):3217–3222, June 2004.

[89] Jennifer B. Dunn, Michael L. Burns, Shawn E. Hunter, and Phillip E. Savage. Hydrothermal stability of aromatic carboxylic acids. *The Journal of Supercritical Fluids*, 27(3):263–274, December 2003.

[90] Jie Fu, Phillip E. Savage, and Xiuyang Lu. Hydrothermal decarboxylation of pentafluorobenzoic acid and quinolinic acid. *Industrial & Engineering Chemistry Research*, 48(23):10467–10471, December 2009.

[91] Joan Fraga-Dubreuil, Juan Garcia-Serna, Eduardo Garcia-Verdugo, Lucinda M. Dudd, Graham R. Aird, W. Barry Thomas, and Martyn Poliakoff. The catalytic oxidation of benzoic acid to phenol in high temperature water. *The Journal of Supercritical Fluids*, 39(2):220–227, December 2006.

[92] Pimu Zhai, Liqiu Wang, Changhou Liu, and Shouchen Zhang. Deactivation of zeolite catalysts for benzene oxidation to phenol. *Chemical Engineering Journal*, 111(1):1–4, July 2005.

[93] Russell L. Holliday, Brenton Y.M. Jong, and Joseph W. Kolis. Organic synthesis in subcritical water: Oxidation of alkyl aromatics. *Journal of Supercritical Fluids, The*, 12(3):255–260, July 1998.

[94] P. A Hamley, T. Ilkenhans, J. M Webster, E. Garcia-Verdugo, E. Venardou, M. J Clarke, R. Auerbach, W. B Thomas, K. Whiston, and M. Poliakoff. Selective partial oxidation in supercritical water: the continuous generation of terephthalic acid from para-xylene in high yield. *Green Chemistry*, 4(3):235–238, 2002.

[95] J. B Dunn, D. I Urquhart, and P. E Savage. Terephthalic acid synthesis in supercritical water. *Advanced Synthesis & Catalysis*, 344(3-4):385392, 2002.

[96] E. Garcia-Verdugo, J. Fraga-Dubreuil, P. A Hamley, W. B Thomas, K. Whiston, and M. Poliakoff. Simultaneous continuous partial oxidation of mixed xylenes in supercritical water. *Green Chemistry*, 7(5):294300, 2005.

[97] Mitsumasa Osada and Phillip E. Savage. Terephthalic acid synthesis at higher concentrations in high-temperature liquid water. 1. effect of oxygen feed method. *AIChE Journal*, 55(3):710–716, 2009.

[98] Y. Chen, J. L Fulton, and W. Partenheimer. A XANES and EXAFS study of hydration and ion pairing in ambient aqueous $MnBr_2$ solutions. *Journal of Solution Chemistry*, 34(9):993–1007, 2005.

[99] S. E Hunter, C. A Felczak, and P. E Savage. Synthesis of p-isopropenylphenol in high-temperature water. *Green Chemistry*, 6(4):222–226, 2004.

[100] Phillip E. Savage, Shawn E. Hunter, Katherine L. Hoffee, Theresa J. Schuelke, and Matthew J. Smith. Bisphenol e decomposition in High-Temperature water. *Industrial & Engineering Chemistry Research*, 45(23):7775–7780, November 2006.

[101] Barbara Kuhlmann, Edward M. Arnett, and Michael Siskin. Classical organic reactions in pure superheated water. *The Journal of Organic Chemistry*, 59(11):3098–3101, June 1994.

[102] Barbara Kuhlmann, Edward M. Arnett, and Michael Siskin. H-D exchange in pinacolone by deuterium oxide at high temperature and pressure. *The Journal of Organic Chemistry*, 59(18):5377–5380, 1994.

[103] J. Kalpala, K. Hartonen, M. Huhdanpää, and M. L Riekkola. Deuteration of 2-methylnaphthalene and eugenol in supercritical and pressurised hot deuterium oxide. *Green Chemistry*, 5(5):670–676, 2003.

[104] Shi Bai, Bruce J. Palmer, and Clement R. Yonker. Kinetics of deuterium exchange on resorcinol in D2O at high pressure and high temperature. *The Journal of Physical Chemistry A*, 104(1):53–58, January 2000.

[105] M. Kubo, T. Takizawa, C. Wakai, N. Matubayasi, and M. Nakahara. Noncatalytic kinetic study on site-selective H/D exchange reaction of phenol in sub-and supercritical water. *The Journal of chemical physics*, 121:960—969, 2004.

[106] Jerry March. *Advance Organic Chemistry: Reactions Mechanisms and Structure*. John Wiley & Sons, 1985.

[107] Ying Yang and Ronald F. Evilia. Deuteration of hexane by 2HCl in supercritical deuterium oxide. *The Journal of Supercritical Fluids*, 15(2):165–172, June 1999.

[108] M. Sasaki, J. Nishiyama, M. Uchida, K. Goto, K. Tajima, T. Adschiri, and K. Arai. Conversion of the hydroxyl group in 1-hexyl alcohol to an amide group in supercritical water without catalyst. *Green Chemistry*, 5(1):95–97, 2003.

[109] Kiyohiko Tajima, Munehiro Uchida, Kimitaka Minami, Mitsumasa Osada, Kiwamu Sue, Toshiyuki Nonaka, Hideo Hattori, and Kunio Arai. Amination of n-Hexanol in supercritical water. *Environmental Science & Technology*, 39(24):9721–9724, December 2005.

[110] Jennifer Marie Brunner Dunn. *The partial oxidation of p-xylene in high-temperature water*. PhD thesis, University of Michigan, United States – Michigan, 2004. Ph.D.

[111] Robert M. Silverstein, Francis X. Webster, and David Kiemle. *Spectrometric Identification of Organic Compounds*. Wiley, 7 edition, January 2005.

[112] Michael B. Smith and Jerry March. *March's Advanced Organic Chemistry: Reactions, Mechanisms, and Structure, 5th Edition*. Wiley-Interscience, 5th edition, January 2001.

[113] Alan R. Katritzky, Franz J. Luxem, and Michael Siskin. Aqueous high-temperature chemistry of carbo- and heterocycles. 6. monosubstituted benzenes with two carbon atom side chains unsubstituted or oxygenated at the .α.-position. *Energy & Fuels*, 4(5):518–524, 1990.

[114] Jingyi An, Laurence Bagnell, Teresa Cablewski, Christopher R. Strauss, and Robert W. Trainor. Applications of High-Temperature aqueous media for synthetic organic reactions. *The Journal of Organic Chemistry*, 62(8):2505–2511, April 1997.

[115] Alan R. Katritzky, M. Balasubramanian, and Michael Siskin. Aqueous high-temperature chemistry of carbo- and heterocycles. 2. monosubstituted benzenes: benzyl alcohol, benzaldehyde and benzoic acid. *Energy & Fuels*, 4(5):499–505, 1990.

[116] Makoto Tokunaga and Yasuo Wakatsuki. The first Anti-Markovnikov hydration of terminal alkynes: Formation of aldehydes catalyzed by a Ruthenium/Phosphane mixture. *Angewandte Chemie International Edition*, 37(20):2867–2869, 1998.

[117] J. Henrique Teles, Stefan Brode, and Mathieu Chabanas. Cationic Gold(I) complexes: Highly efficient catalysts for the addition of alcohols to alkynes. *Angewandte Chemie International Edition*, 37(10):1415–1418, 1998.

[118] P. W. Jennings, J. W. Hartman, and W. C. Hiscox. Alkyne hydration using Pt(II) catalysts. *Inorganica Chimica Acta*, 222(1-2):317–322, July 1994.

[119] Lukas Hintermann and Aurlie Labonne. Catalytic hydration of alkynes and its application in synthesis. *Synthesis*, (8):1121–1150, 2007.

[120] H. Scott Fogler. *Elements of Chemical Reaction Engineering*. Prentice Hall PTR, 4 edition, September 2005.

[121] P. B. Weisz and C. D. Prater. Interpretation of measurements in experimental catalysis. *Advances in Catalysis*, VI:144–196, 1954.

[122] D. S Noyce and M. D Schiavelli. Acid-catalyzed hydration of phenylacetylene. evidence for the vinyl cation intermediate. *Journal of the American Chemical Society*, 90(4):1020–1022, 1968.

[123] D. S Noyce and M. D Schiavelli. Isotope effects in the acid-catalyzed hydration of phenylacetylene. *Journal of the American Chemical Society*, 90(4):1023–1026, 1968.

[124] D. S Noyce and M. D Schiavelli. Kinetics of the acid-catalyzed hydration of 1-phenylpropyne. *The Journal of Organic Chemistry*, 33(2):845–846, 1968.

[125] D. S Noyce, M. A Matesich, O. P. Melvyn, D. Schiavelli, and P. E Peterson. Concerning the Acid-Catalyzed hydration of acetylenes. *Journal of the American Chemical Society*, 87(10):2295–2296, 1965.

[126] Andreas Schmidt, Tobias Habeck, Bohdan Snovydovych, and Wolfgang Eisfeld. Addition reactions and redox esterifications of carbonyl compounds by N-Heterocyclic carbenes of indazole. *Organic Letters*, 9(18):3515–3518, 2007.

[127] Scott E. Denmark and Christopher R. Butler. Vinylation of aryl bromides using an inexpensive vinylpolysiloxane. *Organic Letters*, 8(1):63–66, January 2006.

[128] Paige R. Brooks, Michael C. Wirtz, Michael G. Vetelino, Diane M. Rescek, Graeme F. Woodworth, Bradley P. Morgan, and Jotham W. Coe. Boron Trichloride/Tetra-n-Butylammonium iodide: A mild, selective combination reagent for the cleavage of primary alkyl aryl ethers. *The Journal of Organic Chemistry*, 64(26):9719–9721, December 1999.

[129] T. Shindo, Y. Fukuyama, and T. Sugai. Scope and limitations of Lithium-Ethylenediamine-THF-Mediated cleavage at the α-Position of aromatics: Deprotection of aryl methyl ethers and benzyl ethers under mild conditions. *Synthesis*, 2004(5):692–700, 2004.

[130] Asit K. Chakraborti, Mrinal K. Nayak, and Lalima Sharma. Diphenyl disulfide and sodium in NMP as an efficient protocol for in situ generation of thiophenolate anion: Selective deprotection of aryl alkyl ethers and alkyl aryl esters under nonhydrolytic conditions. *The Journal of Organic Chemistry*, 67(6):1776–1780, March 2002.

[131] Shanthaveerappa K. Boovanahalli, Dong Wook Kim, and Dae Yoon Chi. Application of ionic liquid halide nucleophilicity for the cleavage of ethers: A green protocol for the regeneration of phenols from ethers. *The Journal of Organic Chemistry*, 69(10):3340–3344, May 2004.

[132] J. R Hwu, F. F Wong, J. J Huang, and S. C Tsay. Sodium bis (trimethylsilyl) amide and lithium diisopropylamide in deprotection of alkyl aryl ethers: α-Effect of silicon. *J. Org. Chem*, 62(12):4097–4104, 1997.

[133] M. T Konieczny, G. Maciejewski, and W. Konieczny. Selectivity adjustment in the cleavage of allyl phenyl and methyl phenyl ethers with boron trifluoride-methyl sulfide complex. *Synthesis-Journal of Synthetic Organic Chemistry*, 10:1575–1577, 2005.

[134] A. Talha Yalta. The accuracy of statistical distributions in microsoft excel 2007. *Computational Statistics & Data Analysis*, 52(10):4579–4586, June 2008.

[135] B.D. McCullough and David A. Heiser. On the accuracy of statistical procedures in microsoft excel 2007. *Computational Statistics & Data Analysis*, 52(10):4570–4578, June 2008.

[136] Johannes M. L. Penninger and Johannes M. L. Kolmschate. Chemistry of methoxynaphthalene in supercritical water. In *Supercritical Fluid Science and Technology*, volume 406 of *ACS Symposium Series*, pages 242–258. American Chemical Society, Washington, DC, August 1989.

[137] Sascha R. A. Kersten, Biljana Potic, Wolter Prins, and Wim P. M. Van Swaaij. Gasification of model compounds and wood in hot compressed water. *Industrial & Engineering Chemistry Research*, 45(12):4169–4177, June 2006.

[138] Fernando L. P. Resende, Matthew E. Neff, and Phillip E. Savage. Noncatalytic gasification of cellulose in supercritical water. *Energy & Fuels*, 21(6):3637–3643, November 2007.

[139] Fernando L. P. Resende, Stephanie A. Fraley, Michael J. Berger, and Phillip E. Savage. Noncatalytic gasification of lignin in supercritical water. *Energy & Fuels*, 22(2):1328–1334, March 2008.